

---

# PHOTONIC CORRELATOR BASED ON FOUR WAVE MIXING

A thesis submitted in fulfillment of the requirements for the degree of  
Doctor of Philosophy

**Refat Kibria**

B.Eng., M.Eng.

School of Electrical and Computer Engineering

College of Science, Engineering and Health

RMIT University

Melbourne, Australia

March 2014

## **DECLARATION**

I certify that except where due acknowledgement has been made, the work is that of the author alone; the work has not been submitted previously, in whole or in part, to qualify for any other academic award; the content of the thesis is the result of work which has been carried out since the official commencement date of the approved research program; and, any editorial work, paid or unpaid, carried out by a third party is acknowledged.

-----

**Refat Kibria**

(31/03/2014)

Dedicated to my father

Professor Golam Kibria -

my constant source of inspiration to do better.

## **ACKNOWLEDGEMENT**

First of all, I would like to express my great gratitude to my senior supervisor, Professor Michael Austin, for providing me with excellent research environment, valuable directions, and delicate guidance throughout this research work. His meticulous scholarship impresses me. His great passion towards scientific research work inspires me to work hard. Without his encouragement and patience, this work would have never been finished.

Special thanks to my second supervisor Dr. Lam Bui and Professor Arnan Mitchell for their generosity in sharing their knowledge with me. Their rich knowledge was a constant source of ideas. Sincere thanks to them for their invaluable help in encouraging me to overcome obstacles in the research.

I would like to thank my completion seminar panel members - Professor James Scott and Associate Professor Wayne Rowe for their valuable comments and suggestions on my work to prepare the thesis.

I would also like to thank the current and former colleagues in the Microwave Photonics Research Laboratory at the School of Electrical and Computer Engineering, RMIT University: Paul, Khaled, Kusan, Mehdrad, Jarrod, and Fithri. Their strong support and generous help greatly improved my research work.

Thanks to SGR of RMIT University for funding my research. Without the funding, I would not be able to pursue the research. Also thanks to Associate Professor Alan Wong and Dr. Katrina Neville for giving me the opportunity of tutoring their courses. This not only helped me financially but also provided me with invaluable teaching experience in the course of my PhD.

Finally, I am greatly indebted to my friends and family without whom I cannot be myself. It is a pleasure to remember my dearest friend Robin at the eve of a PhD thesis submission. He is the person who played a great role to allow me to become an engineer and researcher. My fellow friends-



especially- Polash, Iqbal, Chandan, Imrul, Tim and Tanvir, who are living here in Melbourne and offered me a tremendous support all through during my stay. Thanks is never enough for them. Among my family members, first come my parents - my father Professor Golam Kibria, my mother Shahin Kibria who did everything in their capability and sometime beyond to grow me up to this level. I also like to pay tribute to my uncles, especially Dr. Gulam Nabi and Mr. Golam Akbar, both of whom influenced me a lot to become an academic. My brothers, my sister, my sweet niece Fairouz and Fabiha, my only nephew Raeed and my in-laws - especially mother-in-law Dil Afroza Khanom and all of the family members are heavily supportive and carried a lot of pain themselves to smooth up my journey to complete the research. Last but not the least, my loving wife Naharin and my only daughter Rida, both of them sacrificed a lot of their pleasures and accepted a tough life here abroad only to be a source of constant support and inspiration for me. I think my research work is a special gift for my wife who shared many of my parts in rising up a little baby by sacrificing her own career to give me enough scope to pursue my research. They have always been the biggest support, physically and mentally, in my life and study.

## ABSTRACT

Modern high-performance signal processing applications face constantly increasing processing speeds. The use of photonics potentially offers a much higher bandwidth and faster processing than what can be achieved in the electronic domain. This thesis investigates novel photonic techniques based on optical mixing for performing a correlation, a common signal processing task.

The first photonic correlation scheme investigated uses four wave mixing (FWM) in a length of highly nonlinear fibre (HNLF) to mix template or reference wavelengths with a pump wavelength, which has been modulated by an input bit stream in order to produce copies of the input signal at the output idler wavelengths. The idler wavelengths are differentially delayed and summed at a photoreceiver to produce a correlation of the input bit stream and the reference bit pattern. This technique was investigated experimentally and results show that a correlation function is successfully achieved.

A significant advantage of this technique compared to previous photonic correlation techniques is that modulation of the pump wavelength allows the “transmitter” to be remotely located, away from the correlation signal processing equipment. An extension of this technique successfully demonstrated the use of software control of the reference bit pattern using a multi-port photonic signal processor (Waveshaper). This enabled a more versatile form of correlator.

True correlation requires the summation of negative signals. This is difficult for optical signals. A novel photonic technique based on FWM, which allows negative accumulation, was proposed for the first time. In this technique, a number of carrier and pump wavelengths are carefully selected such that individual mixing products occur at the same idler wavelength. Subtraction of optical fields at this wavelength can be achieved by changing the relative phase of pump wavelengths by  $90^\circ$  using a Waveshaper optical processor. This novel concept was verified via a simulation using ‘VPItransmissionMaker 9.0’ software. The simulation demonstrated that negative accumulation of optical signals could be achieved for the first time.

In summary, novel photonic correlation techniques based on nonlinear optical mixing in optical fibre have been demonstrated and subtraction of optical fields using FWM has been demonstrated for the first time.

# TABLE OF CONTENTS

Declaration.....	II
Acknowledgement.....	IV
Abstract.....	VI
List of Figures: .....	XI
1. Introduction.....	1
1.1 Motivation.....	1
1.2 Problem definition.....	2
1.3 Synopsis.....	3
1.4 Thesis Contributions.....	5
2. A Review of Correlation .....	6
2.1 Introduction .....	6
2.2 Correlation.....	6
2.2.1 Theory of Correlation .....	6
2.2.2 Types of Correlator.....	9
2.2.2.1 Correlation using bulk optics.....	10
2.2.2.2 Correlation using photonics.....	11
2.3 Photonic approaches .....	12
2.3.1 Joint Transform Correlators .....	12
2.3.2 Matched Filter Correlators .....	13
2.3.2.1 Time spectral convolution based correlation.....	14
2.3.2.2 Optical time domain correlation.....	15
2.4 Conclusion .....	17
3. Four Wave Mixing .....	18
3.1 Introduction .....	18
3.2 Properties of FWM.....	18
3.3 FWM Efficiency .....	22
3.4 Conclusion .....	23
4. Photonic Correlation using Four Wave Mixing .....	24
4.1 Introduction .....	24
4.2 Time-spectral convolution .....	24
4.3 Proposed Method .....	26
4.4 Experimental Set-up .....	27
4.4.1 Transmitter .....	28

4.4.2	Receiver.....	29
4.4.2.1	Selection of the CW Laser Wavelengths .....	30
4.4.2.2	Nonlinear Mixing in HNLF.....	34
4.4.2.3	Separation of the required idler wavelengths .....	36
4.4.2.4	Applying the wavelength dependent delay .....	41
4.4.3	Correlation Results .....	43
4.5	Discussion.....	45
4.6	Conclusion .....	47
5.	Photonic Correlator with Remote Transmitter .....	48
5.1	Introduction .....	48
5.2	Proposed method.....	49
5.3	Experimental Set-up .....	50
5.3.1.	Transmitter.....	50
5.3.2.	Receiver .....	51
5.3.3.	Results.....	58
5.3.4.	Discussion .....	59
5.4	Conclusion .....	60
6.	Photonic Correlation with Negative Accumulation .....	61
6.1	Introduction .....	61
6.2	Concept of optical negative accumulation.....	61
6.2.1.	Simulation verification of the proposed concept.....	63
6.2.2.	Simulation results.....	64
6.2.3.	Conclusion .....	66
6.3	Proposed correlation concept.....	66
6.3.1.	Simulation using Intensity Modulation .....	67
6.3.1.1.	Characterization and Results .....	69
6.3.1.2.	Conclusion .....	74
6.3.2.	Simulation using Phase Modulation .....	74
6.3.2.1.	Characterization and results.....	75
6.4	Conclusion .....	81
7.	Conclusion and Future Work.....	83
7.1	Outcomes of the work .....	83
7.2	Future work .....	85
7.3	Conclusion .....	86

List of Acronyms .....	87
References: .....	89
Appendix I .....	94
Appendix II .....	96
Appendix III .....	101
Appendix IV .....	106
Appendix V.....	109

## LIST OF FIGURES:

Figure 1.1	Schematic of photonic processing of RF signals [16].	2
Figure 2.1	Visual representation of the convolution, cross-correlation and auto correlation processes [28].	8
Figure 2.2	Block diagram of a joint transform correlator.	12
Figure 2.3	Functional block diagram of a matched filter correlator.	13
Figure 2.4	Functional diagram of a time spectral convolution based correlator [24].	14
Figure 2.5	Functional diagram of optical time domain correlation [27].	16
Figure 3.1	Wavelength conversion using four wave mixing [48].	21
Figure 3.2	Illustration of the FWM process in a HNLf.	22
Figure 3.3	Variation in mixing efficiency with wavelength spacing [53].	23
Figure 4.1	Illustration of the working principle of the time-spectral convolution based correlation scheme demonstrated in [24].	25
Figure 4.2	Illustration of the working principle of the proposed HNLf based correlation scheme.	27
Figure 4.3	Experimental set-up for the proposed HNLf based correlation scheme.	29
Figure 4.4	HP 3760A data generator used in the experiment.	29
Figure 4.5	Newport 8-channel laser array with modular controller.	31
Figure 4.6	Measured channel wavelengths representing 1101 combined with the pump wavelength $\lambda_5$ at the input of the HNLf.	32
Figure 4.7	The 8-Channel AWG used in the experiment.	33
FIGURE 4.8	Measured AWG response with the internal heater circuitry set at 72.2° C.	33
Figure 4.9	High power EDFA used in the experiment.	34
Figure 4.10	PM-HNLf from OFS with low dispersion used in the experiment.	35
Figure 4.11	FWM mixing products measured at the output of the HNLf.	36
Figure 4.12	Low pass filter used in the experiment as a first step of filtering.	37
Figure 4.13	Lo-pass filter characteristics (transmit) [filter manufacturer data sheet].	37
Figure 4.14	Measured spectrum after the first stage of filtering using a low-pass filter.	38

Figure 4.15	Finisar Waveshaper 4000s used in the experiment. ....	39
Figure 4.16	Operation principle of the Waveshaper [21] .....	39
Figure 4.17	Template wavelengths measured at the output of the Waveshaper. ....	40
Figure 4.18	Sensitive New Focus Photoreceiver with DC power supply. ....	41
Figure 4.19	(a) Measured photoreceiver output when only $\lambda_4'$ is present. (Zero delay) (b) Measured photoreceiver output when only $\lambda_3'$ is present. It is differentially delayed by a 1-bit delay. (c) Measured photoreceiver output when only $\lambda_1'$ is present. It is differentially delayed by a 3-bit delay. ....	42
Figure 4.20	Correlation output with matched input signal 1011.....	43
Figure 4.21	Correlation output with a mismatched input signal 1000. ....	44
Figure 4.22	Correlation output with matched input 1011 and worst-case mismatched input signal 1010. ....	44
Figure 5.1	Illustration of the working principle of the proposed HNLF based correlation scheme with possible remote transmitter and software controlled template. ....	49
FIGURE 5.2	Characterization and experimental set-up.....	51
Figure 5.3	Measured CW laser wavelengths channels representing the 4 reference bits combined with the pump wavelength, $\lambda_5$ . ....	52
Figure 5.4	Output of the HNLF after nonlinear mixing. ....	54
Figure 5.5	Output of EDFA2 after passing through the low pass filter. ....	54
Figure 5.6	Software selected template 1101 at the output of the Waveshaper.....	55
Figure 5.7	(a) Pump and CW laser wavelengths at the input of the HNLF, (b) mixing products at the output of the HNLF, (c) amplified output of the low pass filter (filtering the high power pump and the input channels), (d) template representing idler wavelengths measured at the Waveshaper. ....	56
FIGURE 5.8	(a) Measured photoreceiver output when only $\lambda_4'$ is present. (b) Measured photoreceiver output when only $\lambda_3'$ is present. It is differentially delayed by a 1 bit delay compared to $\lambda_4'$ . (c) Measured photoreceiver output when only $\lambda_1'$ is present. It is differentially delayed by a 3 bit delay compared to $\lambda_4'$ . ....	57



Figure 5.9 Measured correlation outputs for all possible combinations of input bit patterns. The solid line indicates the output for a matched bit pattern whilst the dotted lines are for mismatched bit patterns.

58

Figure 6.1 Principle of operation. a) Selection of wavelengths based on the scheme in [56] for addition.  
 b) Illustration of the subtraction process by applying a  $\pi/2$  relative phase shift to one pump wavelength.....62

Figure 6.2 Simulation schematic to achieve optical subtraction. ....63

Figure 6.3 Simulation results illustrating the addition process. a) Signal wavelength  $\lambda_{S1}$  and pump wavelength  $\lambda_{P1}$  generate an idler at  $2\lambda_{P1}-\lambda_{S1}$ . b)  $\lambda_{S2}$  and  $\lambda_{P2}$  mix and generate an idler at the same wavelength  $2\lambda_{P1}-\lambda_{S1}$ . c)  $\lambda_{S1}$ ,  $\lambda_{S2}$ ,  $\lambda_{P1}$  and  $\lambda_{P2}$  generate two idlers at the same wavelength which add in phase, producing a 6 dB increase in optical power. ....64

Figure 6.4 Simulation results illustrating the optical subtraction process. a) Signal wavelength  $\lambda_{S1}$  and pump wavelength  $\lambda_{P1}$  generate an idler at  $2\lambda_{P1}-\lambda_{S1}$ . b)  $\lambda_{S2}$  and  $\lambda_{P2}$ , which is  $90^\circ$  phase shifted with respect to  $\lambda_{P1}$ , generate an idler at the same wavelength as in a) but with a  $180^\circ$  phase shift. c)  $\lambda_{S1}$ ,  $\lambda_{S2}$ ,  $\lambda_{P1}$  and  $\lambda_{P2}$  mix and generate two idlers at the same wavelength which are  $180^\circ$  out of phase, producing a subtraction. ....65

Figure 6.5 Principle of operation of the proposed negative accumulation based correlation with pump wavelengths representing the template 1101. ....66

Figure 6.6 Simulation set-up in VPItransmissionMaker 9.0 used to verify the negative accumulation based correlation scheme for a 4-bit duration pattern length when intensity modulation is used. ....67

Figure 6.7 Proof of concept. a) Individual mixing result of  $\lambda_{S1}$  and  $\lambda_{P1}$ . b) Individual mixing product of  $\lambda_{S2}$  and  $\lambda_{P2}$ . c) Mixing product  $\lambda_{S1}$  and  $\lambda_{P1}$ , and  $\lambda_{S2}$  and  $\lambda_{P2}$ , showing an addition when  $\lambda_{P1}$  and  $\lambda_{P2}$  are in phase. d) Individual mixing result of  $\lambda_{S3}$  and  $\lambda_{P3}$ . e) Individual mixing result of  $\lambda_{S4}$  and  $\lambda_{P4}$ . f) Mixing product of  $\lambda_{S3}$ ,  $\lambda_{P3}$ , and  $\lambda_{S4}$ ,  $\lambda_{P4}$ , showing subtraction when  $\lambda_{P3}$  is  $90^\circ$  out of phase with respect to  $\lambda_{P4}$ . .69

Figure 6.8 Detected electrical waveforms for the matched condition due to the a) mixing of  $\lambda_{S1}$  and  $\lambda_{P1}$ , b) mixing of  $\lambda_{S2}$  and  $\lambda_{P2}$ , c) mixing of  $\lambda_{S3}$  and  $\lambda_{P3}$ , d) mixing of  $\lambda_{S4}$  and  $\lambda_{P4}$  and e) the output correlation function which is a summation of plots a) – d). ....72

<b>Figure 6.9</b>	<b>Detected electrical waveform for a mismatched condition due to the a) mixing of <math>\lambda_{S1}</math> and <math>\lambda_{P1}</math>, b) mixing of <math>\lambda_{S2}</math> and <math>\lambda_{P2}</math>, c) mixing <math>\lambda_{S3}</math> and <math>\lambda_{P3}</math>, d) mixing of <math>\lambda_{S4}</math> and <math>\lambda_{P4}</math> and e) the output correlation function which is a summation of plots a) – d). .....</b>	<b>73</b>
<b>Figure 6.10</b>	<b>Output correlation function obtained for a real time 10Gb/s input bit stream. ....</b>	<b>74</b>
<b>Figure 6.11</b>	<b>Simulation set-up in VPItransmissionMaker 9.0 to verify a negative accumulation based correlation scheme for a 4-bit duration pattern length when a phase modulator (PM) is used. ....</b>	<b>75</b>
<b>Figure 6.12</b>	<b>Received Optical waveforms for the matched condition at the target wavelength due to the a) mixing of <math>\lambda_{S1}</math> and <math>\lambda_{P1}</math>, b) mixing of <math>\lambda_{S2}</math> and <math>\lambda_{P2}</math>, c) mixing of <math>\lambda_{S3}</math> and <math>\lambda_{P3}</math>, d) mixing of <math>\lambda_{S4}</math> and <math>\lambda_{P4}</math> and e) the output correlation function with negative accumulation which is a summation of plots a) – d).....</b>	<b>78</b>
<b>Figure 6.13</b>	<b>Detected electrical waveform at the output of the Photoreceiver. ....</b>	<b>79</b>
<b>Figure 6.14</b>	<b>Received optical waveforms for a mismatched condition due to the. a) mixing of <math>\lambda_{S1}</math> and <math>\lambda_{P1}</math>, b) mixing of <math>\lambda_{S2}</math> and <math>\lambda_{P2}</math>, c) mixing of <math>\lambda_{S3}</math> and <math>\lambda_{P3}</math>, d) mixing of <math>\lambda_{S4}</math> and <math>\lambda_{P4}</math> and e) the output correlation function with negative accumulation which is a summation of plots a) – d).....</b>	<b>80</b>

# 1. INTRODUCTION

## 1.1 MOTIVATION

A major limitation to the electronic processing of broadband radio frequency (RF) signals is the speed of the processing electronics. A solution to this problem is based on processing of broadband RF signals in the optical domain [1]. There is currently much interest in the use of photonic technologies for the processing of RF/microwave signals. This field is known as ‘RF photonics’ which is also alternately referred to as ‘microwave photonics’ [2]. Optical approaches have been utilized to realize a range of RF processing tasks. These include filtering, phase shifting, and frequency up and down conversion. Photonic processing of radio frequency signals has been thoroughly investigated for the past three decades [3] to enhance the performance of RF/Microwave systems and to develop versatile techniques of RF photonic signal processing [4-9]. Microwave photonics offers a lot of advantages such as broad bandwidth, low RF dependent attenuation, immunity to electromagnetic interference, flexibility, etc.[2]. As Figure 1.1 depicts, for photonic processing an input RF signal is typically modulated on to an optical carrier signal and processing of the RF signal then takes place in the optical domain, followed by an optical to electronic (O/E) conversion in a photodetector (PD) resulting in an output RF signal. A variety of optical sources such as continuous wave (CW) lasers [10-12], mode-locked lasers [13] and sliced broadband light [14, 15] and a variety of modulation formats such as intensity modulation in the form of double sideband (DSB) or single-sideband (SSB) modulation [16] have been employed to implement the RF/optical conversion.

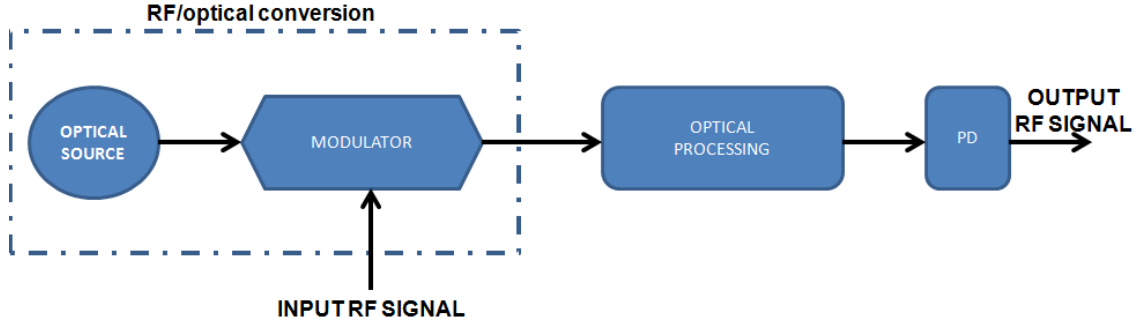


FIGURE 1.1 Schematic of photonic processing of RF signals [16].

A common signal processing task which is very important in communications is the correlation of two signals, which provides a measure of the similarity of the two signals. The correlation function measures the dependence on time delay  $\tau$  of two signals  $r(t)$  and  $s(t)$  and is defined as:

$$C_{rs}(\tau) = \int_{-\infty}^{\infty} r(t) s(t - \tau) dt \quad (1.1)$$

One application of correlation is in the implementation of a matched filter. Matched filters are commonly used in communication systems for maximizing the signal-to-noise ratio (SNR) of a received signal in the presence of additive white Gaussian noise [17]. The correlation of wideband RF signals can be limited by the speed of the processing electronics and hence for real-time wideband applications, the use of photonic approaches to signal processing is becoming popular. The use of photonics to implement matched filters has recently been demonstrated for RF signals [5] and optical signals [9, 20].

## 1.2 PROBLEM DEFINITION

As mentioned in the previous section, electronics has its own bottleneck of low bandwidth (BW) and a photonic approach to realize real time correlation is becoming increasingly popular [2, 5, 6, 23, 24]. However, in order to achieve the accumulation or addition of negative signals, current photonic approaches to correlation use a balanced photodetector to achieve subtraction of electrical signals rather than subtract signals in the optical domain [25-27].

In addition, it is desirable in many practical applications that sophisticated signal processing tasks are done remotely and well away from the source of the signal, e.g. an antenna. However, current approaches to implement a photonic correlator do not allow for separation of the transmitter and the receiver [24, 25] as a Mach-Zehnder modulator (MZM) is typically used to perform the multiplication required for the correlation function.

The aim of this research is to investigate the use of nonlinear Four Wave Mixing (FWM) in highly nonlinear optical fibre (HNLF) to achieve correlation of an input bit stream with a reference template pattern. Furthermore, the goal is to employ FWM to realize negative accumulation optically and thus remove the need for the use of electronic processing even when subtraction between optical signals is required. Four wave mixing is preferred over other fibre based nonlinear effects like self-phase modulation (SPM) or cross-phase modulation (XPM) because it is bit rate independent. In SPM and XPM, intensity modulation of an optical signal results in phase modulation of the same signal or another signal via a time-dependent change of the refractive index. This phase modulation leads to unwanted frequency chirp. FWM involves energy transfer between waves and not a modulation of refractive index. It is therefore transparent to bit rate and data format of the signal [28,34].

### **1.3 SYNOPSIS**

The work in this thesis aims to utilize the four wave mixing property in highly nonlinear optical fibre to demonstrate a photonic correlator which allows remoting of the transmitter from the signal-processing end of the correlator, and also to demonstrate true correlation with accumulation of negative signals.

Chapter 2 of this thesis is a literature review which discusses correlation of signals in general, and photonic correlation approaches in particular. State-of-the-art implementation techniques are analyzed and the problem definition stated above is verified with support from the literature.

Chapter 3 contains an insight on four wave mixing. This research heavily relies on the FWM phenomenon and a detailed analytical explanation as well as inherent properties of FWM are provided and discussed in this chapter.

Chapter 4 presents a practical implementation of a correlation technique utilizing four wave mixing. Optical mixing of template wavelengths with a pump wavelength, which has been modulated by an input bit stream, in order to produce copies of the input signal at the output idler wavelengths, is done in a length of highly nonlinear fibre. This proposed technique is investigated experimentally and the results show that a correlation function is achieved optically.

Chapter 5 illustrates a useful extension of the concept of Chapter 4 by selecting the template with a software controlled optical processor instead of physically turning on/off the laser diodes as was done in the experiment of Chapter 4. This approach allows a true remoting of the transmitter. This proposed technique is also investigated experimentally and performance criteria for such a system are discussed.

Chapter 6 demonstrates an optical technique for the concept of negative accumulation of optical power optically for the first time in the literature. The FWM property is exploited to achieve subtraction between two optical signals. When the relative phase difference between two pump wavelengths is  $\pi/2$  radians, in the mixing process the generated idler has a phase difference of  $\pi$  radians with respect to other idlers at the same frequency and this  $\pi$  radians phase shift leads to negative accumulation of the signal optically. A *VPItransmissionMaker 9.0* based software simulation is performed to prove the concept and demonstrate the correlation scheme with negative accumulation.

Chapter 7 summarizes the work undertaken in the research, draws some conclusions and mentions possible future work.

## 1.4 THESIS CONTRIBUTIONS

The original contributions made by this thesis are:

- i. A novel photonic correlation scheme based on matched filtering using four wave mixing in a length of highly nonlinear optical fibre has been demonstrated [29]. This work was presented at the 2012 IEEE Topical Meeting on Microwave Photonics held at Noordwijk, The Netherlands, in September 2012. A copy of the paper titled “*Nonlinear Mixing Based Photonic Correlation*”, is presented in Appendix II.
- ii. A correlation technique utilizing four wave mixing which allows remoting of the transmitter has been implemented [30]. This work was published in IEEE Photonics Technology Letters, in January 2014. A copy of the paper titled “*HNLF Based Photonic Pattern Recognition using Remote Transmitter*” is presented in Appendix III.
- iii. A novel technique to achieve subtraction of two optical signals based on four wave mixing has been demonstrated [31]. This work was presented at the 2013 IEEE Photonics Conference held at Bellevue, USA, in September 2013. A copy of the paper titled “*Optical Subtraction using Nonlinear Mixing*” is presented in Appendix IV.
- iv. A new photonic correlation scheme based on four wave mixing which achieves subtraction of optical fields and hence allows accumulation of negative signals has been demonstrated [32]. This work has been published in the IEEE Photonics Journal in December 2013. A copy of this paper titled “*A Photonic Correlation Scheme Using FWM with Phase Management to Achieve Optical Subtraction*” is presented in Appendix V.

## **2. A REVIEW OF CORRELATION**

### **2.1 INTRODUCTION**

The aim of this thesis is to investigate the use of FWM in highly nonlinear optical fibre to achieve correlation of an input bit stream with a reference template pattern. Correlation is a very common signal processing task which provides a measure of the similarity between signals. This chapter presents an overview of correlation. First, a brief outline of a generic correlation algorithm is presented. This is followed by an overview of different types of correlator, including electronic correlators and photonic correlators. The final section presents different contemporary photonic correlator implementation techniques.

### **2.2 CORRELATION**

A large number of high-end detection applications such as antenna aperture synthesis, radio imaging, radar, radio astronomy, high-energy physics, and many others, have a common and very computationally intensive part – the wideband correlation of signals. Correlation, or more generally speaking, finding a relation between a set of signals, is a computational core task for a majority of signal processing operations and is critical for computation performance. The result of the cross-correlation function is “a measure of similarity between a pair of signals” [33].

#### **2.2.1 THEORY OF CORRELATION**

The process of correlation provides a measure of the similarity or interdependence between two signals as a function of a shift or lag of one signal with respect to the other. Cross-correlation



refers to the process when the two signals are different and an autocorrelation is when both signals are identical.

The cross-correlation of two continuous signals or functions  $r(t)$  and  $s(t)$  is given by the integral of the product of the two signals after one is shifted by  $\tau$ .

$$C_{rs}(\tau) = \int_{-\infty}^{\infty} r(t) s(t - \tau) dt \quad (2.1)$$

For complex signal Equation 2.1 becomes

$$C_{rs}(\tau) = \int_{-\infty}^{\infty} r^*(t) s(t - \tau) dt \quad (2.2)$$

where  $\tau$  is the time shift or lag between the signals and  $r^*(t)$  is the complex conjugate of the reference signal  $r(t)$ . It is important to note that a correlation between two signals is similar to a convolution between the signals where one signal is reversed in time. The cross-correlation of  $r(t)$  and  $s(t)$  is equivalent to the convolution of  $r(-t)$  and  $s(t)$ . This is the major concept behind the work in this thesis. If we can time-reverse one signal and perform a convolution, then a correlation between signals is achieved.

The time convolution theorem states that if the Fourier transform of  $r(t)$  is  $\mathcal{F}[r(t)] = R(\omega)$ , and the Fourier transform of  $s(t)$  is  $\mathcal{F}[s(t)] = S(\omega)$ , then  $\mathcal{F}[r(t)*s(t)] = R(\omega)S(\omega)$ . Following on from this expression, the Fourier transform of the cross-correlation between  $r(t)$  and  $s(t)$  is equal to  $R(\omega)S(-\omega)$ .

When a signal is correlated with itself, such an operation is called autocorrelation and is often used to find signals in the presence of noise and the measurement of optical spectra and pulse width of very narrow optical pulses. When two different signals are correlated the process is called cross correlation.

Figure 2.1 is a visual representation of the three processes of convolution, cross-correlation and autocorrelation.

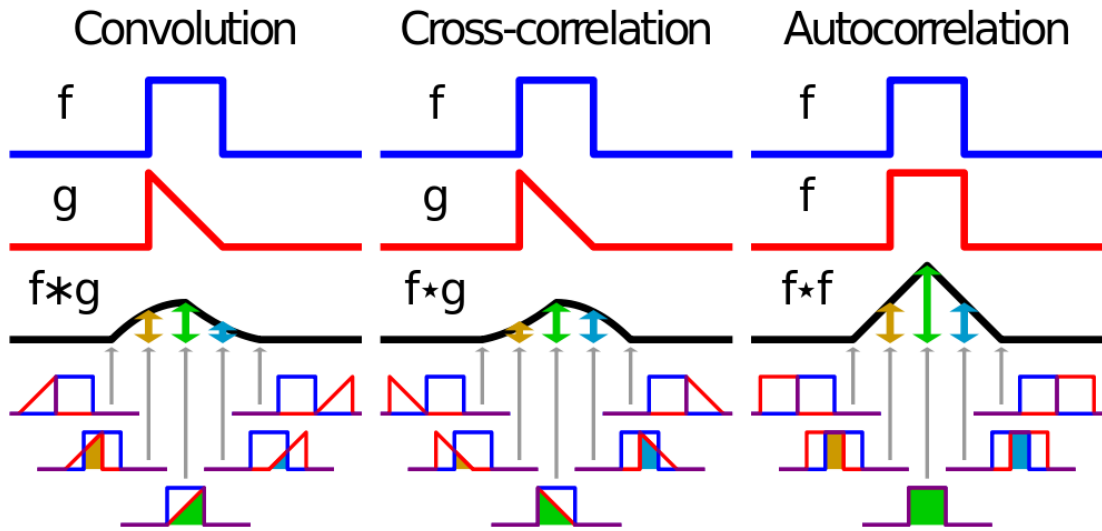


FIGURE 2.1 Visual representation of the convolution, cross-correlation and auto correlation processes [28].

A measure of similarity between a pair of discrete signals, such as digital data signals or sampled analogue signals,  $r[k]$  and  $s[k]$  is given by the cross-correlation  $c_{rs}[n]$  sequence:

$$c_{rs}(n) = \sum_k r[k]s[k - n] \quad (2.3)$$

where  $k$  is the time index and the lag index  $n = [-N/2, N/2 - 1]$  where  $N$  is the number of lags or time shifts between the signals and is typically a power of two. The lag term denotes a time-shift between the pair of signals with negative ( $n < 0$ ) and positive ( $n \geq 0$ ) lags being distinguished. For an analogue correlator the number of lags defines how many points or output values the correlation produces. In real life applications, where for example the correlation function is used together with a Fourier transform, the number of lags determines the resolution of the correlation function [33]. However, for a bit pattern correlator, each lag is equal to a bit period and the number of lags equals the number of bits in the bit pattern to be correlated.

One should note the incurred execution time or time complexity for wideband correlation. For a wideband signal, the time shift between correlation points needs to be small and hence the processing involves the computation of a larger number of samples and hence the processing duration increases [16].

### 2.2.2 TYPES OF CORRELATOR

As mentioned before, the number of lags defines the resolution capabilities of a correlator. The larger the number of lags and hence correlation points, the better a correlator can “tell” how similar two signals are (in the analogue domain) or can correlate longer bit patterns (in the digital domain). In this thesis, the number of wavelengths available to represent the template is the defining parameter for the number of bit in the reference bit pattern and hence the number of lags. A correlator that can work with a digital bit pattern or a stream of digitized samples  $s[n]$  from a continuous analogue signal  $s(t)$  can be implemented in two general ways:

- i) Electronics method
- ii) Photonics method

Since it is generally easier to produce a delay and multiplication using electronics, the use of electronics is generally considered as the more convenient way of implementing a correlator. However, it is limited by the bandwidth of the electronics. An electronic correlator can be implemented in either hardware or software. Normally, hardware correlators are designed and purpose-built for a specific application and are implemented using field-programmable gate arrays (FPGAs) which are reconfigurable devices that are more versatile than application-specific integrated circuits (ASICs) [34]. As an example, the Australia Telescope National Facility (ATNF) compact array uses a high speed hardware correlator to process signals from six antennas of the array. This is known as the Compact Array Broadband Backend (CABB) correlator [35]. The CABB correlator has a bandwidth of 2 GHz with either 32 x 64MHz channels or 2048 x 1MHz channels. Two other hardware correlators are the Australian Long Baseline Array S2 correlator and the Very Long Baseline Array correlator. These are compared in [34] .

As for software correlators, they are usually implemented as a set of libraries or computer programs to perform the designated task of correlation of a given set of signals and typically run in a multiprocessor environment. An example of a software correlator which has been developed in Japan by the National Institute of Information and Communications Technology (NICT) for use in very long

baseline interferometry (VLBI) is known as the K5 Software Correlator. The current version of this correlator known as K5/VSSP32 (Versatile Scientific Sampling Processor) has a maximum sampling rate of 64 MHz [36]. Deller et al. [34] discuss a software correlator known as DiFX (Distributed Fourier transform and multiplication) which has been developed at the Swinburne University of Technology for VLBI and which has now replaced the S2 hardware correlator at the ATNF. Software correlators used for VLBI are known for their flexibility and possible high spectral resolution along with broad bandwidth [34]. However, the promise of high resolution and broad bandwidth requires massive parallel computing systems and very high performance processors. Furthermore, software correlators are generally deemed unfit for real time data processing as this requires conversion and storage of data to process it [33]. As a result, despite very high speed processing, software correlators are not a solution for real time correlation. So, where real-time broadband processing is required, photonic approaches are becoming increasingly popular [2, 9, 23, 24, 37, 38].

For a real time ultrafast correlation scheme, an optical approach remains the only viable solution and a growing interest in photonic correlators for high frequency signals and image processing [2, 9] is unsurprising. The two possible ways for implementation of an optical correlator are:

- i) Correlation using bulk optics
- ii) Correlation using photonics based on optical fibre technology

#### 2.2.2.1 *Correlation using bulk optics*

The correlation of two signals may be obtained by utilizing the Fourier transforming properties of a lens. An early example of this type is described in [39]. It is commonly used in image processing, however in recent times it has also been used for image recognition [22, 40]. This type of correlator depends on spatial processing of a signal and often fails to give any temporal information of the correlation peak. Furthermore, this scheme is unsuitable for implementation as part of a signal-processing unit in a compact device. Therefore, the use of bulk optics is out of the scope of this thesis.

### 2.2.2.2 *Correlation using photonics*

In an attempt to increase the processing speed, an optical fibre digital correlator was proposed by Jackson and Jones in 1986 [41]. To implement the time delays, the correlator used an optical fibre tree as a splitter terminated by fibre delay lines with multiples of lag time  $T$ . The main disadvantage of this proposal is the rigidity in the channel delay times, which is strictly determined by the delays in the optical fibre tree. Therefore, it is not at all flexible and not easy to implement. It is also not suitable for signals with a small delay requirement. A combined system was proposed in [42] to cope with both short and long time scales but this still suffers from implementation complexity.

Another approach to implement a photonic correlator is to find the Fourier Transform (FT) of the received data and to multiply the FT with the complex conjugate of the FT of the matching replica of the transmitted signal [43]. However, this brute force correlation approach causes severe overhead on the latency of the system. The latency in processing a large data window of received signal is the most serious overhead for critical real time applications [44] in optoelectronic methods.

The use of a photonic system in signal processing applications can offer significant advantages over an equivalent electronic or mixed approach. Several photonic correlators have recently been proposed [9, 16, 24-27] to realize ultrafast broadband correlation, with viable practical applications in digital communications, detection and in image recognition. Based on the implementation technique, two recent approaches are categorized as being a:

- i) Joint transform correlator
- ii) Matched filter correlator

An overview of these two techniques is given in the next section.

## 2.3 PHOTONIC APPROACHES

Photonic processing based on the use of optical fibre technology benefits from properties such as large bandwidth, immunity to electromagnetic interference, tunability and programmability compared to electronic processing. Therefore, radio frequency photonic techniques can be utilized to enhance the performance of analogue radio frequency systems in the detection and filtering of ultra-broadband signals. Several photonic-based microwave correlator schemes have been suggested in recent years and in this thesis they are categorized in two categories based on the implementation principle. This section will briefly illustrate the two implementation principles.

### 2.3.1 JOINT TRANSFORM CORRELATORS

The joint transform correlation method is one of the most frequently applied methods in the field of photonic classification and identification. It is used to quantify the degree of similarity between multiple patterns. Optical joint transform correlators allow parallel processing. Figure 2.2 below shows a block diagram for a joint transform correlator [40].

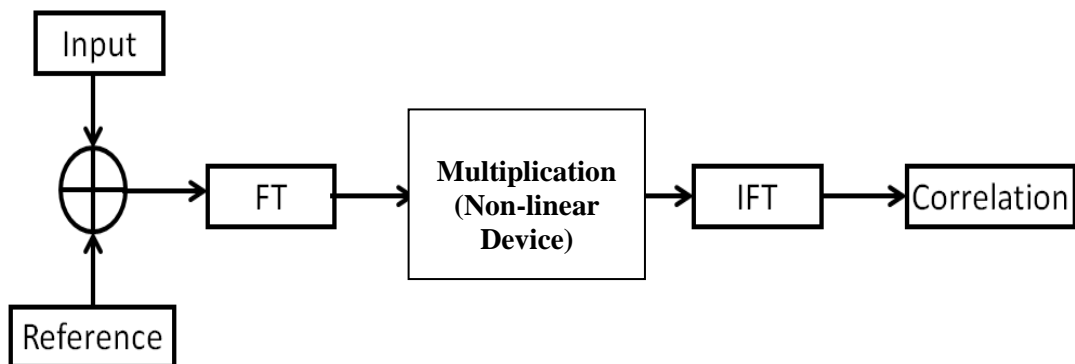


FIGURE 2.2 Block diagram of a joint transform correlator.

In this type of implementation both an input pattern and an optical reference pattern are added and then a Fourier transform is performed in a length of optical fibre to get a joint power spectrum [26].

The frequency domain components are multiplied using nonlinear devices and then an Inverse Fourier Transform is applied using negative dispersion. This type of correlator often suffers from very low correlation contrast [22]. Whilst it is a very well known technique for recognizing fixed images, for real time recognition of ultra-fast patterns it is not a popular implementation technique. For this sort of detection, a matched filtering based correlation technique is widely used. Implementation of this technique is discussed in the next section.

### 2.3.2 MATCHED FILTER CORRELATORS

Matched filter correlators are a better choice and are preferred over joint transform correlators because of their high sensitivity and a relatively enhanced contrast of the correlation peak with respect to joint transform correlators. Most of the recent photonic correlation schemes for compact applications use a matched filter type implementation [9, 24, 25, 27]. Figure 2.3 below illustrates the operational principle of this type of correlator.

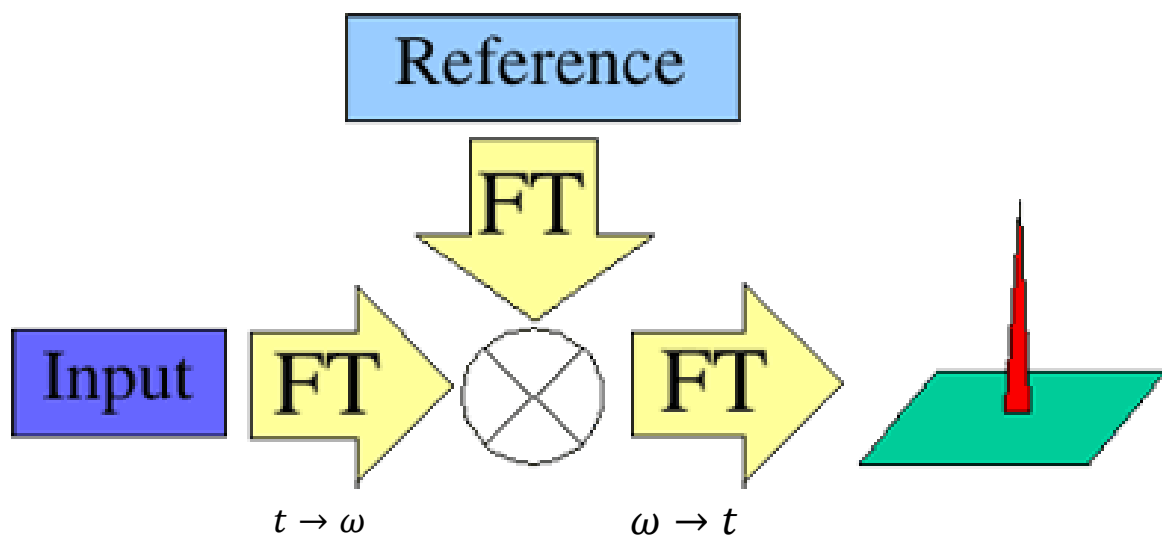


FIGURE 2.3 Functional block diagram of a matched filter correlator.

Unlike the joint transform based implementation, in this approach a separate Fourier transform is applied on both the input pattern and the reference pattern and these are then multiplied in the frequency domain, which is then Fourier transformed again to provide a correlation. The Fourier transform is achieved via a time to wavelength conversion using the wavelength dependent dispersion in a length of optical fibre to obtain a frequency (wavelength) to time mapping. Since this thesis investigates a matched filter based correlation technique, this is discussed more elaborately in the following sub sections.

State-of-the-art photonic correlation techniques which are based on a matched filter approach are:

- i) Time spectral convolution based correlation
- ii) Optical time domain correlation

Based on current research directions, these approaches are discussed only for the case of digital signals in the sections below:

### 2.3.2.1 Time spectral convolution based correlation

Recently, [24, 25] reported a new photonic implementation technique for a matched filter correlator based on time spectral convolution as illustrated in Figure 2.4.

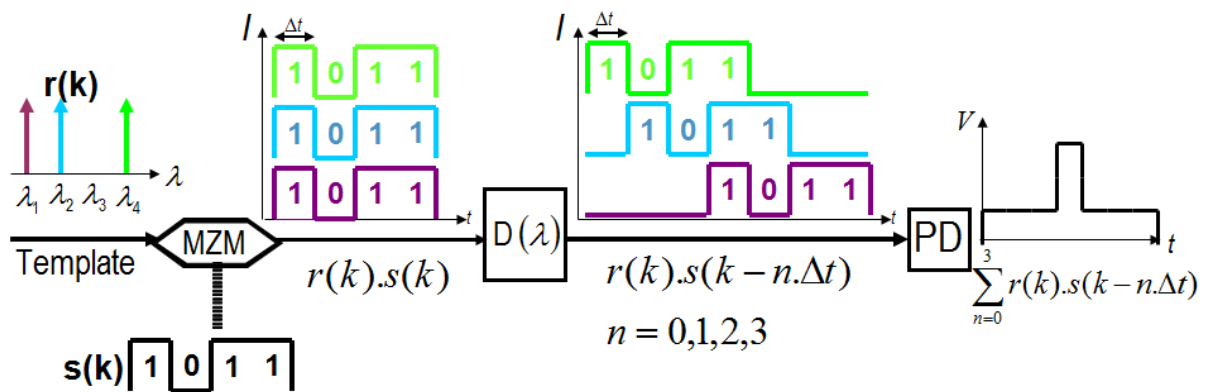


FIGURE 2.4 Functional diagram of a time spectral convolution based correlator [24].



In this approach, an electrical input bit pattern  $s(k)$  is modulated on to (multiplied by) a number of optical wavelengths which represent the 1's and 0's of a time inverted version of the template or reference bit pattern  $r(k)$ , by their presence and absence and which have a defined wavelength spacing. The multiplication is done using a Mach-Zehnder modulator (MZM) and gives an output  $r(k).s(k)$ . The modulated optical wavelengths then face a wavelength dependent delay, which is carefully engineered so that each wavelength faces a delay based on its bit position in the bit pattern. The delay is achieved using the wavelength dependent dispersion in a length of fibre which inherently performs a frequency to time mapping (and reversely, a time to frequency mapping) and hence implements a Fourier transform. The output of the delay network is given by  $r(k).s(k-n\Delta t)$  where  $n.\Delta t$  represents the delay of each wavelength relative to that of the first wavelength ( $n=0$ ) which represents the first bit of the input bit pattern. The multiplied and delayed signals are then integrated (summed up for bits) using a photodetector to realize the entire correlation function as in the equation below.

$$\sum_{n=0}^{N-1} r(k).s(k - n. \Delta t) \quad (2.3)$$

where N is number of bits in the reference bit pattern.

### 2.3.2.2 *Optical time domain correlation*

Serialized time encoded amplified microscopy (STEAM) is a recent invention that can perform ultrafast image acquisition [24]. It operates by firstly slicing a broadband optical source (short optical pulses in the time domain) to represent an input bit pattern in the frequency (wavelength) domain. The spectrally encoded data is then converted to serialized time domain data by passing the signal through a dispersive single mode fibre. STEAM produces a huge amount of data due to its very high speed capturing capability but this huge amount of data cannot be compared in real time due to the limitations of electronics. The common practice is to store the bulk data and then to analyze them in digital domain using high speed computer program. However, in this approach too, it requires huge storage ability to store all the data out of STEAM. It is necessary to get the STEAM data sorted in real

time and store only the required data to storage to increase efficiency. In order to reduce the amount of data that needs to be processed in computer, pattern recognition techniques which are compatible with STEAM are required to eliminate undesired data and obtain the desired information. Thus, there is a need for all optical pattern recognition techniques, which are also compatible with STEAM, to obtain only the desired information.

An ultra-fast pattern recognition technique which was recently reported [24] and which is compatible with a STEAM output signal uses an optical time domain correlation scheme as illustrated in Figure 2.5.

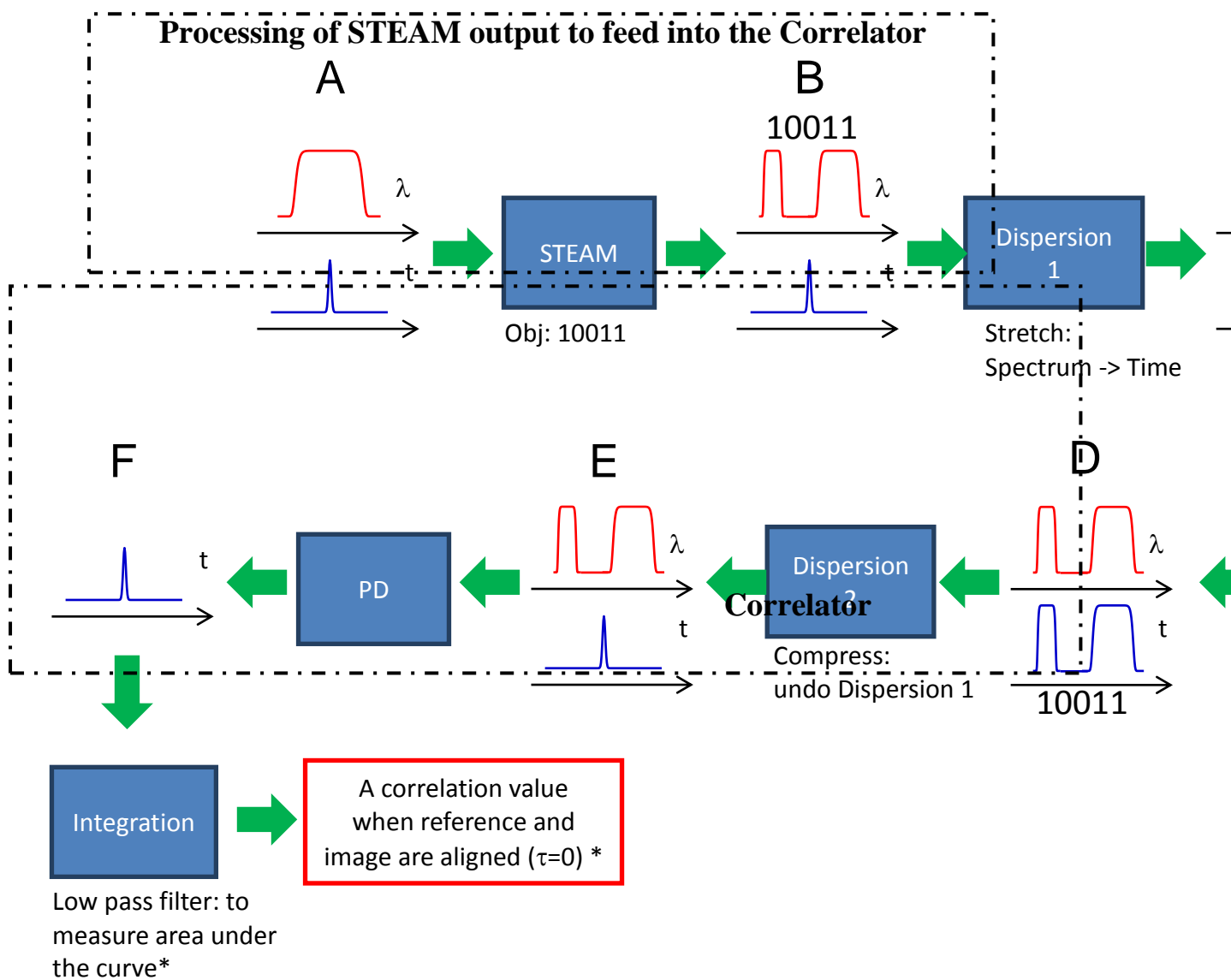


FIGURE 2.5 Functional diagram of optical time domain correlation [27].

Here a broadband optical signal (A) is sliced up to represent the input bit pattern in the frequency domain (B). Then this sliced-up optical signal passes through a dispersive medium to generate a frequency to time mapping (Fourier transform) (C). The signal is stretched in the time domain and looks similar to the wavelength representation with some distortion. The time domain signal is then multiplied with a reference bit pattern in the time domain (D) using a Mach-Zehnder modulator and then negative dispersion is applied (E) to compress the signal in the time domain and the result is integrated to get the final correlation peak (F).

## **2.4 CONCLUSION**

This chapter has presented an overview of correlators. An explanation of the correlation process and general equations for both the correlation and the related convolution process have been given. Examples of electronic correlators, both purpose built hardware correlators and software correlators, were presented and their advantages and disadvantages discussed. For real time, high bandwidth correlation or photonic correlation has distinct advantages. The major types of photonic correlators, joint transform and matched filter, were then discussed. Some recent examples of these were presented. The matched filter type correlator can be further divided into a time spectral convolution based correlator and an optical time domain correlator. This thesis investigates matched filter type correlators implemented using nonlinear four wave mixing (FWM) in highly nonlinear optical fibre. The next chapter will introduce the FWM process.

## 3. FOUR WAVE MIXING

### 3.1 INTRODUCTION

The photonic correlators investigated in this thesis use four wave mixing (FWM) in highly nonlinear optical fibre as a key processing technique. For this reason, this chapter discusses the basics and principles of FWM.

Four-wave mixing is a nonlinear effect arising from a third-order optical nonlinearity, as is described by a  $\chi^{(3)}$  coefficient. The concept of three electromagnetic fields interacting to produce a fourth field is central to the description of all four-wave mixing processes. It is a nonlinear phenomenon which allows optical wavelength conversion. It can occur if at least two different frequency components propagate together in a nonlinear medium such as a highly nonlinear optical fibre (HNLF) or a semiconductor optical amplifier (SOA). In the area of signal processing, optical four wave mixing has been used to perform frequency conversion [45], spatial information processing [26] and frequency measurement [8].

### 3.2 PROPERTIES OF FWM

There are two categories of nonlinear effects in optical fibre. The first category happens because of the interaction of light waves with phonons (molecular vibrations) in the silica medium of an optical fibre. The two main effects in this category are stimulated Brillouin scattering (SBS) and stimulated Raman scattering (SRS).

The second category of nonlinear effects is caused by a nonlinear polarisation of the dielectric medium. The most important nonlinear effects in this category are self-phase modulation (SPM), cross-phase modulation (XPM) and four-wave mixing (FWM).

Physically, we may understand this second process by considering the individual interactions of the optical fields within a dielectric medium. The first input field causes an oscillating polarization in the dielectric, which re-radiates with some phase shift determined by the damping of the individual dipoles. The application of a second optical field will also drive the polarization of the dielectric, and the interference between the two waves will cause intermodulation products in the polarization at the sum and difference frequencies. Now, the application of a third field will also drive the polarization, and this will beat with both the other input fields as well as the sum and difference frequencies. This beating with the sum and difference frequencies is what gives rise to the fourth field in four-wave mixing. Since each of the beat frequencies produced can also act as a new source of optical fields, a large number of interactions and fields may be produced from this basic process [46].

The origin of the FWM process lies in the nonlinear response of bound electrons of a material to an applied optical field. To understand the FWM effect, let us consider a WDM signal, which is a sum of ‘n’ monochromatic plane waves. Following the approach described in [46], we can consider the total electric field of a signal as a summation of ‘n’ plane waves as in Equation 3.1;

$$E = \sum_{p=1}^n E_p \cos(\omega_p t - k_p z) \quad (3.1)$$

where  $E_p$  is the amplitude,  $\omega_p$  is the frequency and  $k_p$  is the propagation constant of the optical fields. The nonlinear polarization is given by

$$P_{nl} = \epsilon_0 \mathcal{X}^{(3)} E^3 \quad (3.2)$$

As in [46], by considering the total electric field as that expressed by Equation 3.1, Equation 3.2 becomes,

$$P_{nl} = \epsilon_0 \mathcal{X}^{(3)} \sum_{p=1}^n \sum_{q=1}^n \sum_{r=1}^n E_p \cos(\omega_p t - k_p z) E_q \cos(\omega_q t - k_q z) E_r \cos(\omega_r t - k_r z) \quad (3.3)$$

By expansion of Equation 3.3 we get,

$$P_{nl} = \frac{3}{4} \epsilon_0 \mathcal{X}^{(3)} \sum_{p=1}^n \left( E_p^2 + 2 \sum_{q \neq p} E_p E_q \right) E_p \cos(\omega_p t - k_p z)$$

$$\begin{aligned}
& + \frac{1}{4} \varepsilon_0 \mathcal{X}^{(3)} \sum_{p=1}^n E_p^3 \cos(3\omega_p t - 3k_p z) \\
& + \frac{3}{4} \varepsilon_0 \mathcal{X}^{(3)} \sum_{p=1}^n \sum_{q \neq p} E_p^2 E_q \cos\{(2\omega_p - \omega_q)t - (2k_p - k_q)z\} \\
& + \frac{3}{4} \varepsilon_0 \mathcal{X}^{(3)} \sum_{p=1}^n \sum_{q \neq 1} E_p^2 E_q \cos\{(2\omega_p + \omega_q)t - (2k_p + k_q)z\} \\
& + \frac{6}{4} \varepsilon_0 \mathcal{X}^{(3)} \sum_{p=1}^n \sum_{q > p} \sum_{r > q} E_p E_q E_r \left\{ \begin{array}{l} \cos((\omega_p + \omega_q + \omega_r)t - (k_p + k_q + k_r)z) + \\ \cos((\omega_p + \omega_q - \omega_r)t - (k_p + k_q - k_r)z) + \\ \cos((\omega_p - \omega_q + \omega_r)t - (k_p - k_q + k_r)z) + \\ \cos((\omega_p - \omega_q - \omega_r)t - (k_p - k_q - k_r)z) \end{array} \right\} \quad (3.4)
\end{aligned}$$

The first term in Equation 3.4 includes intensity dependent refractive index terms which represent the effect of SPM and XPM. The second, third and fourth terms can be neglected because of a phase mismatch which evolves between the optical fields as they propagate along the fibre. The reason behind this phase mismatch is that in an optical fibre the propagation constant is frequency dependent so that  $k(3\omega) \neq 3k(\omega)$ . When there is a varying phase mismatch between the propagating waves the coupling of energy between waves with distance averages to zero. The phase mismatch can also be understood as the mismatch in phase between different signals travelling within the fibre at different group velocities. These terms can be neglected because they contribute little effect. The last term in Equation 3.4 represents the phenomenon of four-wave mixing [47]. If the wavelengths in the WDM system are closely spaced so that the relative fibre dispersion is small, or they are located near the zero dispersion wavelength of the fibre, then the propagation constants of the wavelength channels are nearly constant and the phase-matching condition is nearly satisfied. When this is so, the power generated at these sum and difference frequencies can be quite significant [48].

FWM is often used for wavelength conversion in photonic signal processing applications. Among the various nonlinear phenomena exploited for fibre-based wavelength conversion, FWM is regarded

as advantageous due to its transparency both in terms of modulation format and bit rate [34, 49]. FWM-based wavelength converter have been demonstrated in a range of optical fibres including W-type soft glass fibre [50], highly nonlinear photonic crystal fibre [51] and highly nonlinear holey fibre [52]. Figure 3.1 shows a schematic of FWM based wavelength conversion.

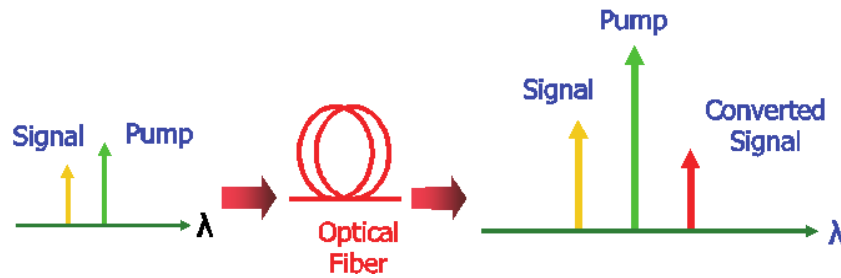


FIGURE 3.1 Wavelength conversion using four wave mixing [48].

In basic terms, FWM is the mixing of three wavelengths to produce a fourth wavelength such that  $\omega_4 = \omega_1 + \omega_2 - \omega_3$ . Note that for the special case when  $\omega_1 = \omega_2$ , two frequencies can produce a third such that  $\omega_4 = 2\omega_1 - \omega_3$ . Commonly, a high power pump laser at  $\omega_p$  can be used to convert a signal frequency  $\omega_s$  to a new frequency at  $2\omega_p - \omega_s$ , which is often known as the idler frequency,  $\omega_i$ . In terms of wavelength,  $\lambda_i \approx 2\lambda_p - \lambda_s$ . Similarly, an idler can be produced at  $2\lambda_s - \lambda_p$ . According to the finding in Mishra et al, the table below is a comparison of different third order nonlinear phenomena.

Nonlinear Phenomenon's	SPM	XPM	FWM
Bit rate	Dependent	Dependent	Independent
Origin	Nonlinear susceptibility	Nonlinear susceptibility	Nonlinear susceptibility
Effects	Phase shift	Phase shift	New waves generated
Shape of broadening	Symmetric	Symmetric or asymmetric	No effect
Channel spacing	No effect	Dependent.	Dependent.

Table: 3.1 Performance comparison of SPM, XPM and FWM [34]

It is evident from the above finding that for ultrafast bit rate processing, FWM is the superior among the different third order nonlinearities. Figure 3.2 below depicts the generation of two idler wavelengths of equal power due to FWM of two equal power wavelengths in a length of HNLF using a *VPITransmissionMaker* simulation.

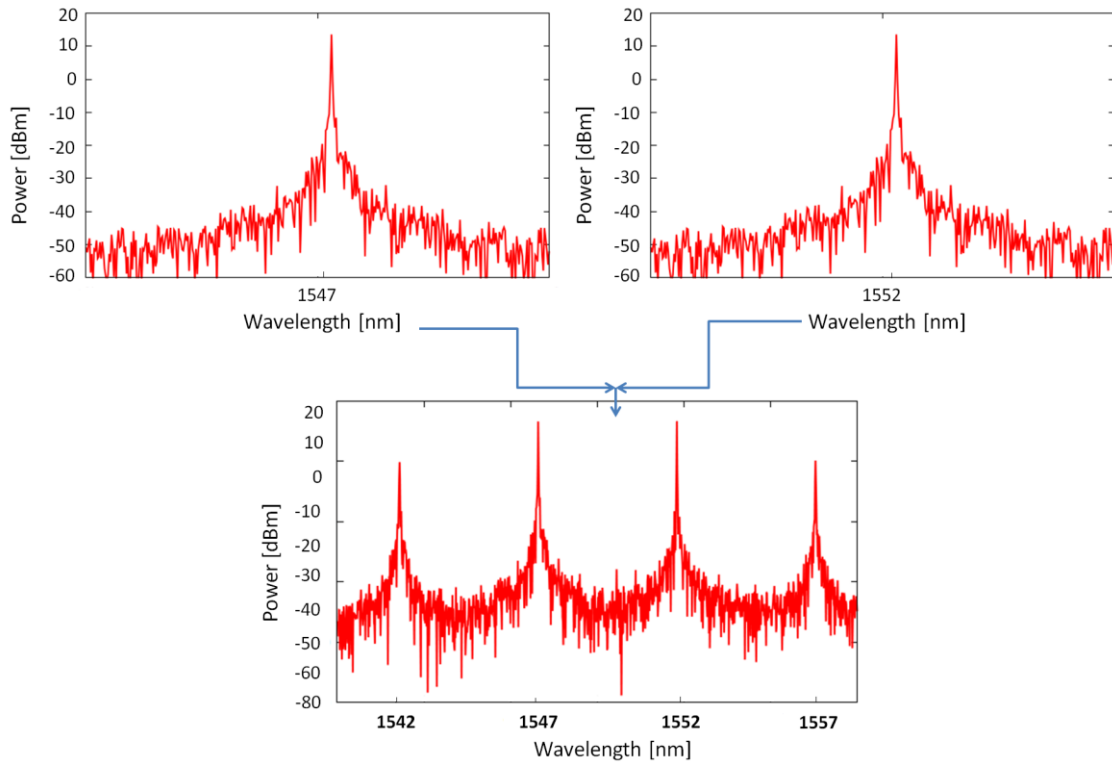


**FIGURE 3.2** Illustration of the FWM process in a HNLF.

### 3.3 FWM EFFICIENCY

As discussed above, FWM requires phase matching of the propagating waves. This requires small chromatic dispersion in the fibre and/or small wavelength spacing between the propagating waves. FWM mixing efficiency scales inversely with wavelength or channel spacing when the fibre dispersion is non-zero. The wavelength spacing must decrease as the fibre dispersion increases in order to maintain a given mixing efficiency. Figure 3.3 is a plot of calculated FWM mixing efficiency



as a function of channel spacing for various values of fibre dispersion [53]. It can be proven in theory and is evident in Figure 3.3 that the smaller the dispersion or the smaller the wavelength spacing, the larger the FWM mixing efficiency.

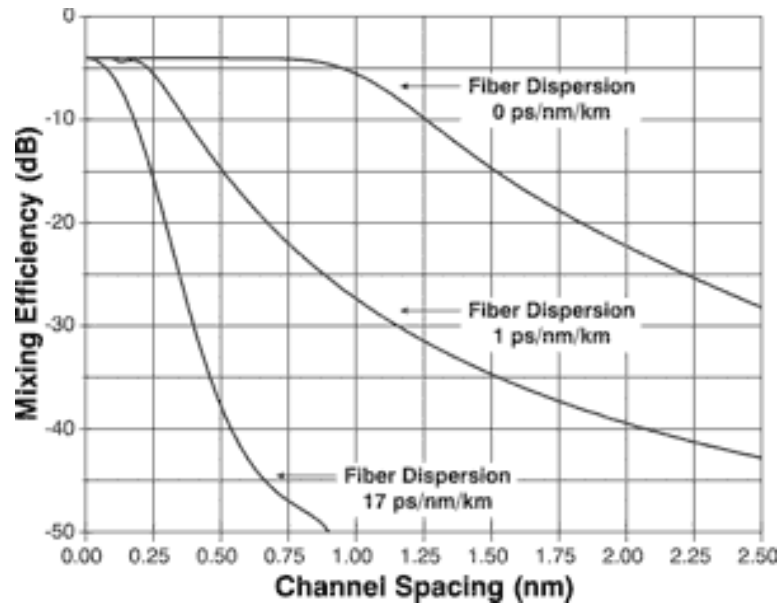


FIGURE 3.3 Variation in mixing efficiency with wavelength spacing [53].

### 3.4 CONCLUSION

In this chapter, the nonlinear four wave mixing effect is discussed and analyzed. An analytical expression for FWM is presented and explained and the use of FWM for wavelength conversion is presented. The next chapter will discuss the implementation of a novel optical correlator exploiting the FWM effect in a length of highly nonlinear optical fibre.

## 4. PHOTONIC CORRELATION USING FOUR WAVE MIXING

### 4.1 INTRODUCTION

In Chapter 2, the need for correlation and various types of existing correlation schemes were discussed and explained. The principle of FWM is covered in Chapter 3. This chapter discusses the development of a novel photonic correlation technique using FWM in a length of Highly Nonlinear Fibre (HNLF). This correlation technique has been experimentally demonstrated. FWM has been used to mix wavelength channels with a pump wavelength which has been modulated by an input bit stream in order to produce copies of the input signal at the output idler wavelengths [29]. These idler wavelengths are differentially delayed and summed at a photoreceiver to produce the required correlation function.

This chapter describes the experimental process and the results of this novel nonlinear mixing based technique to achieve bit pattern correlation.

### 4.2 TIME-SPECTRAL CONVOLUTION

A microwave photonics based approach to realize ultrafast correlation is becoming popular considering the potential very broad bandwidth of photonic technologies. In recent years, numerous research groups have worked in this particular area and an overview of the approaches implemented by them was discussed in Chapter 2. Here a more detailed background review will be given for the key principle utilized in this research.

The concept of obtaining a correlation from a time-spectral convolution was first proposed by Park and Azana in [24]. The convolution process is defined by the equation 4.1.

$$r(\tau) * s(\tau) = \int_{-\infty}^{\infty} r(\tau)s(\tau - t)dt \quad (4.1)$$

Recalling Equation 2.1 for correlation given in Chapter 2, it is observed that the only difference between convolution and correlation is that one of the signals needs to be time inverted in the correlation process. So, a time spectrum convolution technique can be used efficiently to get a correlation function when one signal is a time-inverted copy of the original signal. For correlation of bit patterns, the discrete form of the correlation function is more appropriate. Below is the equation which was presented as Equation 2.4 to represent correlation for discrete signals.

$$c_{rs}(n) = \sum_k r[k]s[k - n] \quad (2.4)$$

In selecting the time inverted signal, the template is chosen to be time inverted rather than the input signal pattern as it is obviously advantageous to handle the reference pattern than the unknown signal pattern. Hence, the reference pattern is made to represent a time-inverted copy of the original expected pattern. For example if 1011 is the expected or desired matched pattern then the reference needs to be set as 1101. Figure 4.1 below illustrates the operating principle of the time-spectral convolution based correlation technique in [24].

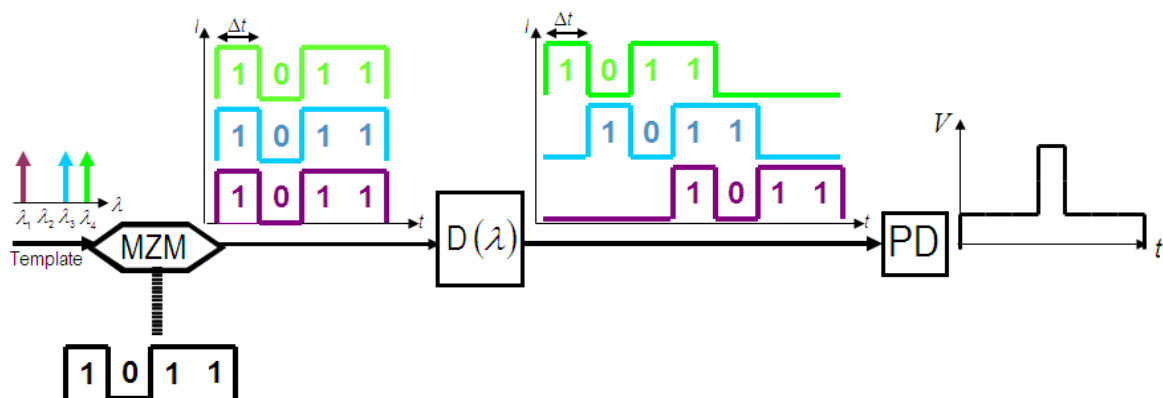


FIGURE 4.1 Illustration of the working principle of the time-spectral convolution based correlation scheme demonstrated in [24].

The correlation system in [24] used a reference bit pattern encoded on to discrete optical wavelengths. In particular, the reference bit pattern is inverted in time and '1's and '0's are represented by the presence and absence of optical wavelengths respectively. The pattern 1101 is represented by  $\lambda_4$ ,  $\lambda_3$  and  $\lambda_1$ . These wavelengths are combined and modulated by the input bit pattern

using a Mach-Zehnder Modulator (MZM). The wavelengths are then differentially delayed using the dispersion in 64 km of single-mode fibre (SMF) to provide time delays equal to multiples of a bit period at a bit rate of 2.4 Gbps. The wavelengths and the dispersion are selected such that after the dispersive delay, the wavelength channels separate in time according to the bit position that they represent. The wavelengths are then combined and the summed optical power is measured using a high frequency photodetector. This produces the desired correlation function of the binary input signal and the encoded reference bit pattern.

A disadvantage with this technique is that all the photonic processing is done near the source of the input bit pattern whereas in a practical system it may be desirable to isolate the signal processing from the source of the input signal.

### **4.3 PROPOSED METHOD**

The correlation method proposed here is also based on the basic principle of the time-spectrum convolution technique. In this new system, the bit pattern on one wavelength is copied on to several other wavelengths using wavelength conversion; in particular, FWM wavelength conversion is used. The proposed method is shown in Figure 4.2. A pump wavelength is first modulated by the unknown input bit stream. This part of the system is called the transmitter (TX) and can be done at a remote location. The modulated pump is then sent to the receiver (RX) where it is mixed with a number of CW wavelength channels in a length of HNLF. FWM in the HNLF creates numerous idler wavelengths, each with a copy of the input bit stream. The reference bit pattern or template is represented by the idler wavelengths which are created during the FWM process. These are determined by the choice of the CW wavelength channels which are mixed with the pump wavelength. The idler wavelengths are filtered and differentially delayed with delays corresponding to multiples of a bit period and then summed at a photoreceiver to provide the correlation function.

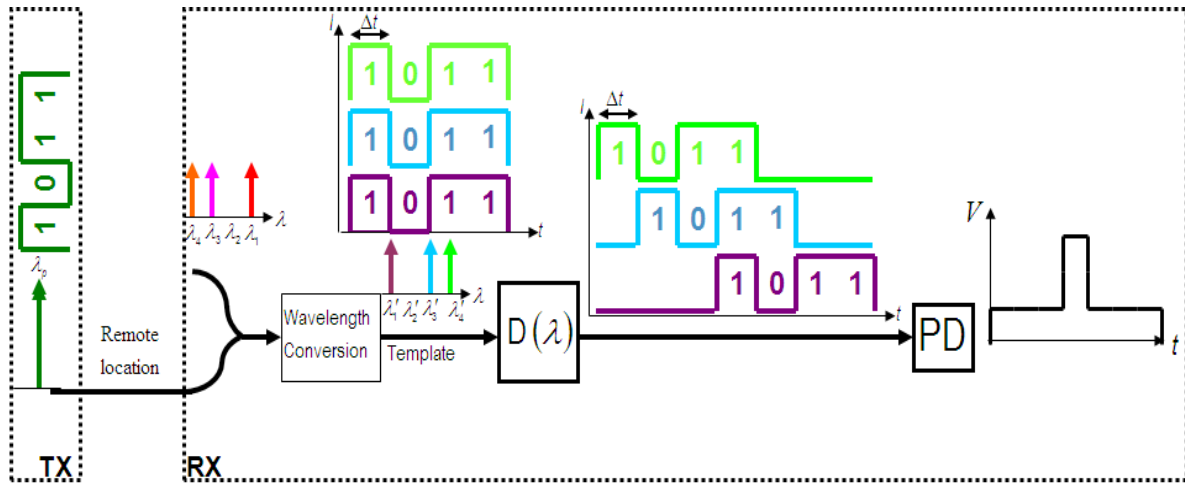


FIGURE 4.2 Illustration of the working principle of the proposed HNLf based correlation scheme.

An advantage of this system is that the pump wavelength can be modulated with the signal and transmitted from a remote location to the receiver for correlation with the reference bit pattern. The input to the correlation or signal processing unit is an optical waveform rather than an electrical waveform.

#### 4.4 EXPERIMENTAL SET-UP

The experimental set-up for the proposed system is shown in Figure 4.3. As discussed before, the proposed system consists of two parts.

1. A transmitter, where a pump wavelength is modulated by the input bit stream.
2. A receiver to process the transmitted signal and provide an output correlation function.

The transmitter (TX) contains a high power pump laser, Mach-Zehnder modulator (MZM) and a signal pattern generator. The pump wavelength is modulated by the input bit stream using the MZM and is then transmitted to the receiver (RX) where it is mixed with a number of CW wavelength channels. The receiver consists of all the signal processing components including the CW laser

diodes, the HNLF, the optical amplifiers, optical filters, wavelength delay network and photoreceiver. A description of the components used and the operation of the system follows.

#### 4.4.1 TRANSMITTER

At the transmitter, the pump wavelength ( $\lambda_5$  in Figure 4.3) is modulated by the input bit pattern using a MZM. Selection of the pump wavelength is very critical. It depends on available laser sources and on the filter response of the low pass optical filter which is used to separate the required idler wavelengths from the high power pump and other unwanted wavelengths. The laser diode used for the pump is one from an 8-channel laser diode array manufactured by Newport. The pump wavelength was carefully selected to be 1546.95 nm as at this wavelength the low pass optical filter has very high attenuation (46 dB). The filter passes all wavelengths below 1545 nm with an insignificant loss of less than 0.3 dB. It is important to have much more attenuation for the pump wavelength at the receiver as ultimately after wavelength conversion only the idler wavelengths of interest are to be passed by the receiver filter.

The input bit pattern originates from a programmable pattern generator. This was an HP3760A data generator, shown in Figure 4.4. Unfortunately, this is an old model which has a maximum data rate of only 150 Mb/s. To demonstrate the proposed system, the input bit pattern was chosen to be a 4 bit long binary word of 1011 with a bit duration of  $T=10$  ns (bit rate = 100 Mbps). The amplitude of the 1's from the data generator was set to be 0.8V to drive the MZM. The MZM used was a lithium niobate device fabricated at RMIT University. The  $V_\pi$  of the modulator was 5.7volts. The MZM was biased carefully to maximize the difference between the '1' and '0' levels measured at the photoreceiver output.

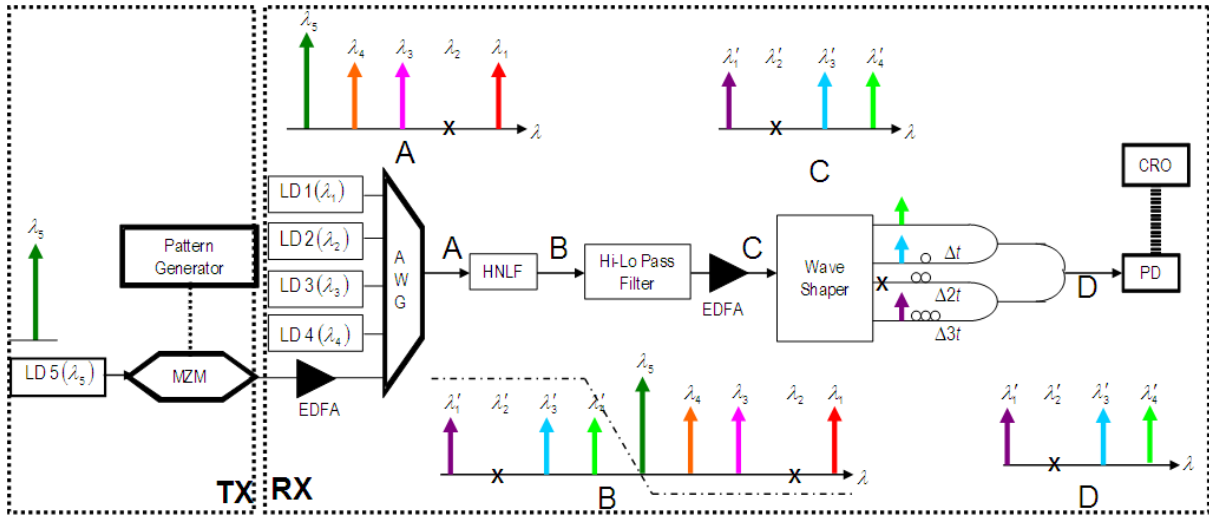


FIGURE 4.3 Experimental set-up for the proposed HNLf based correlation scheme.

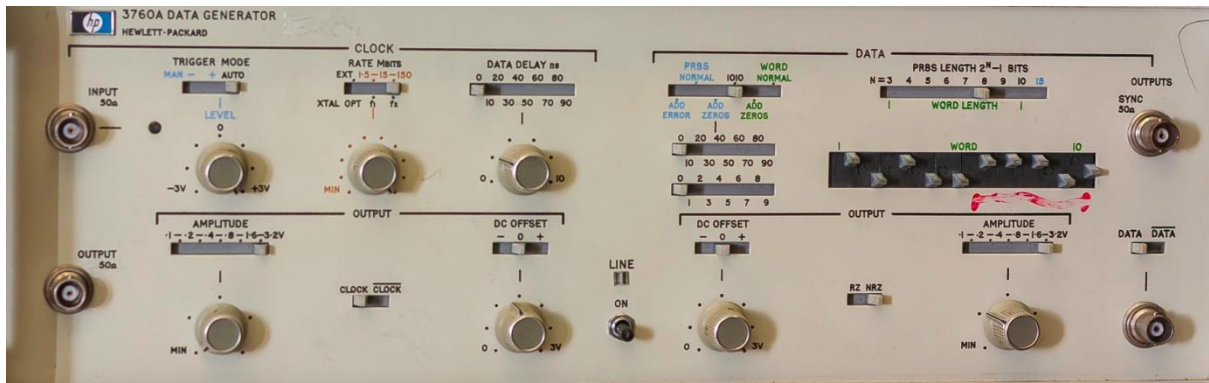


FIGURE 4.4 HP 3760A data generator used in the experiment.

#### 4.4.2 RECEIVER

At the receiver, four CW lasers with wavelengths  $\lambda_1 - \lambda_4$  are used to represent the number of bits in the pattern. The modulated pump wavelength is amplified by an EDFA to ensure that it has high power for efficient FWM and then it is combined with the CW wavelength channels an AWG before passing to the HNLf. The key steps to setting up the receiver are:

- i. Selecting the CW laser wavelengths
- ii. Combining the CW laser wavelengths with the pump wavelength.
- iii. Mixing the combined wavelengths in a length of HNLF.
- iv. Separation of the required idler wavelengths.
- v. Applying wavelength dependent delays to the idler wavelengths.
- vi. Measure the output correlation function after the photoreceiver.

To ensure that the pump and CW laser wavelengths are polarized in the same direction to maximize the FWM in the HNLF, all the equipment used in the experiment is polarization maintaining (PM) equipment. This includes the fibres, couplers and amplifiers.

#### *4.4.2.1 Selection of the CW Laser Wavelengths*

The template is selected following exactly the same procedure as in [24] in which a reference bit pattern is encoded on to discrete optical wavelengths. In particular, the reference bit pattern is inverted in time and ‘1’s and ‘0’s are represented by the presence and absence of optical wavelengths respectively. As mentioned before, the input bit pattern for this experiment was chosen to be 1011, so the reference bit pattern or template would be 1101, which is a time-inverted version of 1011. However, the selection of wavelengths to represent the ‘1’s in a template was much more challenging than anticipated. First, the range of available wavelengths in the laboratory was limited. An 8-channel laser array with modular controller manufactured by Newport was available with wavelength spacing of approximately 1.6nm from 1542.3nm to 1553.5nm (Figure 4.5). Each of the lasers emits a fixed wavelength with a maximum output power of +17 dBm (50mW). A high power (+15 dBm) tunable laser was also available.

From the discussion on FWM in Chapter 3, it is clear that the selection of wavelengths is critical for efficient FWM. The efficiency of the FWM conversion process is closely related to both



the power and the separation of the wavelengths in the mixing process [45, 54]. For successful operation of the proposed system, the most critical part is the power level of furthest idler, which is generated as a mixing product of the pump and the furthest wavelength channel from the pump. Due to the wider separation between them, the efficiency of the FWM is smaller and the power at that idler is smaller than at the other idlers. For the experimental system, a critical requirement was that the pump power has to be around 6 dB higher than the furthest channel wavelength power to ensure efficient idler generation. FWM between the LD wavelengths could cause interfering cross-products on a desired idler wavelength. Assuming an undesired cross-product has a power level which is 20dB less than the desired idler to be deemed insignificant, the pump needs to be about 10dB larger than the LD powers.

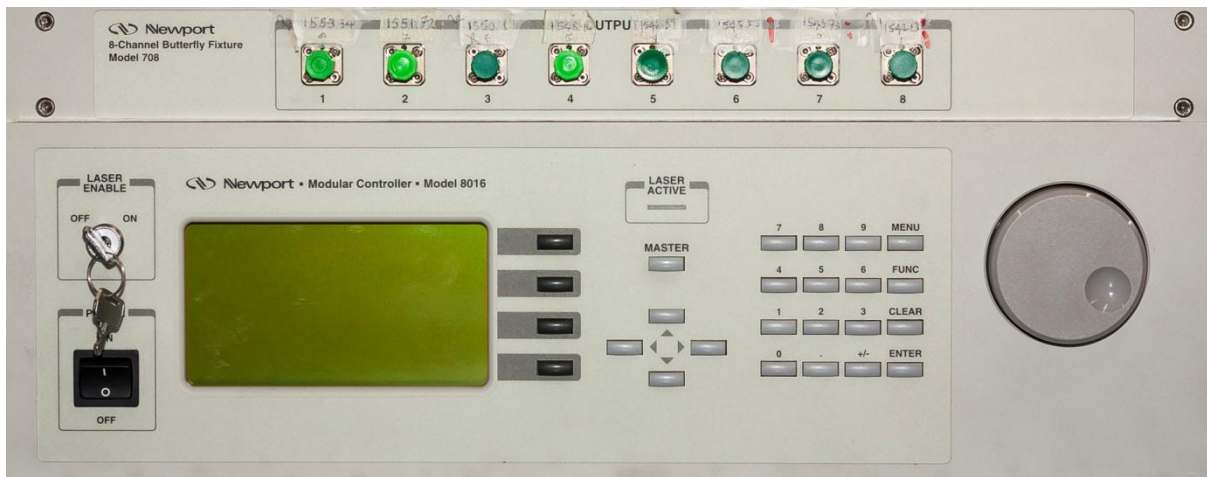


**FIGURE 4.5** Newport 8-channel laser array with modular controller.

Following above discussion on selection criteria, the wavelengths of the four CW channels were selected to be 1549.41 nm ( $\lambda_4$ ), 1550.2 nm ( $\lambda_3$ ), 1551.84 nm ( $\lambda_2$ ) and 1553.63 nm ( $\lambda_1$ ) and the modulated pump wavelength ( $\lambda_5$ ) is at 1546.95 nm. Wavelengths  $\lambda_1$ ,  $\lambda_2$ ,  $\lambda_3$  and  $\lambda_5$  are emitted from the Newport laser array whilst  $\lambda_4$  comes from the tunable laser. A particular template is set by turning required lasers on or off. For this experiment, 1101 is the template (which means a matched bit pattern is 1011). To set this template,  $\lambda_2$  is turned off to represent '0' while  $\lambda_4$ ,  $\lambda_3$  and  $\lambda_1$  are turned on to represent the three '1's in 1101.

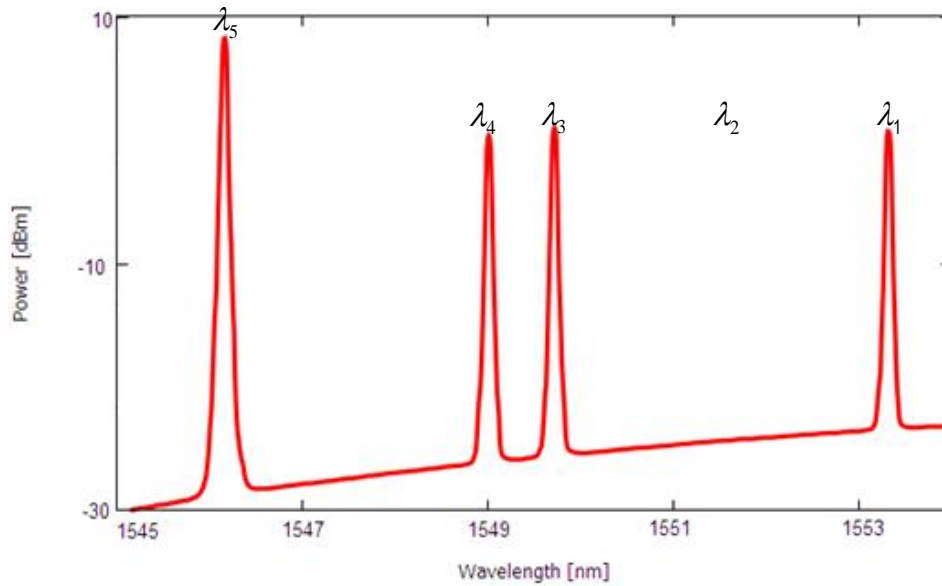


**FIGURE 4.6** Measured channel wavelengths representing 1101 combined with the pump wavelength  $\lambda_5$  at the input of the HNLF.

Figure 4.6 shows the laser wavelengths used in this experiment measured at the input of the HNLF (Figure 4.3 [A]). They were measured using an Anritsu MS9710C optical spectrum analyzer (OSA). The optical power of  $\lambda_4$ ,  $\lambda_3$  and  $\lambda_1$  is +1 dBm and the power of the modulated pump wavelength is +8 dBm.

The CW laser or channel wavelengths are combined with the pump wavelength using an Arrayed Waveguide Grating (AWG). The AWG is a software controlled filtering device with 8 input ports and 1 output port (or vice versa) manufactured by ANDevices. The input ports of the AWG pass certain wavelength channels. The centre wavelength of each channel is changeable by varying the AWG temperature which is controlled by a software controlled internal heater circuitry. The AWG channels were adjusted to have centre wavelengths which match the CW channel and pump laser wavelengths. Implementing a trial and error method, it was found that with an internal temperature of 72.2° C, the centre wavelengths of the AWG channels matched the laser wavelengths. Figure 4.7 below displays the device actually used in the experiment and Figure 4.8 shows the measured AWG

response to a broadband noise emitted from an EDFA. The response was measured using an Anritsu MS9710C optical spectrum analyzer.



FIGURE 4.7 The 8-Channel AWG used in the experiment.

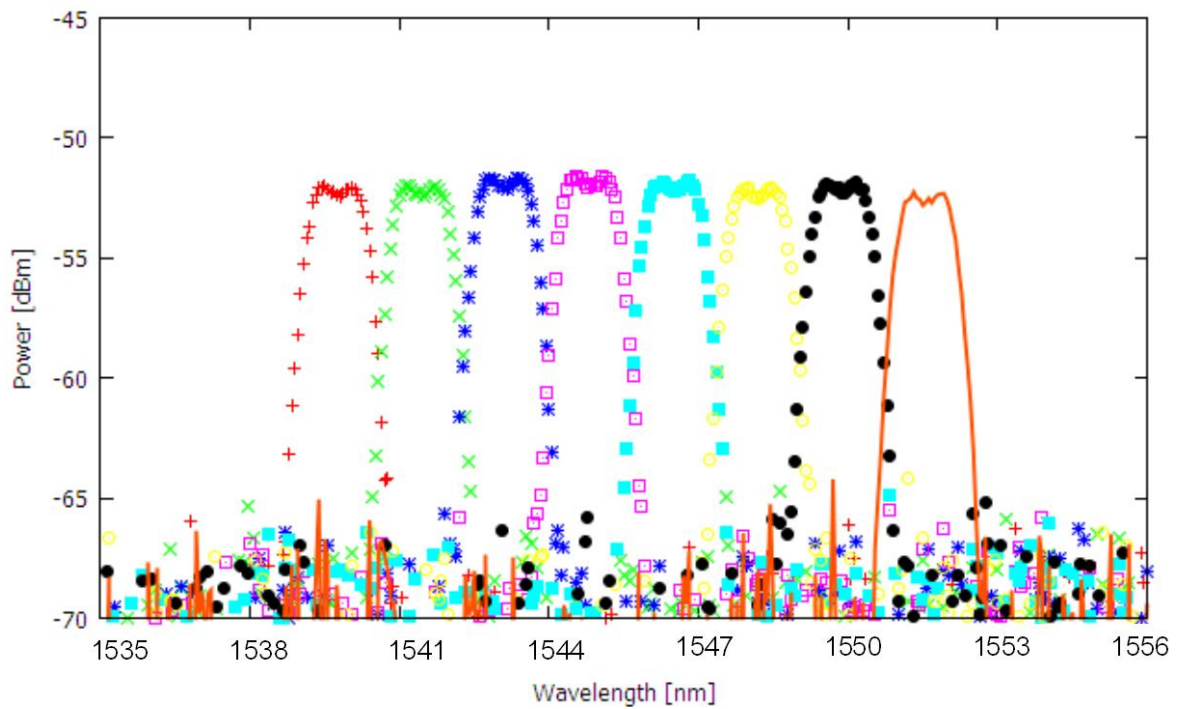


FIGURE 4.8 Measured AWG response with the internal heater circuitry set at 72.2° C.

All the centre wavelengths of the AWG channels visible in Figure 4.8 align with the emitted wavelengths of the laser array. Approximately 6 dB of insertion loss was observed for each of the optical wavelengths in the AWG channels.

To keep the modulated pump power a lot higher than the CW wavelengths, the pump wavelength was amplified using an EDFA which is shown in Figure 4.9. The EDFA is a high power EDFA with a 1W pump laser manufactured by PriTel. The EDFA was not run with maximum output power however precautions were taken not to burn the fibres and the EDFA connecting ports. As visible in Figure 4.6, at the input of the HNLF, the pump power is around 7 dB higher than the other wavelengths for this experiment with a power of +8 dBm, where the selected wavelength channels have a power of +1 dBm each.

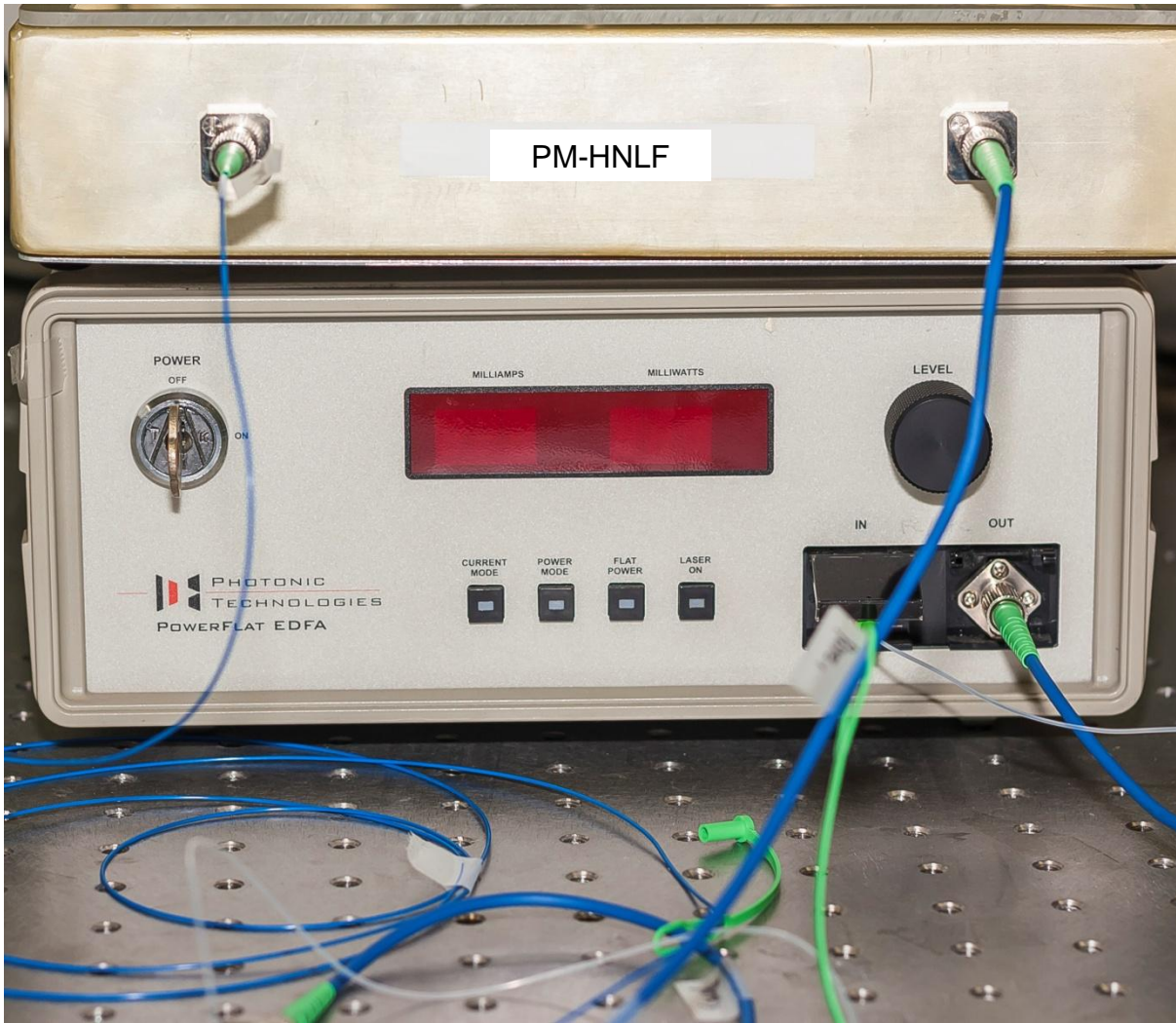


FIGURE 4.9 High power EDFA used in the experiment.

#### 4.4.2.2 Nonlinear Mixing in HNLF

The combined pump and wavelength channels were then fed into 1 km of HNLF. The HNLF used for this experiment is standard PM-HNLF from OFS (<http://ofscatalog.specialtyphotronics.com>), as shown in Figure 4.10.





**FIGURE 4.10** PM-HNLF from OFS with low dispersion used in the experiment.

This fibre has a very high nonlinear coefficient ( $\gamma = 20 \text{ W}^{-1}\text{km}^{-1}$ ) compared to the value of  $1.2 \text{ W}^{-1}\text{km}^{-1}$  for SMF. It also has very low dispersion ( $-0.19 \text{ ps} / \text{nm}\cdot\text{km}$ ) in the 1540-1560 nm band. Nonlinear mixing between the pump and the three input wavelength channels generated numerous idler wavelengths as shown in Figure 4.11. The mixing product of each wavelength channel and the pump carries the pump information and thus the new idler wavelengths are created with a copy of the input bit pattern on them [55].

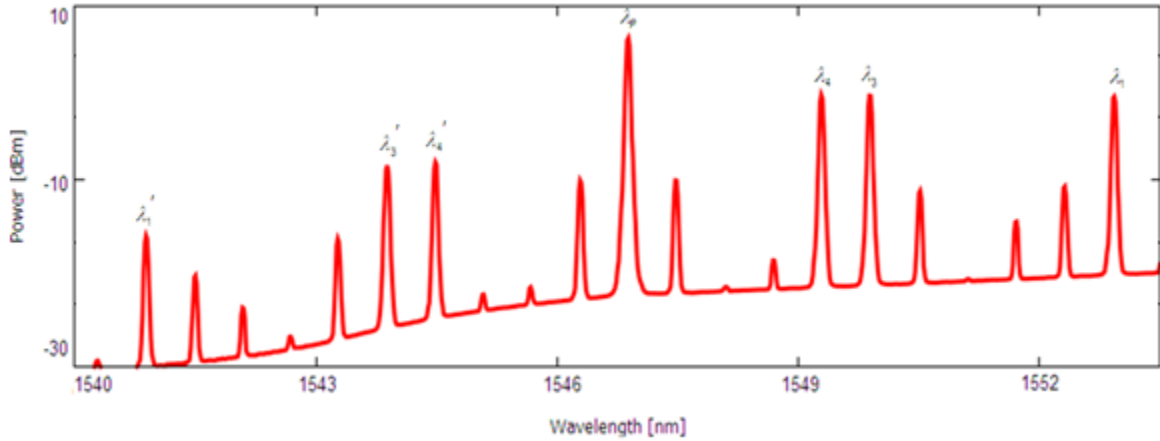


FIGURE 4.11 FWM mixing products measured at the output of the HNLF.

#### 4.4.2.3 Separation of the required idler wavelengths

The information carrying idler wavelengths are now the wavelengths of interest and the challenge is to remove all other remaining wavelengths including the pump wavelength in order to process the idlers to obtain the required correlation function. Since the pump power at the output of the HNLF is more than 20 dB higher than that of the lowest power idler  $\lambda_1'$ , only one stage of filtering is not enough to remove the pump wavelength. As previously stated, in the wavelength selection process the pump wavelength was carefully selected to be 1546.95 nm and the four wavelength channels were chosen to be 1549.41 nm ( $\lambda_4$ ), 1550.2 nm ( $\lambda_3$ ), 1551.84 nm ( $\lambda_2$ ) and 1553.63 nm ( $\lambda_1$ ). The wavelength separation is not uniform because of laser and filter compatibility. To create the 1011 template,  $\lambda_2$  is turned off. Figure 4.11 shows the numerous wavelengths, including the pump and the original wavelength channels, measured at the output of the HNLF (Figure 4.3 [B]). The target idler wavelengths are  $\lambda_4'$ ,  $\lambda_3'$ , and  $\lambda_1'$ . These idlers are created with unequal powers. It can be seen that the power of  $\lambda_1'$  is less than that of  $\lambda_3'$  and  $\lambda_4'$ . This is because the FWM efficiency decreases as the separation between the pump and channel wavelengths increases.

The problem is to remove all other wavelengths in the spectrum and obtain a spectrum which only contains  $\lambda_4'$ ,  $\lambda_3'$ , and  $\lambda_1'$ . This was achieved by utilizing a two-step filtering process.

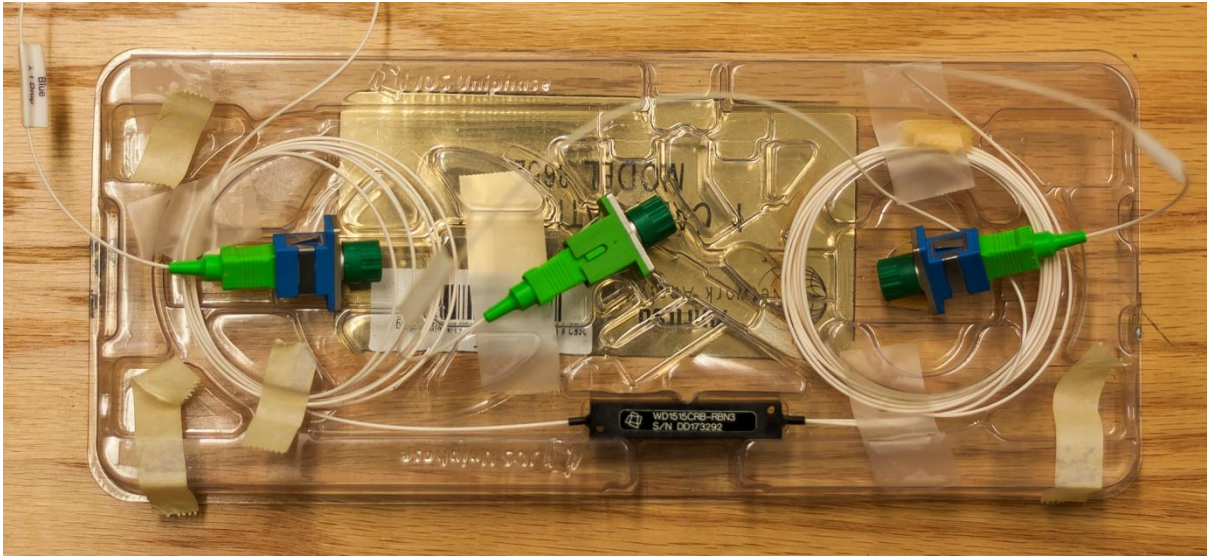


FIGURE 4.12 Low pass filter used in the experiment as a first step of filtering.

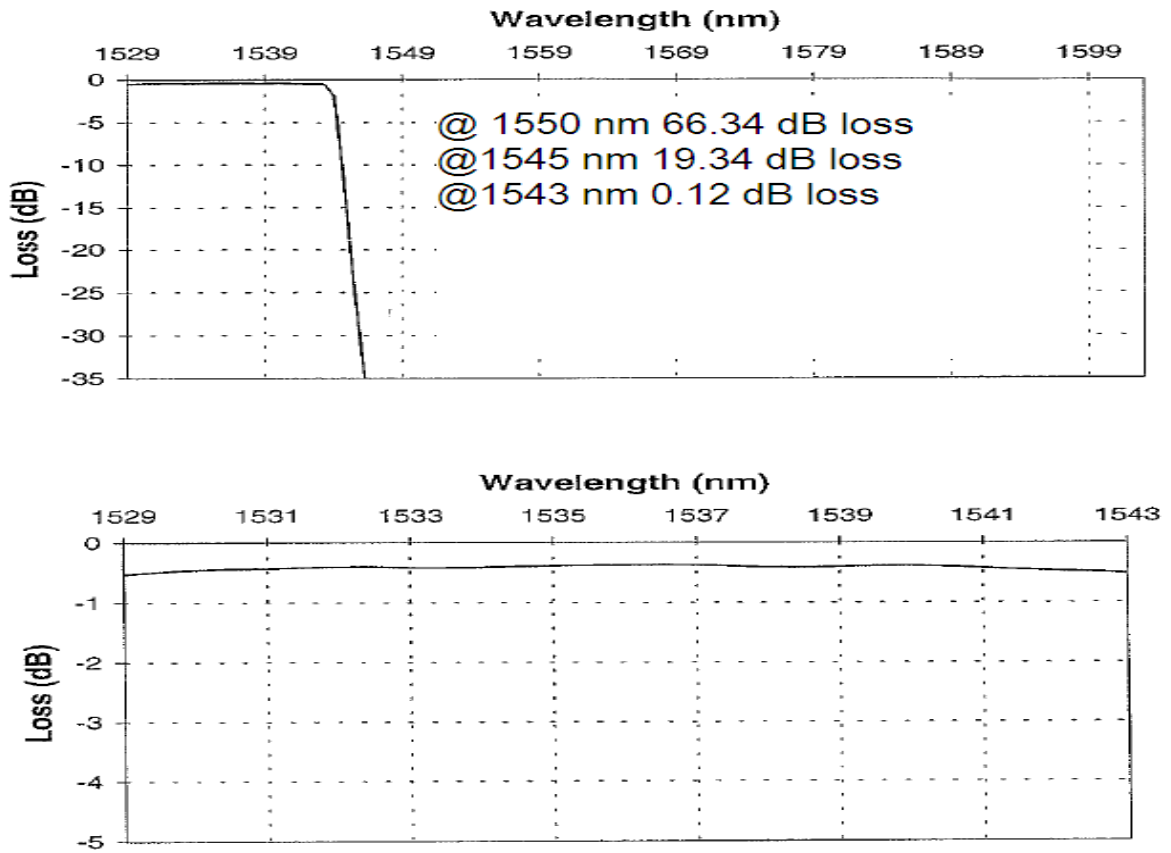
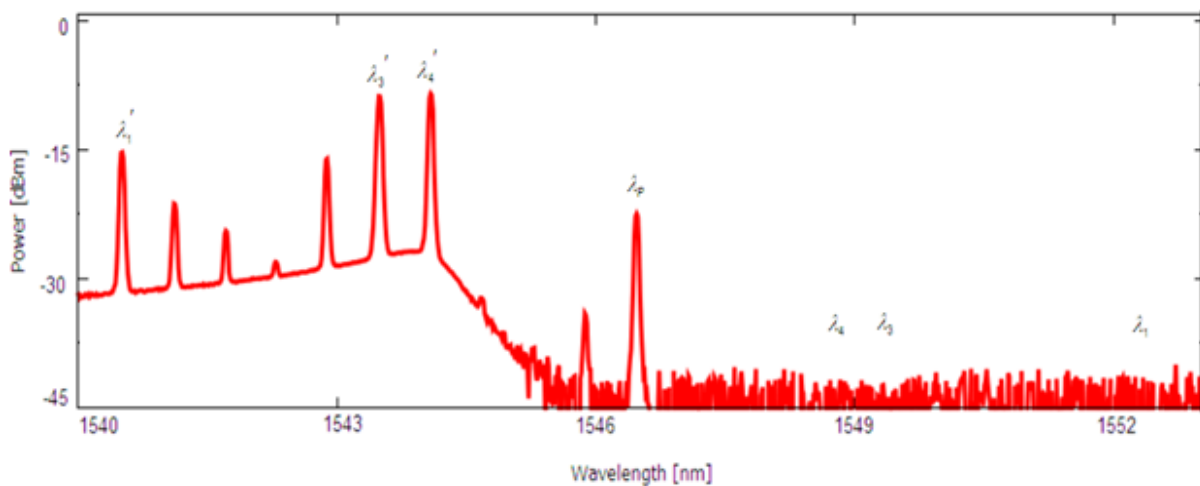


FIGURE 4.13 Lo-pass filter characteristics (transmit) [filter manufacturer data sheet].

The first filter used is a low-pass filter with a cut-off (-20 dB) wavelength of 1545.4nm. Figure 4.12 shows filter used in the experiment. It has three ports and can be used as either low pass or high pass filter. For this experiment, it is used as a low pass filter and Figure 4.13 shows the measured filter characteristics from the filter data sheet.

The filter shown in Figure 4.12 has 46 dB of attenuation at 1546.95 nm (which is the pump wavelength). By employing this filter, the high power pump and the original wavelength channels are attenuated significantly. Only the required idler wavelengths along with a few other low power unwanted idlers remain in the spectrum as shown in Figure 4.14. This spectrum was measured before the second EDFA (Figure 4.3 [C]).



**FIGURE 4.14** Measured spectrum after the first stage of filtering using a low-pass filter.

The output of the first stage filter is then fed into a Waveshaper (which is a multiport optical processor) for further filtering. The Waveshaper used in this research is a Finisar Waveshaper 4000s as shown in Figure 4.15. This is a five port optical processor with four input ports and one output port (or vice-versa).





FIGURE 4.15 Finisar Waveshaper 4000s used in the experiment.

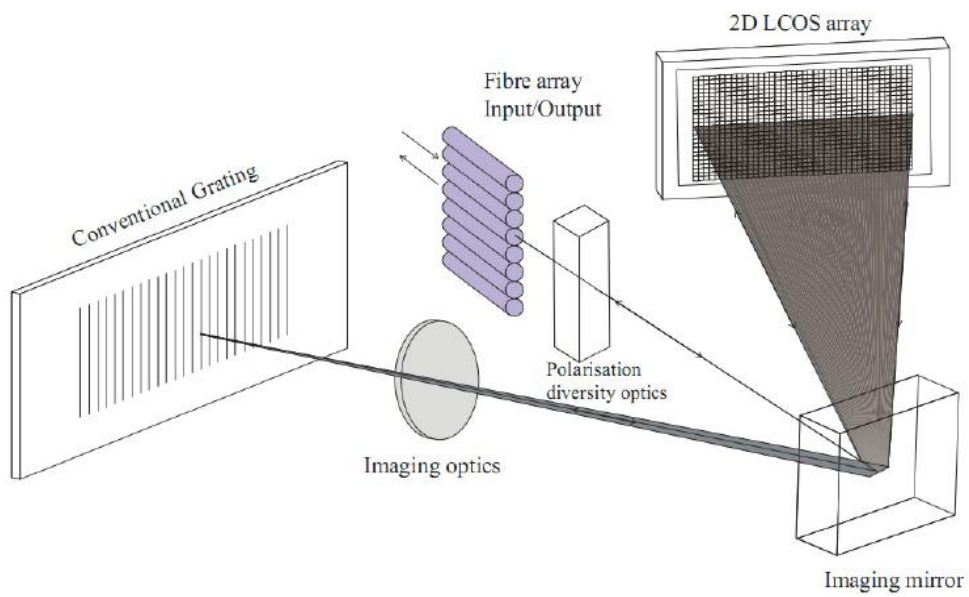
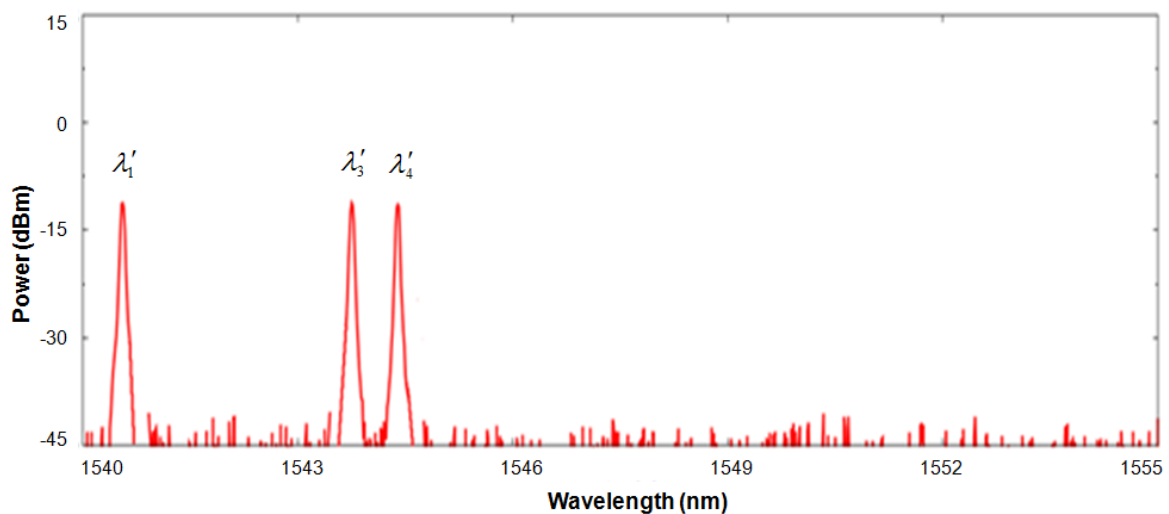


Figure 4.16 Operation principle of the Waveshaper [21].

The Waveshaper is a programmable optical filter with full control of filter amplitude and phase characteristics. Covering the entire C- or L-band or the C+L band, the Waveshaper combines precise control of filter wavelength, bandwidth, shape, and phase with the ability to switch and combine multiple signals in an “Add” or “Drop” configuration. The controllable separation bandwidth is as low as 20 GHz or 0.16 nm and it can add up to 20 dB of attenuation to the neighboring rejection band. The general operating principle of a Waveshaper is given in Figure 4.16 as described in [21].

At the output of the Waveshaper, all the unwanted wavelengths were removed and the required template was obtained as shown in Figure 4.17. To adjust for the variation of power among the different idler wavelengths seen in Figure 4.14, the Waveshaper software was set to apply a variable amount of attenuation to the different idler wavelengths such that the output of each port had an equal power level of -11 dBm (as shown in Figure 4.17).



**FIGURE 4.17** Template wavelengths measured at the output of the Waveshaper.

The experimental system was limited to only 4 bits because only a 4 port Waveshaper is available. The Waveshaper can filter out signals with a resolution of 20 GHz. For longer bit patterns a large number of closely separated wavelengths are able to be filtered using multiple Waveshapers or a Waveshaper with a large number of output ports to do so. The use of a Waveshaper is preferred over other types of optical filters because they are software controllable. .

#### 4.4.2.4 Applying the wavelength dependent delay

To generate the desired correlation function, the template wavelengths at the output ports of the waveshaper are required to undergo a wavelength dependent delay based on the bit position which they represent in the template. In [24], the wavelengths were differentially delayed using the dispersion in a length of single-mode fibre to provide time delays equal to multiples of a bit period. In this thesis work, a differential delay network formed by using different lengths of single-mode fibre patch cord was used instead of using the dispersion in a length of single-mode fibre because for the low bit rate used, a delay of one-bit period would require a fibre length of ~600km. The differential delay between each output port of the Waveshaper was adjusted to a 1 bit duration ( $\Delta t = 10\text{ns}$ , equivalent to the time delay in a 2m long fibre patch). Based on their relative bit position, a zero relative delay is applied to  $\lambda_4$  at port 1 of the waveshaper, a 1 bit delay is applied to  $\lambda_3$  at port 2 and  $\lambda_1$  at port 4 faces a 3 bit delay. The outputs of the different ports are then combined using 3 dB couplers and the combined optical signal is detected using a using a New Focus 1514 6 GHz photoreceiver module which is shown in Figure 4.18 below. This receiver has a gain of approximately 4500 V/W.



FIGURE 4.18 Sensitive New Focus Photoreceiver with DC power supply.

Figure 4.19 shows the measured photoreceiver output due to the bit pattern on each wavelength and the relative time delay introduced by the fibre delay network. The measured results show the expected relative time delays. The fibre delay network introduces a loss of  $\sim 6\text{dB}$  and hence the average received power per wavelength is  $-18\text{ dBm}$ . An Agilent DSOX 3024A oscilloscope was used to detect the output voltage from the photo receiver module.

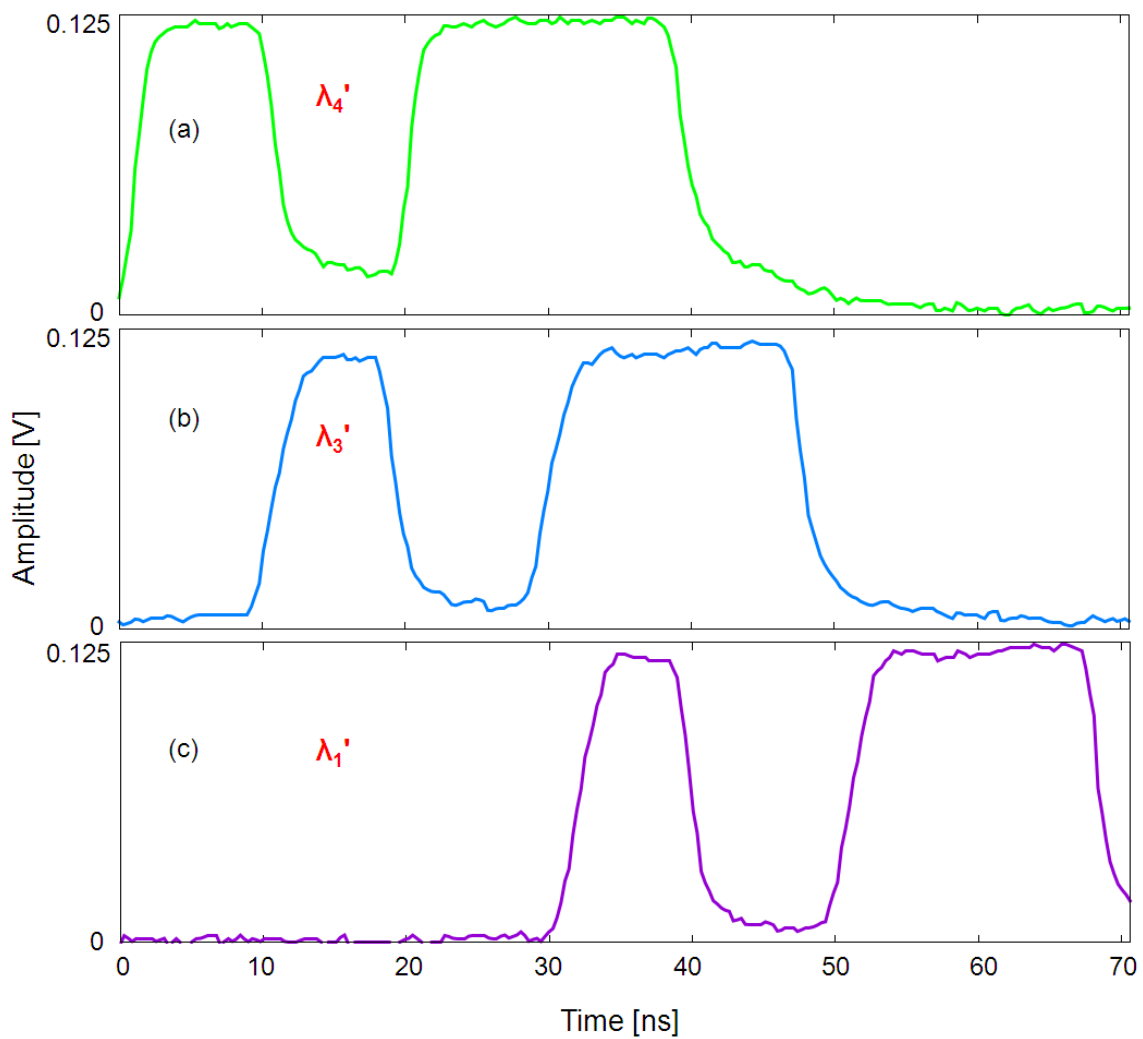


**FIGURE 4.19** (a) Measured photoreceiver output when only  $\lambda_4'$  is present. (Zero delay) (b) Measured photoreceiver output when only  $\lambda_3'$  is present. It is differentially delayed by a 1-bit delay. (c) Measured photoreceiver output when only  $\lambda_1'$  is present. It is differentially delayed by a 3-bit delay.

### 4.4.3 CORRELATION RESULTS

Having characterized the system and showed that it performs as expected, the correlation function for matched and mismatched input bit patterns is demonstrated. In Figure 4.20, the solid blue line shows the measured correlation function at the photoreceiver output when all three idler wavelengths are present and the input bit pattern (1011) matches the reference bit pattern. When there is a match between the input bit pattern and the reference bit pattern, a correlation peak occurs at the middle of the correlation function, which is at the end of the original bit pattern (bit 4). The height of the correlation peak is equal to the height of a detected '1' multiplied by the number of '1's in the template, which in this case is 3 ( $3 \times 0.125 \text{ V} = 0.375 \text{ V}$ ).

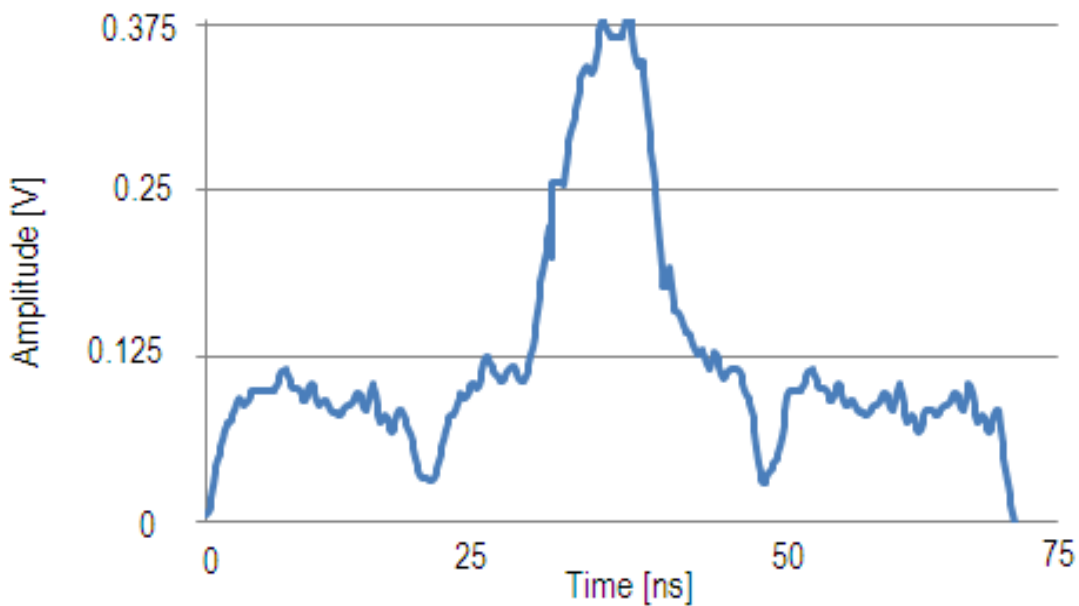


**FIGURE 4.20** Correlation output with matched input signal 1011.

Figure 4.21 demonstrates the output correlation function with a mismatched input pattern. Here the input pattern is 1000 which is different from the reference pattern 1011. It is a large mismatch case and the peak of the output correlation function for the mismatched pattern is only '1' unit which is equal to the amplitude of only one '1' of the system. In this case this is  $1 \times 0.125 \text{ V} = 0.125 \text{ V}$ .

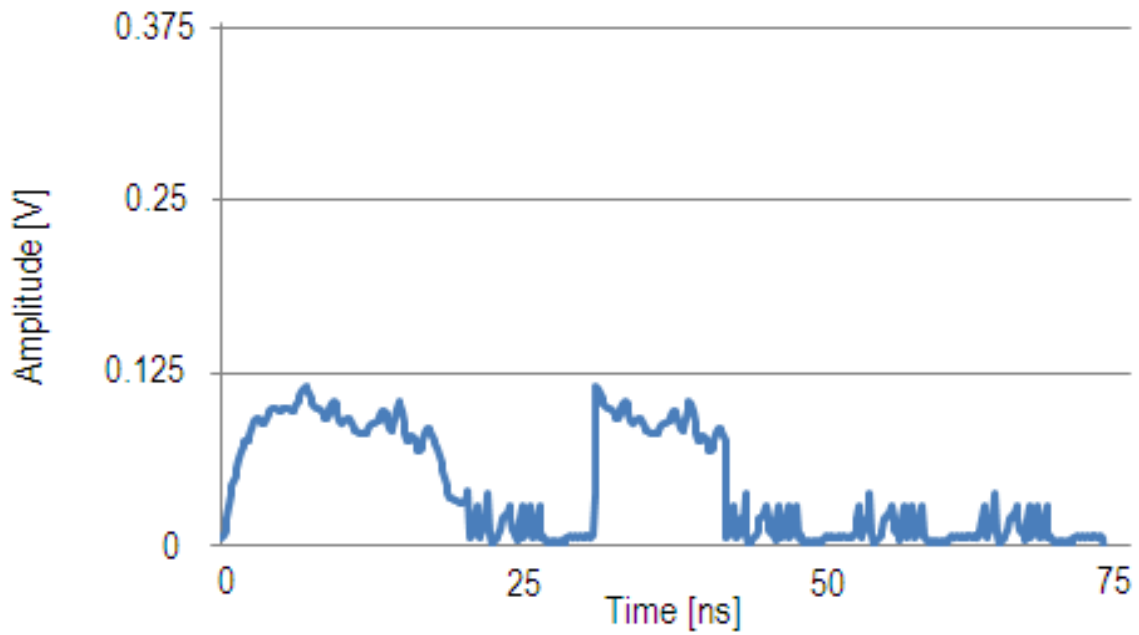


FIGURE 4.21 Correlation output with a mismatched input signal 1000.

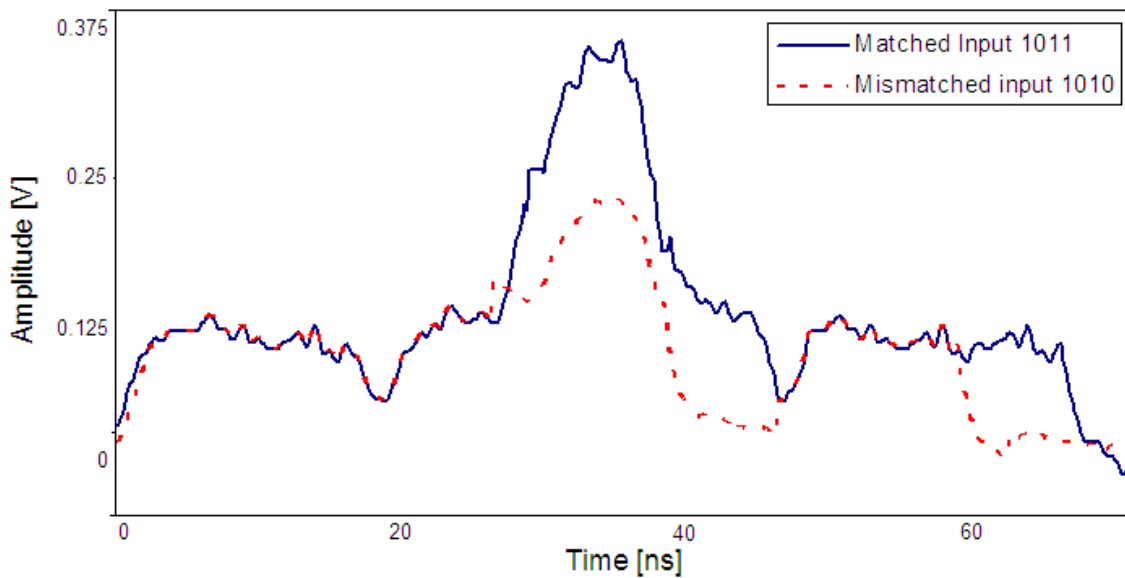


FIGURE 4.22 Correlation output with matched input 1011 and worst-case mismatched input signal 1010.

Figure 4.22 compares the measured output for the matched input matched (input 1011) with a worst-case mismatched input (input 1010). This worst-case input was determined from a truth table

exercise. As is visible in the figure 4.22 the correlation peak for the matched case is at least '1' unit larger than that for a mismatched signal.

## 4.5 DISCUSSION

In the experiment described in this chapter, photonic correlation of a 4 bit pattern with a reference bit pattern has been demonstrated using a novel approach using four wave mixing. In setting up the experiment, several issues had to be addressed. Filtering out the high power pump and the wavelength channels was a challenge and therefore the wavelengths were carefully selected using available laser sources to match the available filter cut-off wavelength.

Although the proposed concept has been demonstrated here using only a 4 bit pattern, it is important to note that the technique is scalable to larger bit patterns. In the work reported here, the 4 bits was a limitation of the number of output ports on the Waveshaper which was used to filter out the idler wavelengths, each representing a bit. A multiport Waveshaper would enable the filtering of more wavelengths, allowing more bits in the bit pattern. Scalability depends on a number of factors. Firstly, it depends on the number of idler wavelengths which can be efficiently generated and filtered using four wave mixing. Efficient four wave mixing requires HNLFF with low dispersion. The HNLFF used here exhibits low dispersion ( $-0.19$  ps/km.nm) over the wavelength range 1540-1560nm. This determines the range of possible signal wavelengths. The wavelength spacing in this range depends on the resolution of the filter used to filter out the idler wavelengths. Assuming a filter resolution of 20GHz, an upper limit on the number of possible wavelengths in this 20nm range, and therefore the number of signal bits, is 125.

A second issue to note is that although a fiber delay network was used here, this is not necessary. A simple dispersive medium could be used to achieve the required wavelength dependent time delays. Unfortunately, the concept was demonstrated with a bit rate of only 100 Mb/s due to the unavailability of a high speed pattern generator. In this case it was easier to use a fibre delay network instead of a dispersive fibre to achieve the large time delays corresponding to multiples of a bit

period. At higher bit rates than that used here, single-mode fiber could be used as a dispersive medium to achieve the required time delays for the idler wavelengths, as in [6]. Generating a several bit delay would be easier and with much less insertion loss than using the fiber delay network which was used here.

The required time delay increases as the number of bits increases. For  $N$  bits, a maximum time delay of  $(N-1) \times$  the bit duration is required. At 40Gb/s, the bit duration is 25ps. For a 16 bit pattern, a maximum delay of 375 ps is required. Assuming wavelength spacing of 0.8nm, a length of 1.84km of SMF could be used to achieve the delays (delay = 17 ps/nm/km  $\times$  0.8 nm  $\times$  1.84 km = 25ps between wavelengths).

Another factor which can limit the scalability of this scheme, as well as that demonstrated in [6], is the visibility of the correlation peak for the matched case, i.e. how different is the correlation peak for the matched signal from the maximum output for a mismatched signal. Since the output of the photoreceiver is due to the summation of several optical signals at different wavelengths, and each wavelength produces a signal current plus a noise current, successful detection of the matched case depends on the signal current produced by each '1' as well as the noise current produced by each wavelength.

For the matched case, the maximum value of the output signal will be due to the number of '1's in the signal ( $N$ ), whereas the maximum output for a mismatched case will be proportional to  $(N-1)$  times the output for each '1', as seen in Figure 4.22. The maximum output current when  $N$  wavelengths are incident on the photoreceiver will include  $N$  noise currents, whereas the maximum output for a mismatched case will include  $(N-1)$  noise currents. Using the concept of the quality factor or  $Q$  factor which is a figure of merit commonly used in digital optical fiber systems, where the  $Q$  factor is defined as the difference between the average levels of '1's and '0's divided by the sum of their standard deviations due to the noise, it can be shown that the  $Q$  factor for the detected signal in the matched case will be proportional to  $(2N-1)^{-1}$ . Therefore, for this correlation technique, the visibility of the matched case decreases as the number of '1's in the reference bit pattern increases.



## 4.6 CONCLUSION

A novel photonic correlation technique which uses four wave mixing in a length of nonlinear optical fibre has been proposed and demonstrated. Modulation of the pump is done at the transmitter end of the system whilst the FWM, signal filtering and correlation is done at the receiver. Contrary to the scheme in [24], the technique discussed here will allow the use of a remote transmitter. A conference paper on this work was presented at the 2012 IEEE International Topical Meeting on Microwave Photonics in Noordwijk, The Netherlands, in September 2012. This paper is included in Appendix II.

In the next Chapter a software controlled implementation of the template using an optical processor to achieve realistic remoting of the transmitter is discussed.

## 5. PHOTONIC CORRELATOR WITH REMOTE TRANSMITTER

### 5.1 INTRODUCTION

In [24], a pattern recognition technique based on a matched filter was presented in which the reference or template bit pattern is encoded as discrete optical wavelengths. These wavelengths are each modulated by the input bit pattern and then differentially delayed in a dispersive medium before they are summed and detected with a high frequency photoreceiver. Correlation of the binary input signal and the encoded reference bit pattern is obtained at the photoreceiver output.

A key problem with this technique in [24] is that all the photonic processing is done near the source of the input bit pattern whereas in a practical system it may be desirable to isolate the signal processing from the source of the input signal. In addition, for this technique a new reference bit pattern requires a new template, which is selected by physically turning lasers on and off, which has obvious disadvantages.

In Chapter 4 a different correlation technique based on FWM was proposed and experimentally demonstrated. In that technique, the template was also selected by physically turning laser diodes on or off. In this chapter, a nonlinear mixing based correlation scheme is discussed where the template is selected using software control of an optical processor. This is a key difference. Because of the software controlled filtering of wavelengths, changing and controlling the template pattern can be done from a remote location. As in Chapter 4, the proposed correlation scheme in this Chapter uses four wave mixing in a length of highly nonlinear fibre to mix a number of CW laser wavelengths with a pump wavelength which has been modulated by an input bit stream in order to produce copies of the input signal at the output idler wavelengths [55].

## 5.2 PROPOSED METHOD

In the correlation scheme proposed in this chapter, the reference bit pattern or template is determined by selecting particular idler wavelengths generated by the FWM process using a software controlled optical processor (Waveshaper). These idler wavelengths are differentially delayed using lengths of fibre with delays corresponding to multiples of a bit period and then summed at a photoreceiver to provide the correlation function. Once again, a fibre delay network is used only because of the low bit rate which is used because of equipment limitations. This technique allows the pump wavelength to be modulated with the input bit pattern and transmitted from a remote location for correlation. A key difference between this technique and that described in Chapter 4 is that, instead of selecting the reference template by turning lasers on or off, all the lasers at the receiver are kept on and particular idler wavelengths are selected for the reference template. Figure 5.1 shows the proposed system. A software controlled Waveshaper is used to select the idlers of interest to set the template.

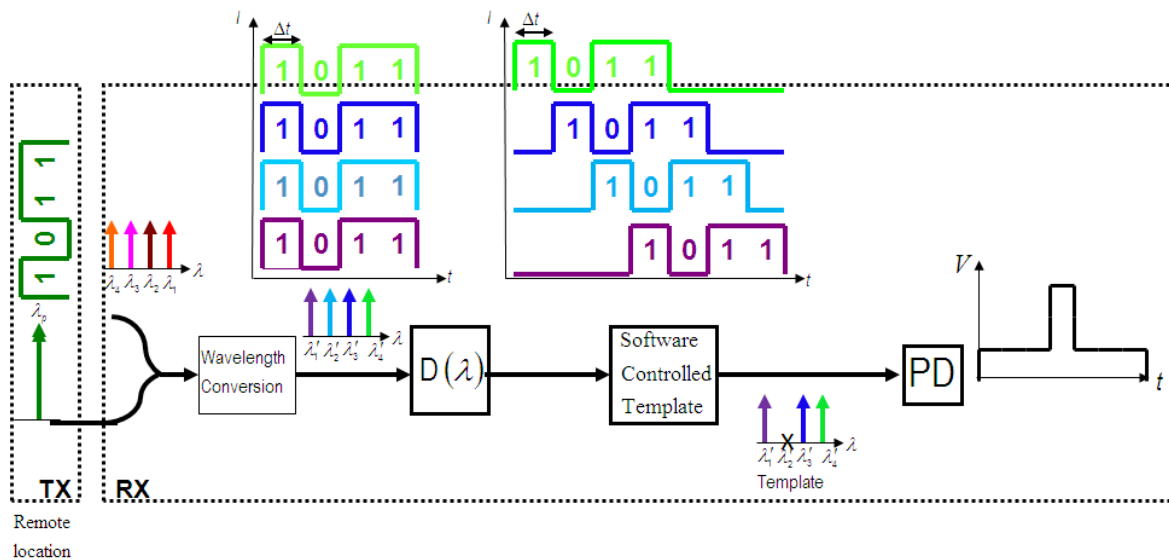


FIGURE 5.1 Illustration of the working principle of the proposed HNLF based correlation scheme with possible remote transmitter and software controlled template.

## 5.3 EXPERIMENTAL SET-UP

The experimental set-up is similar to that described in Chapter 4. The system consists of a transmitter where a MZM is used to modulate a pump wavelength with the input bit stream, and a receiver where wavelength conversion, differential delays, selection of idler wavelengths and detection of the correlation function occur.

### 5.3.1. Transmitter

As stated in Chapter 4, the transmitter end of the system contains a high power pump laser and a Mach-Zehnder modulator. As described in the previous experiment of Chapter 4, the pump wavelength was carefully selected to be 1546.95 nm because after the four wave mixing in the HNLF, the pump wavelength needs to be filtered out and at this wavelength the wavelength selective filter has a very high attenuation (66 dB).

The pump wavelength is modulated by the input bit pattern using the MZM. The HP3760A programmable data generator was used to generate the input bit pattern with a bit duration of  $T=10$  ns (bit rate = 100 Mbps). In this case, the amplitude of the 1's from the data generator was set to be 1.6 Volts. . For this experiment, the MZM was a commercial device from Codeon with a  $V_{\pi}$  of 4 volts. Once again, the MZM was biased such that the drive voltage produced a maximum on-off contrast or 'eye-opening' for the modulated signal. The modulated pump wavelength is then transmitted to the receiver. The transmitter could be located several km from the receiver if the fibre losses are small and the received signal can be amplified to a useful power level.

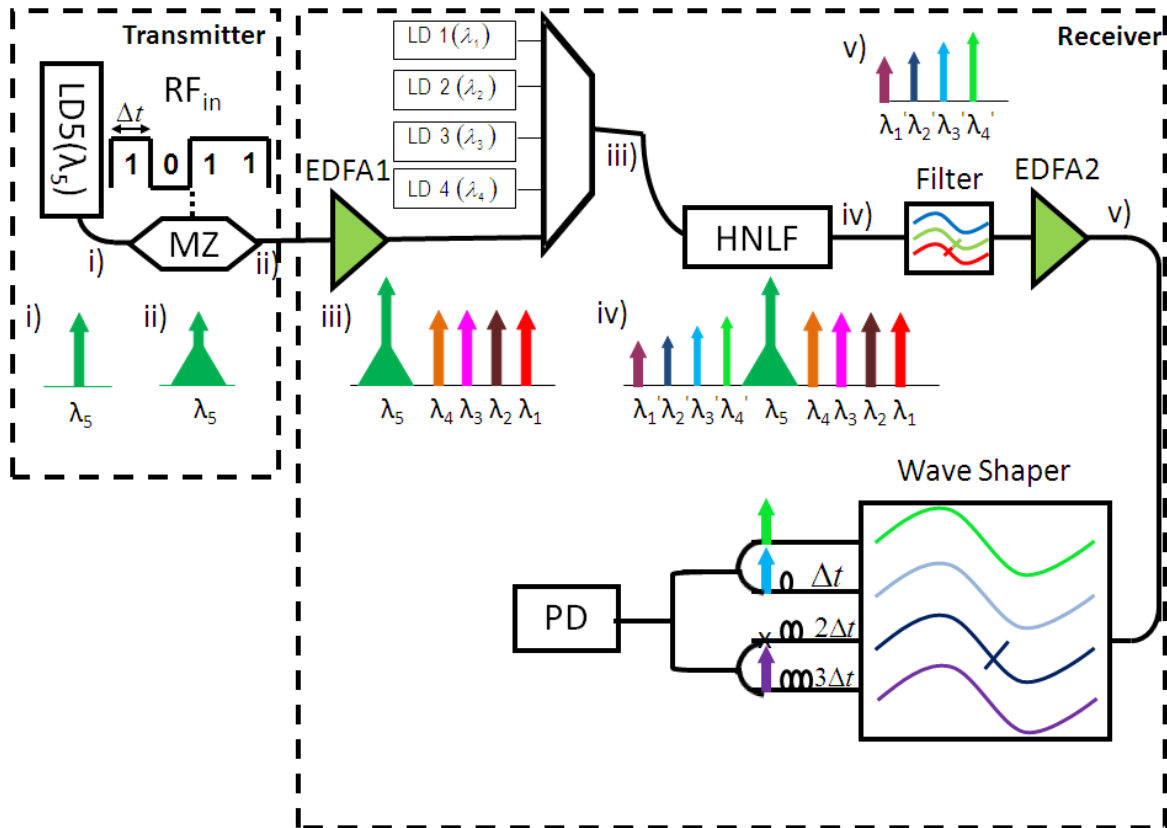


FIGURE 5.2 Characterization and experimental set-up.

### 5.3.2. Receiver

At the receiver, the modulated pump is amplified by an EDFA (EDFA1 in Figure 5.2) which has a gain of 20dB and combined with a number of CW laser wavelengths using the Arrayed Waveguide Grating (AWG) described in Chapter 4 (Figure 5.2 [iii]). The number of CW laser wavelengths, ‘n’, is equal to the number of bits to be correlated. Unlike the experiment in Chapter 4, the CW lasers are always on, regardless of the number of ‘1’s in the bit pattern.

The modulated pump wavelength and the CW laser wavelengths are then mixed in a length of HNLF, (Figure 5.2 [iv]). After the HNLF the generated idler wavelengths are separated from the pump wavelength and original CW laser wavelengths using the optical low pass filter described in Chapter 4 (Figure 5.2 [v]). After the filter, the idler wavelengths are amplified in a second EDFA (EDFA2 in Figure 5.2) and then pass to a software controlled multiport optical processor (Waveshaper) which is used to further filter out the unwanted wavelengths and select the required

template wavelengths. A key point here is that the required idler or template wavelengths can be selected using software control. After the Waveshaper the selected idler wavelengths pass through a bit position dependent time delay network based on the bit position they represent, before being summed and detected at the photoreceiver.

As in Chapter 4, the input bit pattern for this experiment was chosen to be 1011 with a bit duration of 10 nS. Because the desired bit pattern is 4 bits long, the template will contain four wavelengths to represent the 4 bits. The actual template is selected later using software control of the Waveshaper. The same laser array which was used for the experiment in Chapter 4 was used here with the same set of wavelengths and the same amount of output power. The wavelengths of the four CW channels were selected to be 1549.41 nm ( $\lambda_4$ ), 1550.2 nm ( $\lambda_3$ ), 1551.84 nm ( $\lambda_2$ ) and 1553.63 nm ( $\lambda_1$ ) and the modulated pump wavelength ( $\lambda_5$ ) is at 1546.95 nm. Wavelengths  $\lambda_1$ ,  $\lambda_2$ ,  $\lambda_3$  and  $\lambda_5$  are emitted from the Newport 8-channel laser array whilst  $\lambda_4$  comes from a separate high power tunable laser.

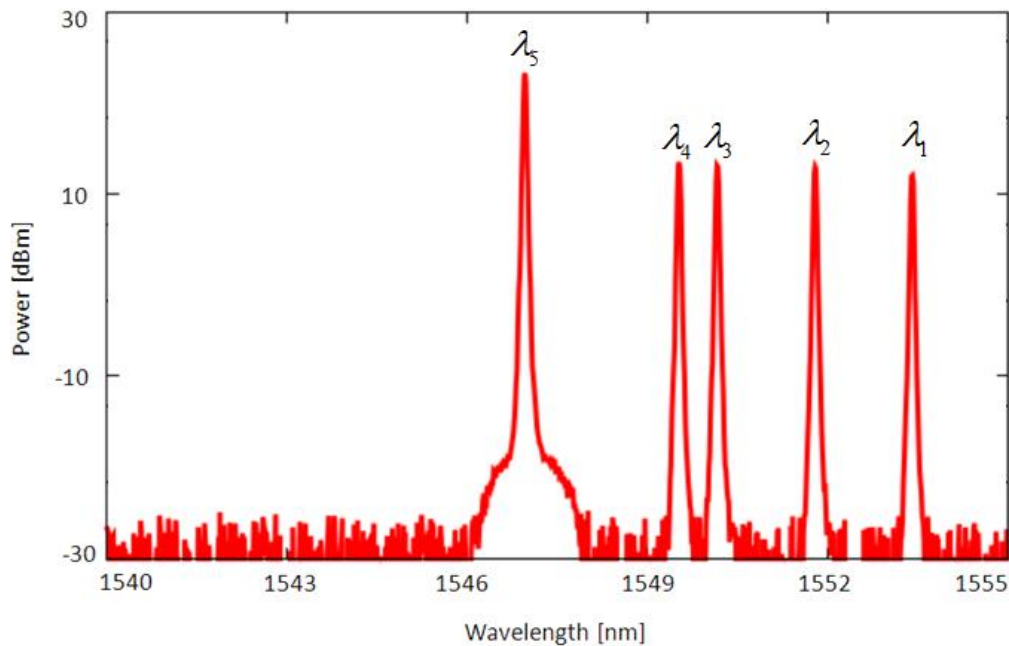


**FIGURE 5.3** Measured CW laser wavelengths channels representing the 4 reference bits combined with the pump wavelength,  $\lambda_5$ .

Figure 5.3 shows the measured CW laser wavelengths used in this experiment,  $\lambda_1$ ,  $\lambda_2$ ,  $\lambda_3$  and  $\lambda_4$ , and the pump wavelength,  $\lambda_5$ , which is modulated by the input bit pattern that is to be correlated. These wavelengths were measured at the output of the AWG (Figure 5.2 [iii]).

The combined pump and CW wavelength channels are fed into a 1 km length of HNLF. This is the same HNLF that was used in the experiment of Chapter 4. Nonlinear mixing between the pump and the four input wavelength channels generates numerous idler wavelengths. The measured optical spectrum at the output of the HNLF (Figure 5.2 [iv]) is shown in Figure 5.4. The spectrum contains the high power pump wavelength, the high power original CW wavelength channels and many lower power idler wavelengths. A key point is that the mixing products of the individual CW wavelength channels and the pump each carry the pump information and thus new wavelengths are created with the input information copied on to them [55].

Since the template is to be selected from the four target idlers, all the rest of the spectrum components need to be removed. The filter shown at v) in Figure 5.2 provides around 30 dB of attenuation to wavelengths higher than 1544nm which is not enough to eliminate the pump and other unwanted high power components and hence a two stage filtering scheme is implemented as described in Chapter 4. The output of the first stage of filtering with the low pass filter is shown in Figure 5.5 after amplification by EDFA2 which has a gain of 20 dB. The wavelengths then pass to the Waveshaper for a second stage of filtering and selection of the template wavelengths. The Waveshaper was described in Chapter 4. As well as filtering out undesirable wavelengths, the Waveshaper can also be used to equalize the power of each template wavelength.

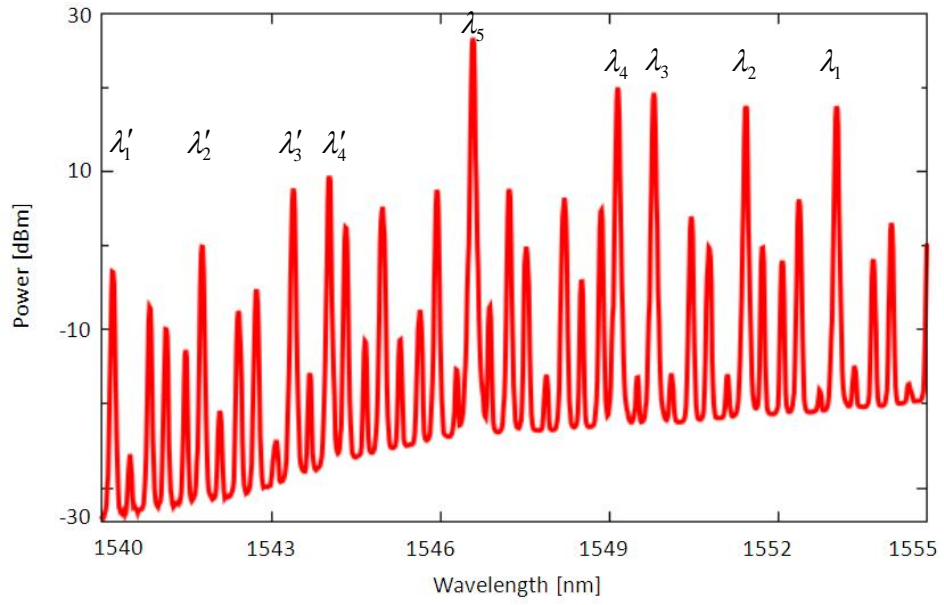


**FIGURE 5.4** Output of the HNL after nonlinear mixing.

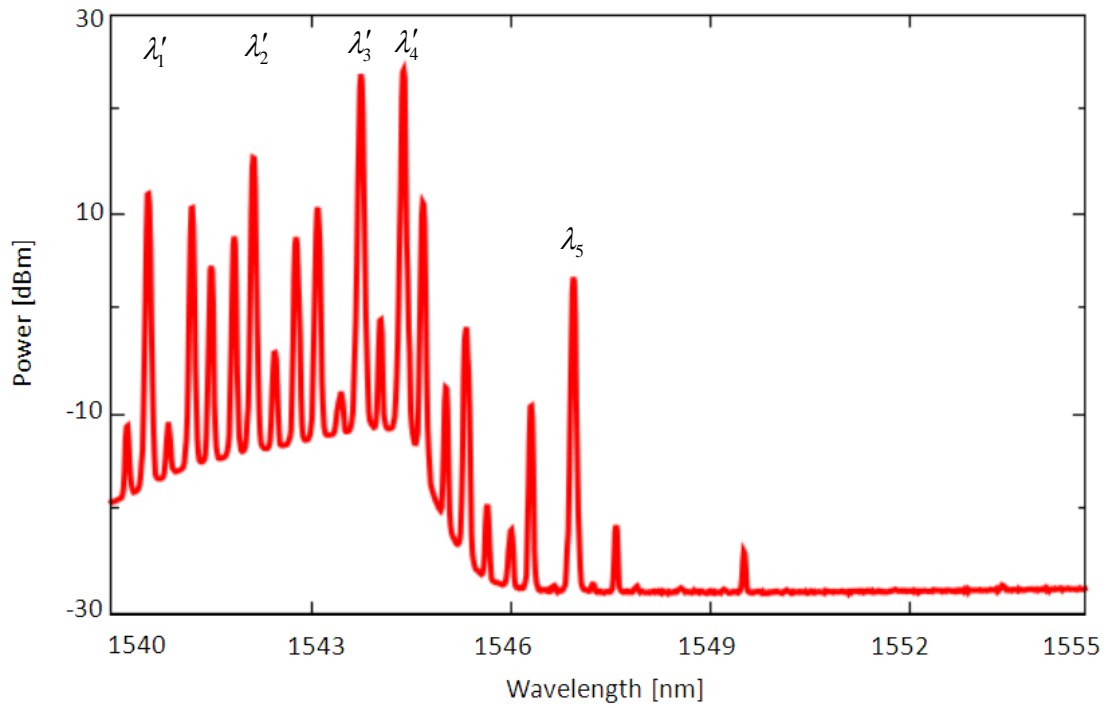


**FIGURE 5.5** Output of EDFA2 after passing through the low pass filter.



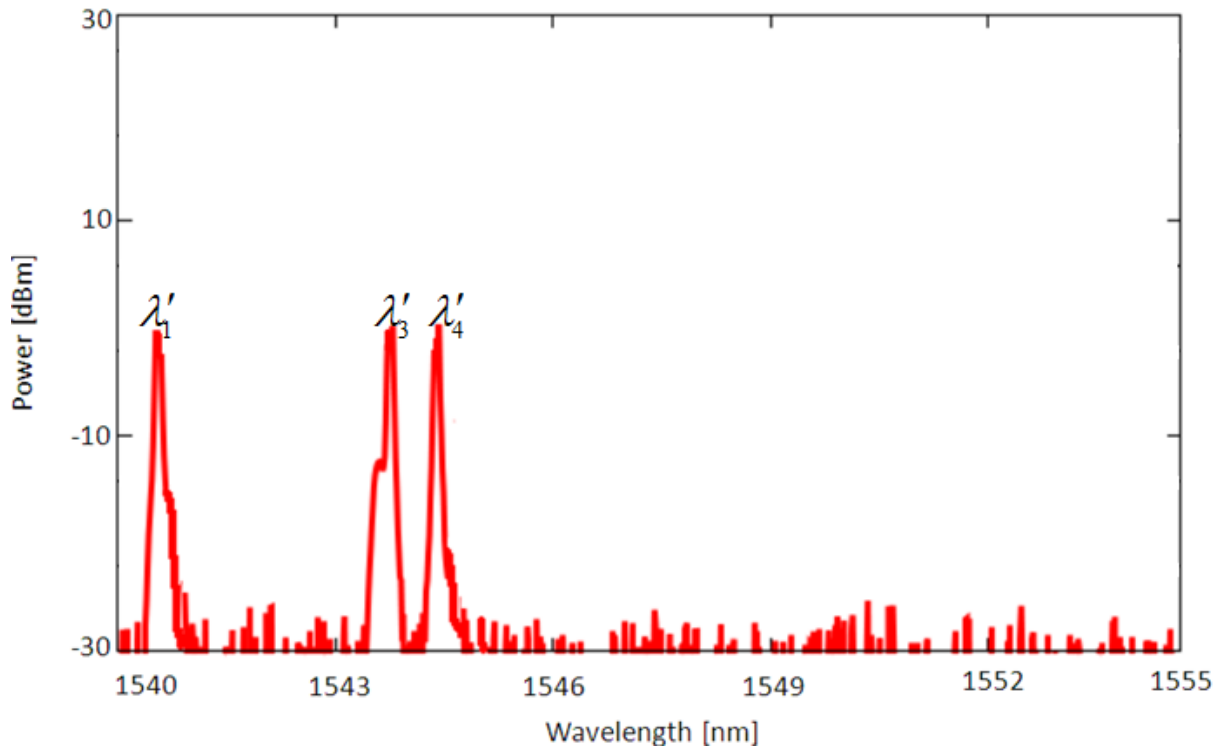


FIGURE 5.6 Software selected template 1101 at the output of the Waveshaper.

In the current example,  $\lambda_2'$  is discarded to represent the template 1101 as seen in Figure 5.6 and all the other unwanted idler wavelengths are also removed from the spectrum. The power level at the Waveshaper for each wavelengths is +1.2 dBm. The three wavelengths which represent the template all carry the input signal information from the pump. They are fed to the wavelength dependent delay at this stage to get the final correlation output at the photoreceiver. The power level of each wavelength at the photoreceiver is approximately -8dBm.

Figure 5.7 depicts a summary of the measured spectra at various stages of the experimental set-up, clearly displaying the input wavelengths and the conversion to get the template.

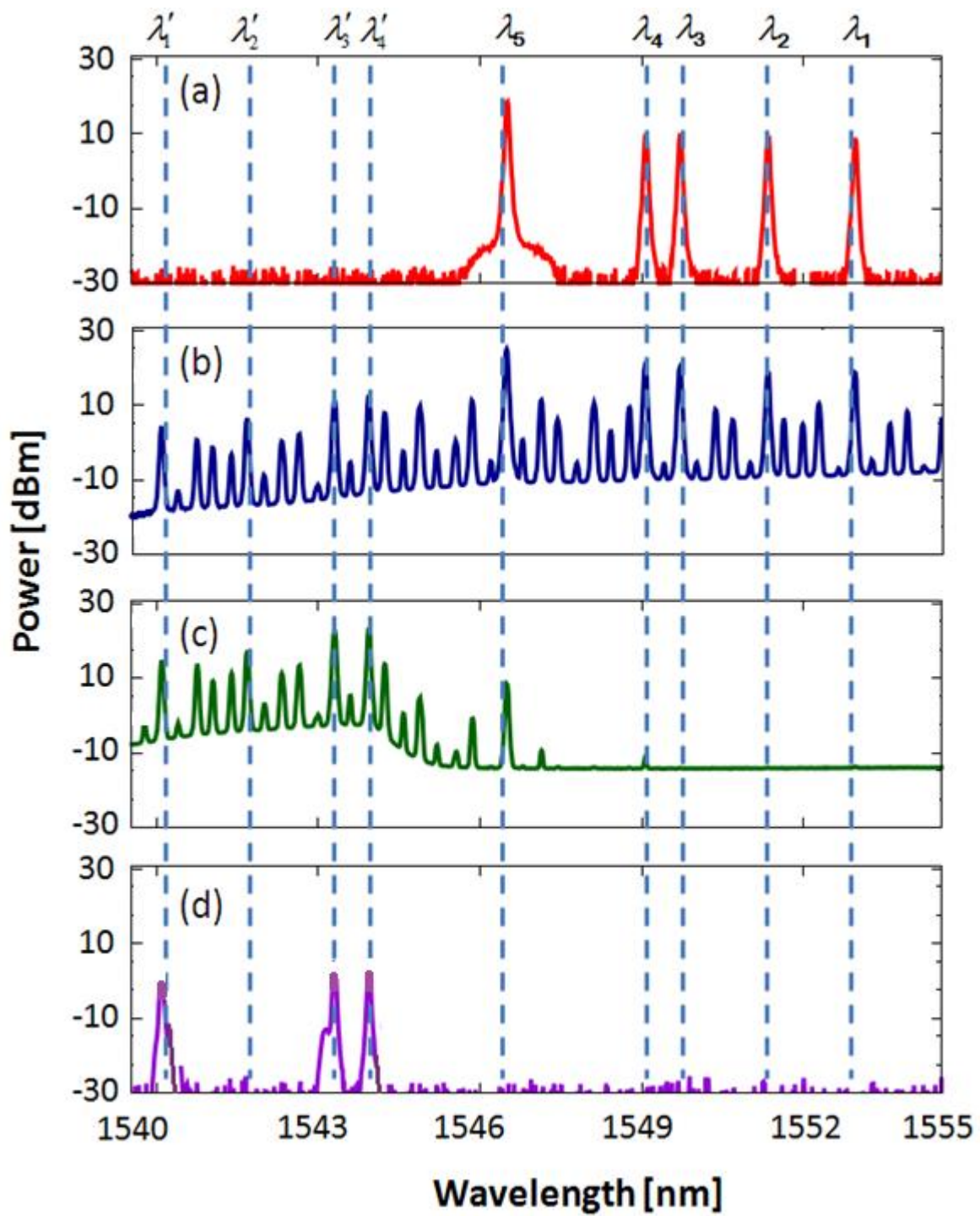
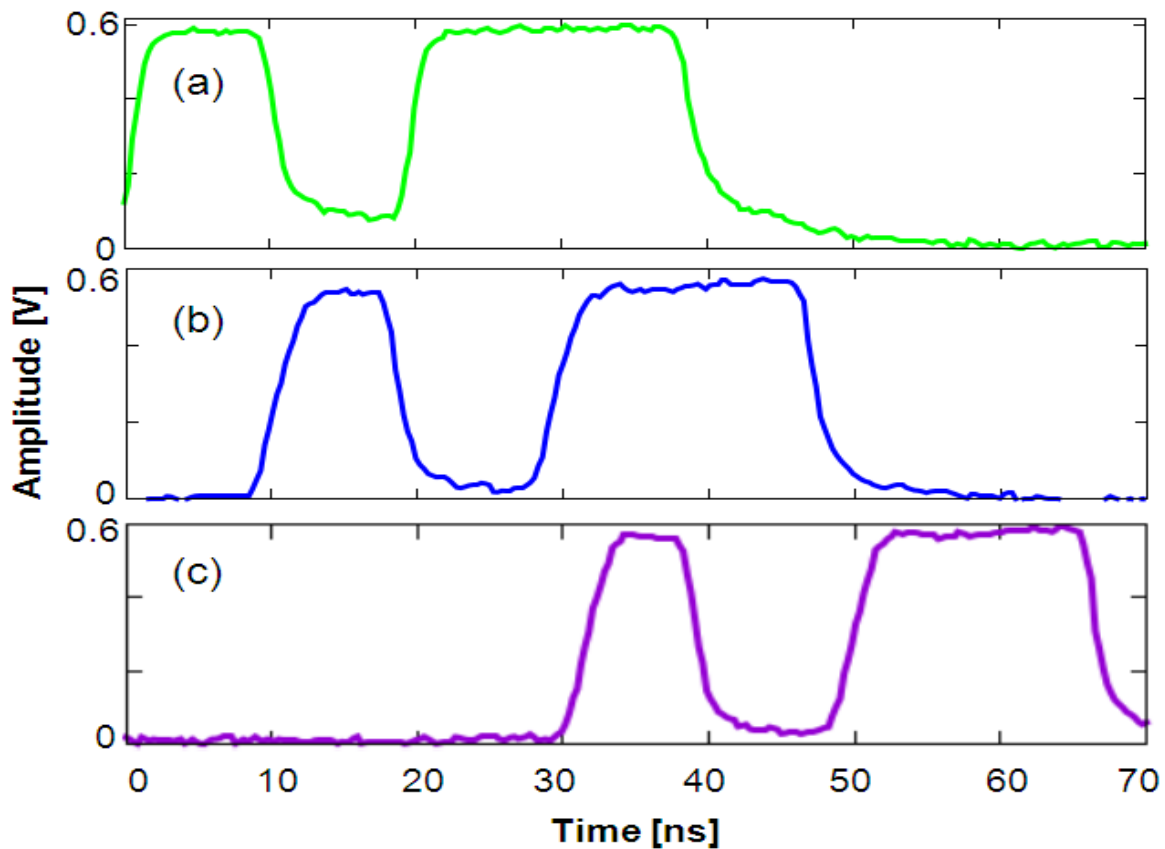


FIGURE 5.7 (a) Pump and CW laser wavelengths at the input of the HNLF, (b) mixing products at the output of the HNLF, (c) amplified output of the low pass filter (filtering the high power pump and the input channels), (d) template representing idler wavelengths measured at the Waveshaper.

The template wavelengths at the output port of the waveshaper face a time delay network based on the bit position they represent in the template. Figure 5.6 shows the representation of the template 1101 where  $\lambda_4'$  and  $\lambda_3'$  represent the first two '1' bits. After that a zero means the absence of a wavelength and again a '1' is represented by  $\lambda_1'$ . Based on their bit position a relative zero delay is applied to  $\lambda_4'$  at port 1 of the Waveshaper, a '1' bit delay is applied to  $\lambda_3'$  at port 2. There is no wavelength present at port 3 as  $\lambda_2'$  is eliminated here and a '3' bit delay is applied to  $\lambda_1'$  at the output of port 4. Figure 5.8 shows the measured photoreceiver output due to each wavelength and the relative delays due to the delay network. When all three wavelengths are incident upon the photoreceiver, the output of the receiver will be a summation of the signal due to each wavelength.



**FIGURE 5.8** (a) Measured photoreceiver output when only  $\lambda_4'$  is present. (b) Measured photoreceiver output when only  $\lambda_3'$  is present. It is differentially delayed by a 1 bit delay compared to  $\lambda_4'$ . (c) Measured photoreceiver output when only  $\lambda_1'$  is present. It is differentially delayed by a 3 bit delay compared to  $\lambda_4'$ .

### 5.3.3. Results

Having characterized the system and showed that it performs as expected, it was then used to demonstrate the correlation of the input bit stream and the reference bit pattern. In Figure 5.9, the thick solid line shows the measured correlation function at the photoreceiver output when all three idler wavelengths are present and the input bit pattern (1011) matches the reference bit pattern. When there is a match between the input bit pattern and the reference bit pattern, a correlation peak occurs at the middle of the correlation function, which occurs at the end of the original bit pattern. The height of the measured correlation peak is equal to the height of a '1' detected for each wavelength (0.6 V) multiplied by the number of '1's in the template, which in this case is 3 ( $3 \times 0.6 \text{ V} = 1.8 \text{ V}$ ).

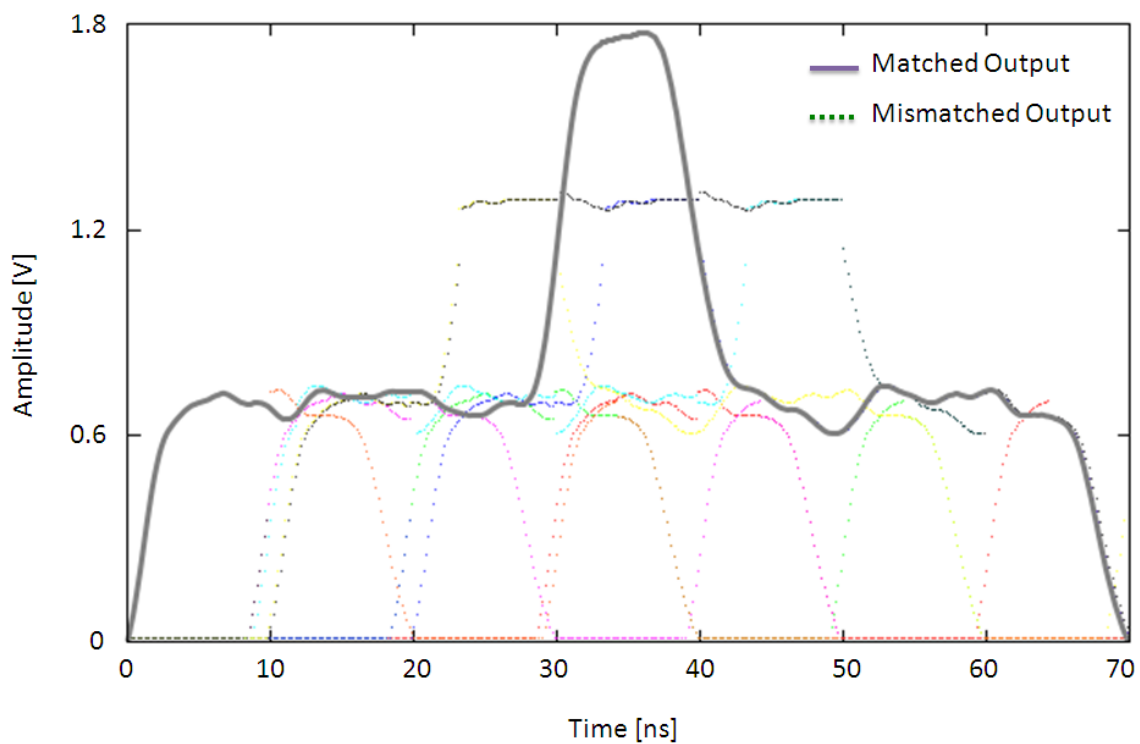


**FIGURE 5.9** Measured correlation outputs for all possible combinations of input bit patterns. The solid line indicates the output for a matched bit pattern whilst the dotted lines are for mismatched bit patterns.

The dotted plots in Figure 5.9 show the measured correlation functions for all possible mismatched conditions. The height of the correlation peak is always smaller than that for the matched case. The maximum output for a mismatched signal is  $2 \times 0.6 = 1.2$  V. The results achieved here are similar to those obtained using the scheme in [24, 29].

#### 5.3.4. Discussion

The work described in this Chapter uses software control of the template. This allows rapid change of the template using a PC. The CW lasers are ‘on’ all the time and therefore are more stable than being switched ‘on’ and ‘off’. The set-up described in this Chapter is easier to use than that in Chapter 4.

The proposed system is an incoherent optical system in which the output of the receiver is due to the summation of several optical signals at different wavelengths. Each wavelength produces a signal current plus a noise current.

An assessment of satisfactory operation of the system can be estimated using the concept of the Q factor which is a figure of merit commonly used in digital optical fibre systems to express the ‘eye-opening’ of a received digital signal. The Q factor is defined as the difference between the average levels of ‘1’s and ‘0’s divided by the sum of their standard deviations due to the noise. For the correlation system considered here, successful detection of the matched case depends on the signal current produced by each 1 as well as the noise current produced by each wavelength. The Q factor issue will have a similar effect in this approach as it had in the approach discussed in Chapter 4 and will follow the same analysis discussed there.

## 5.4 CONCLUSION

A novel photonic correlation technique based on matched filtering using FWM has been proposed and demonstrated. Contrary to the systems in [24, 29] and in Chapter 4, the scheme proposed here uses software control of the template. This allows all the CW lasers to remain ‘on’ all the time, rather than switching them on and off as required, and also allows the use of a remote transmitter. This work is a useful extension of the work done in Chapter 4 and enables a more versatile form of correlator. A paper describing this work has been published in the IEEE Photonics Technology Letters (Appendix III). In the next Chapter a novel technique for realising optical subtraction is described which is used to achieve a correlation with negative accumulation.

## **6. PHOTONIC CORRELATION WITH NEGATIVE ACCUMULATION**

### **6.1 INTRODUCTION**

Subtraction is a widely used phenomenon required for various signal processing tasks. In photonic correlation schemes such as [27, 38], a high speed balanced photoreceiver is used to obtain the difference between two optical signals. The signal processing to achieve a correlation is then done in the electronic domain. However, an inherent bottleneck of electronic systems is their limited bandwidth.

Correlation of negative signals is difficult using photonics since optical signals are always positive. In this chapter a novel FWM based scheme is presented to achieve subtraction optically. Optical wavelengths for the mixing process are selected carefully following the principle of [56], so that the mixing product for several pump and signal wavelengths produces idlers at the same wavelength. Changing the phase of pump wavelengths produces a subtraction of power at the idler wavelength. This subtraction principle is utilized in a correlator scheme to achieve a negative accumulation based correlator which gives better contrast and noise floor with respect to previously demonstrated photonic correlation schemes.

### **6.2 CONCEPT OF OPTICAL NEGATIVE ACCUMULATION**

The key concept of achieving optical negative accumulation in this work, is to utilize the inherent property of four wave mixing to achieve the subtraction of two optical signals optically. FWM of signal and pump wavelengths creates idlers at sum and difference wavelengths which carry information from the original wavelengths. If a number of signal and pump wavelengths are selected such that the signal wavelengths have a separation of twice that of the pump wavelengths, then FWM of each signal and pump will create idlers at a common target wavelength, as shown in Figure 6.1.

The optical power at this target idler wavelength depends on the relative phase of each mixing term at that wavelength. Subtraction of an idler can be achieved if the pump of that mixing product has a  $\pi/2$  radians phase shift with respect to the other pumps. The resultant idler for that particular mixing term will have a  $\pi$  radians phase difference with respect to the other idlers and their sum will be a subtraction between two optical signals by subtraction of electric fields.

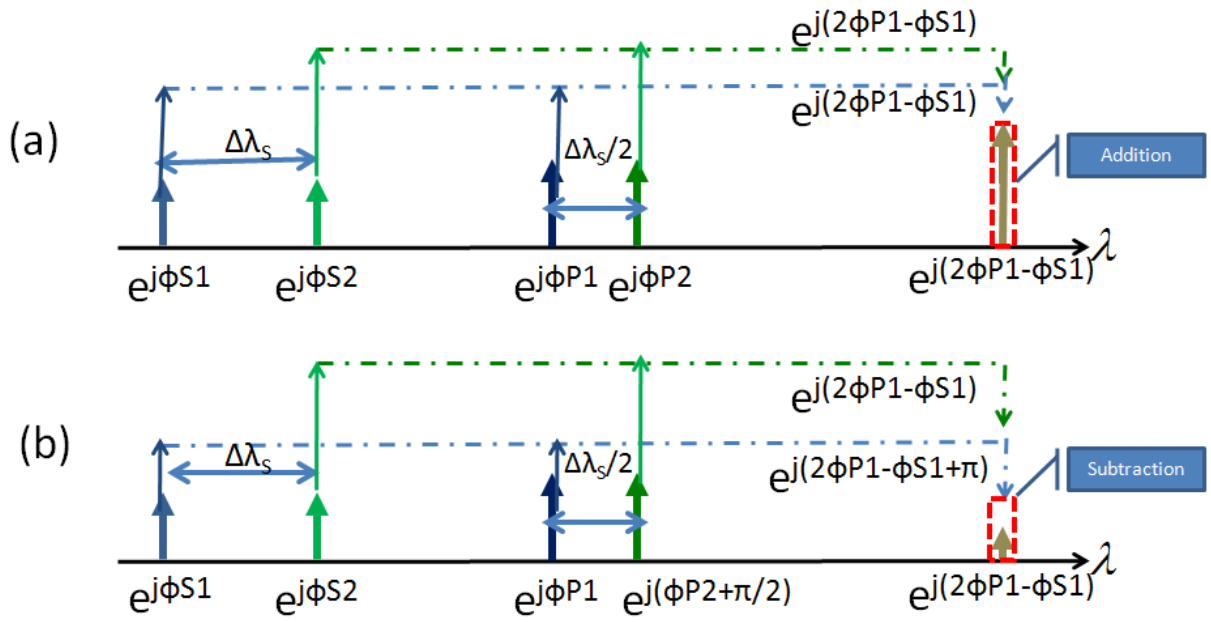


**FIGURE 6.1** Principle of operation. a) Selection of wavelengths based on the scheme in [56] for addition. b) Illustration of the subtraction process by applying a  $\pi/2$  relative phase shift to one pump wavelength.

In Figure 6.1, the signal wavelengths are  $\lambda_{S1}$  and  $\lambda_{S2}$  ( $= \lambda_{S1} + \Delta\lambda_s$ ) and the pump wavelengths are  $\lambda_{P1}$  and  $\lambda_{P2}$  ( $= \lambda_{P1} + \Delta\lambda_s/2$ ). In terms of frequency, the signal frequencies are  $\omega_{S1}$  and  $\omega_{S2}$ , where  $\omega_{S2} = \omega_{S1} + \Delta\omega_s$ , and the pump frequencies are  $\omega_{P1}$  and  $\omega_P$ , where  $\omega_{P2} = \omega_{P1} + \Delta\omega_s/2$ . Four wave mixing of  $\omega_{P1}$  and  $\omega_{S1}$  produces an idler frequency at  $2\omega_{P1} - \omega_{S1}$  ( $\approx 2\lambda_{P1} - \lambda_{S1}$ ). Likewise, FWM of  $\omega_{P2}$  and  $\omega_{S2}$  produces an idler at  $2(\omega_{P1} + \Delta\omega_s/2) - (\omega_{S1} + \Delta\omega_s) = 2\omega_{P1} + \Delta\omega_s - \omega_{S1} - \Delta\omega_s = 2\omega_{P1} - \omega_{S1}$  ( $\approx 2\lambda_{P1} - \lambda_{S1}$ ). If the pump wavelengths are in phase (Figure 6.1a), the resultant idlers add at the common wavelength. If  $\lambda_{P2}$  has a phase shift of  $\pi/2$  radians compared to  $\lambda_{P1}$  (Figure 6.1b), the mixing



product due to  $\lambda_{p2}$  has a phase shift of  $\pi$  radians compared to the mixing product due to  $\lambda_{p1}$  resulting in subtraction of the optical fields.

### 6.2.1. Simulation verification of the proposed concept

A simulation of this proposed concept was performed using *VPITransmissionMaker 9.0* software (Figure 6.2). A WDM comb generator is used as an optical source to obtain wavelengths with a deterministic phase relationship. A Waveshaper (optical processor or filter) was designed to pass signal wavelengths in one arm and pump wavelengths in the other arm. The Waveshaper can also change the phase of a pump wavelength as required. The pump and signal wavelengths are then combined and fed into a length of HNLF. The output of the HNLF contains the nonlinear FWM products. The comb generator is a mode locked laser with all the wavelengths locked in phase.

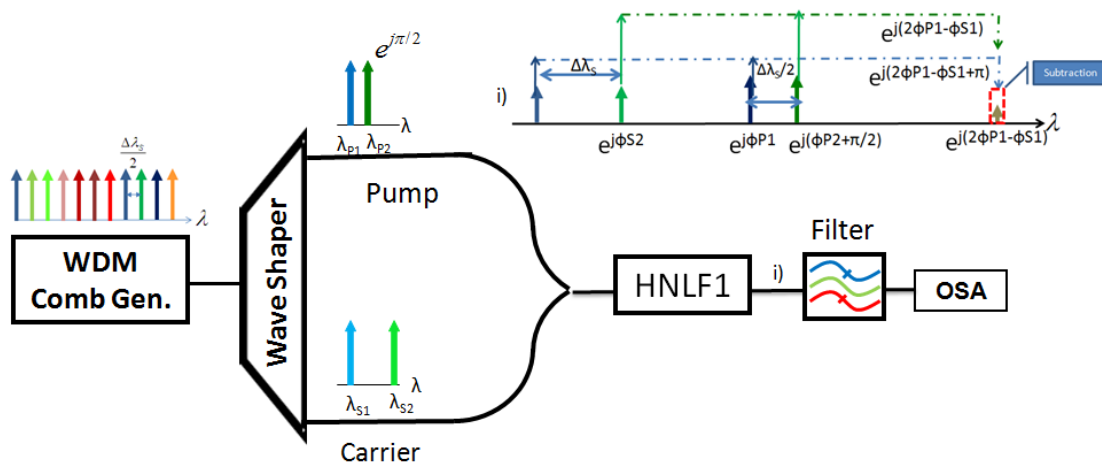
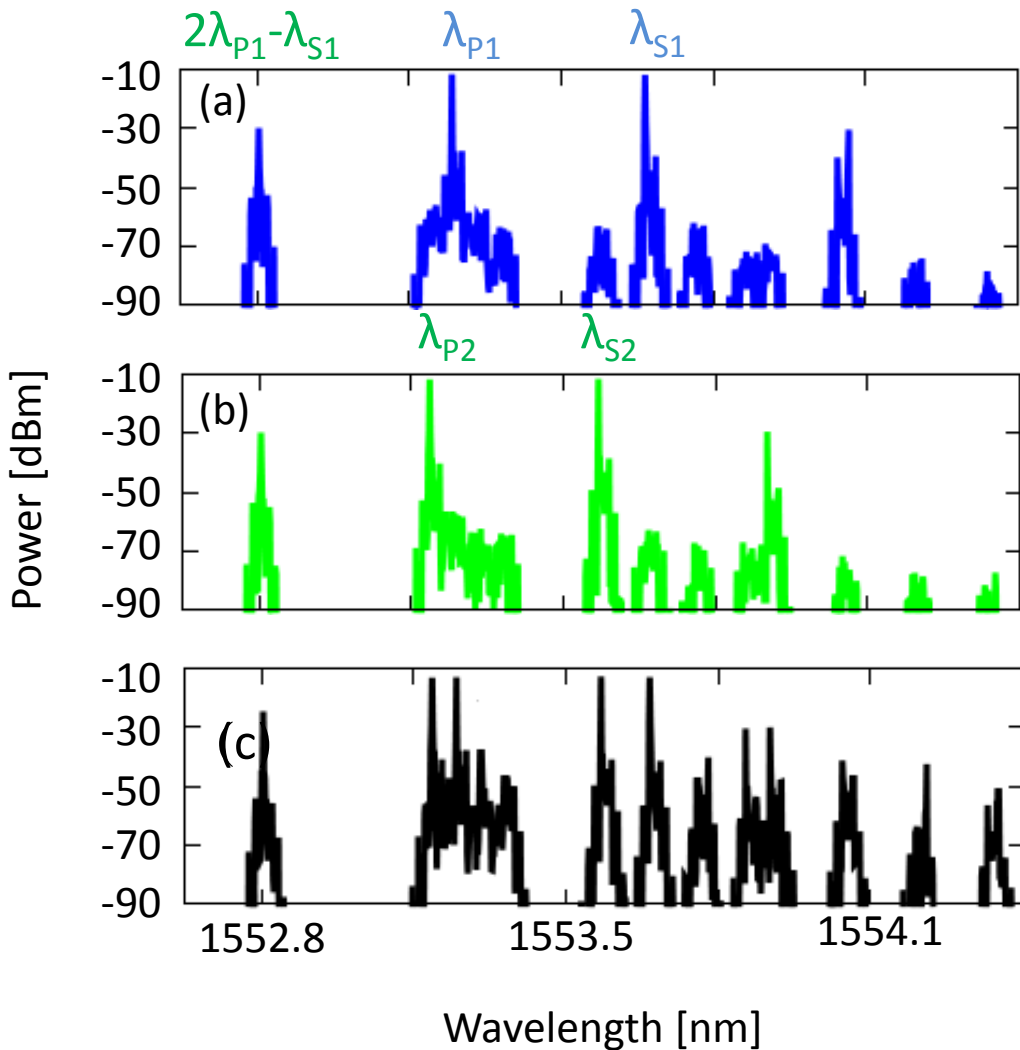


FIGURE 6.2 Simulation schematic to achieve optical subtraction.

A bandpass filter is used to pass only the mixing products at the required idler wavelength and eliminate all other wavelength components. The power level at the target idler is monitored using an OSA to observe the addition and subtraction processes.

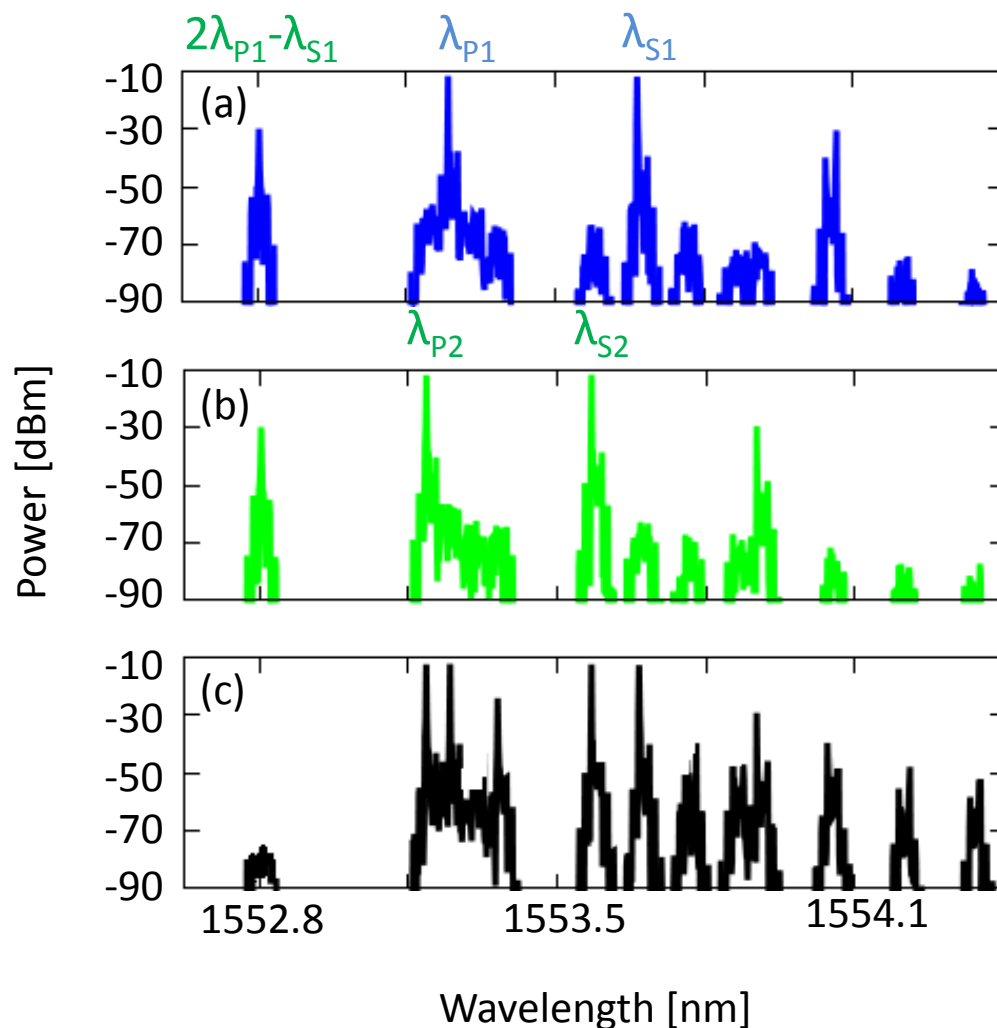
### 6.2.2. Simulation results

Figure 6.3 shows the simulation results when the signal and pump wavelengths are all in phase. In Figure 6.3a signal  $\lambda_{S1}$  and pump  $\lambda_{P1}$  mix and generate an idler at  $2\lambda_{P1}-\lambda_{S1}$  with a power level of -30 dBm. Likewise in Figure 6.3b,  $\lambda_{S2}$  and  $\lambda_{P2}$  generate an idler at the same wavelength with the same power level of -30dBm. When  $\lambda_{S1}$ ,  $\lambda_{S2}$ ,  $\lambda_{P1}$  and  $\lambda_{P2}$  are all present (Figure 6.3c), the optical fields of the two idlers add in phase, resulting in a power level of -24 dBm, a 6 dB power increase caused by a doubling of the optical field.



**FIGURE 6.3** Simulation results illustrating the addition process. a) Signal wavelength  $\lambda_{S1}$  and pump wavelength  $\lambda_{P1}$  generate an idler at  $2\lambda_{P1}-\lambda_{S1}$ . b)  $\lambda_{S2}$  and  $\lambda_{P2}$  mix and generate an idler at the same wavelength  $2\lambda_{P1}-\lambda_{S1}$ . c)  $\lambda_{S1}$ ,  $\lambda_{S2}$ ,  $\lambda_{P1}$  and  $\lambda_{P2}$  generate two idlers at the same wavelength which add in phase, producing a 6 dB increase in optical power.

Figure 6.4 shows the simulation results when the phase of pump  $\lambda_{p2}$  is phase shifted by  $90^\circ$  ( $\pi/2$  radians) with respect to  $\lambda_{p1}$ . As before, the mixing of  $\lambda_{s1}$  and  $\lambda_{p1}$  produces an idler at  $2\lambda_{p1}-\lambda_{s1}$  with a power level of -30 dBm, as does the mixing of  $\lambda_{s2}$  and  $\lambda_{p2}$ . However, the two idlers are now  $180^\circ$  ( $\pi$  radians) out of phase. When  $\lambda_{s1}$ ,  $\lambda_{s2}$ ,  $\lambda_{p1}$  and  $\lambda_{p2}$  are all present, the optical fields of the idlers subtract and produce a power level of -80 dBm.



**FIGURE 6.4** Simulation results illustrating the optical subtraction process. a) Signal wavelength  $\lambda_{s1}$  and pump wavelength  $\lambda_{p1}$  generate an idler at  $2\lambda_{p1}-\lambda_{s1}$ . b)  $\lambda_{s2}$  and  $\lambda_{p2}$ , which is  $90^\circ$  phase shifted with respect to  $\lambda_{p1}$ , generate an idler at the same wavelength as in a) but with a  $180^\circ$  phase shift. c)  $\lambda_{s1}$ ,  $\lambda_{s2}$ ,  $\lambda_{p1}$  and  $\lambda_{p2}$  mix and generate two idlers at the same wavelength which are  $180^\circ$  out of phase, producing a subtraction.

### 6.2.3. Conclusion

In this section, the concept of subtraction of optical signals using FWM has been demonstrated for the first time. This concept was presented and published in the IEEE Photonics Conference held in Bellevue, USA, in September 2013 (see Appendix IV). A discussion on the application of the concept in different real-time signal processing schemes is covered in the following sections.

## 6.3 PROPOSED CORRELATION CONCEPT

The concept of subtraction of optical signals using FWM is now demonstrated for correlation. Consider a scenario of correlation of a bit pattern with a 4 bit duration. To represent four bits, four wavelengths are to be selected to act as carrier wavelengths. These carrier wavelengths are modulated with the input electrical bit stream to be correlated and then dispersed in such a way that neighbouring wavelengths experience a relative delay of one bit duration delay between them. The template is to be represented by four pump wavelengths of equal power. Pump wavelengths representing a ‘0’ will face a  $\pi/2$  radians phase shift with respect to the wavelengths representing a ‘1’. The spacing between the pump wavelengths is selected to be half the spacing between the signal wavelengths such that the individual mixing processes generates the same unique idler wavelength [56].

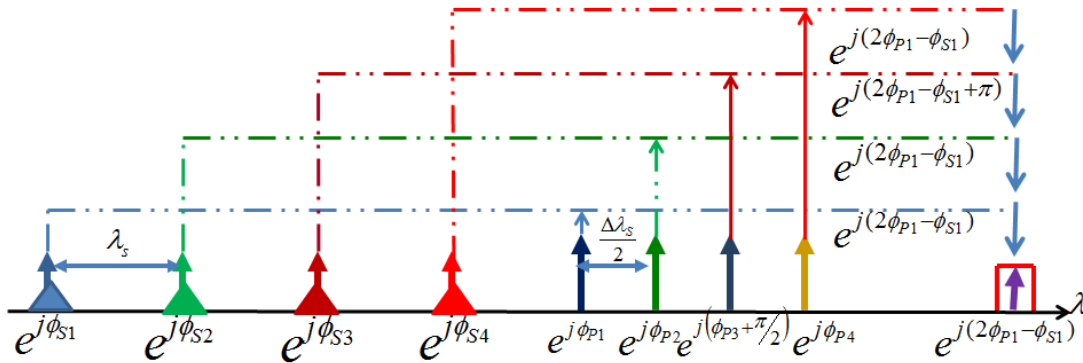
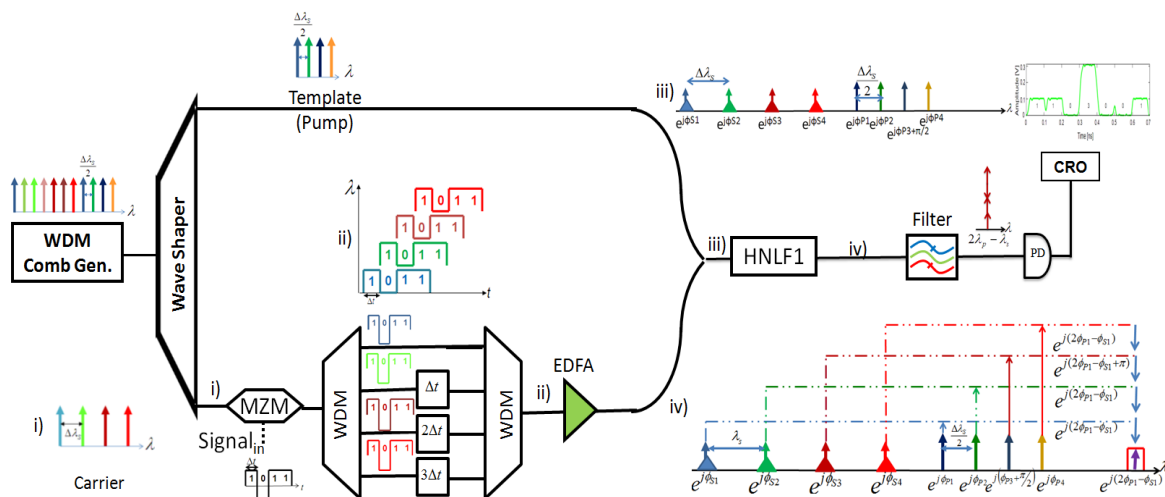


FIGURE 6.5 Principle of operation of the proposed negative accumulation based correlation with pump wavelengths representing the template 1101.

As shown in Figure 6.5 above, there are four carrier wavelengths which are each modulated by the input signal (let it be 1011, for example) and four pump wavelengths which represent the template (1101 in this case). The phase of the third pump wavelength representing the ‘0’ has a  $\pi/2$  radians phase shift with respect to the wavelengths representing a ‘1’. FWM of the carrier and pump wavelengths produces idlers at  $2\lambda_{p1}-\lambda_{s1}$  with three additive idlers and one  $180^\circ$  out of phase idler which will subtract from the others. The output at  $2\lambda_{p1}-\lambda_{s1}$  provides a correlation coefficient with negative accumulation.

### 6.3.1. Simulation using Intensity Modulation

A simulation of the proposed correlation concept was performed using “*VPITransmissionMaker 9.0*” software to validate the concept. The simulation set-up for the correlation scheme using intensity modulation to modulate the signal wavelengths is shown in Figure 6.6.



**FIGURE 6.6** Simulation set-up in VPITransmissionMaker 9.0 used to verify the negative accumulation based correlation scheme for a 4-bit duration pattern length when intensity modulation is used.

Figure 6.6 above demonstrates the correlation result when an intensity modulator is used to modulate the carrier wavelengths with the input data (in this case it is 1011). A WDM comb generator

is used to generate numerous wavelengths of equal spacing from which the carrier wavelengths and pump wavelengths were selected using a Waveshaper module. It is important to get the carrier and the pump wavelengths from the same mode locked source because it is a prerequisite of the proposed concept that all the carrier and pump wavelengths have a deterministic phase relationship and in this case, they are of the same phase.

The waveshaper module consists of filters and a phase shifter which can manipulate the phase of any input wavelength and can also process any frequency in the spatial domain. In the laboratory the waveshaper or multiport optical processor enables software control to shape any pulse or frequency comb. The WDM comb generator module was used to generate a wavelength comb with a  $\Delta\lambda_s/2$  spacing between them. The waveshaper processes the incoming wavelength comb in such a way that one output port provides 4 optical wavelengths with a  $\Delta\lambda_s$  spacing between them with no manipulation of their phase. These wavelengths represent the carrier wavelengths. The other output port has 4 optical wavelengths with  $\Delta\lambda_s/2$  spacing between them. The phase of these wavelengths can be manipulated to represent the template. In this case, to represent 1101 the phase of the third wavelength was altered to have a  $\pi/2$  radians phase difference with respect to the other wavelengths at this port. Therefore, at this output port the four pump wavelengths representing 1101 each had the same power level with one wavelength phase shifted by  $\pi/2$  radians.

The output port which provides the carrier wavelengths is connected to a quadrature biased MZM which is driven by an input 1011 bit pattern at 10 Gbps. As a result all the carrier wavelengths are modulated by the input bit stream. Since intensity modulation is utilized in this simulation the '1' is represented by the presence of optical power whereas an absence indicates a '0'. The wavelengths then face a differential delay depending on the bit position they represent and are then amplified and combined with the wavelengths representing the template before being fed into a 1 km length of HNLF. The HNLF has a nonlinear coefficient  $\gamma = 20 \text{ W}^{-1}\text{km}^{-1}$  and zero dispersion in the 1540 nm to 1560 nm range.

The FWM of pump and carrier wavelengths produces numerous idlers, but one unique idler at  $2\lambda_{P1}-\lambda_{S1}$  is produced for all individual mixings and this particular wavelength is filtered out to obtain the correlation function.

### 6.3.1.1. Characterization and Results

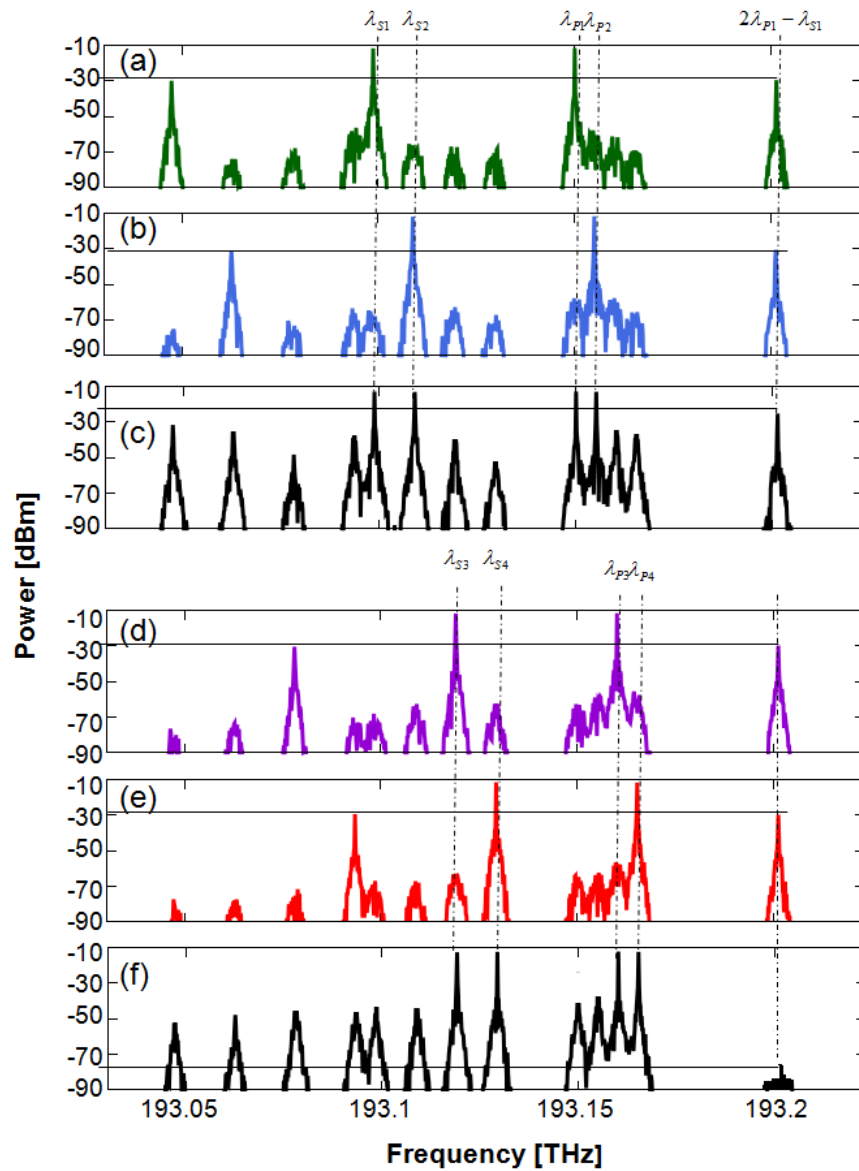


**FIGURE 6.7** Proof of concept. a) Individual mixing result of  $\lambda_{S1}$  and  $\lambda_{P1}$ . b) Individual mixing product of  $\lambda_{S2}$  and  $\lambda_{P2}$ . c) Mixing product  $\lambda_{S1}$  and  $\lambda_{P1}$ , and  $\lambda_{S2}$  and  $\lambda_{P2}$ , showing an addition when  $\lambda_{P1}$  and  $\lambda_{P2}$  are in phase. d) Individual mixing result of  $\lambda_{S3}$  and  $\lambda_{P3}$ . e) Individual mixing result of  $\lambda_{S4}$  and  $\lambda_{P4}$ . f) Mixing product of  $\lambda_{S3}$ ,  $\lambda_{P3}$ , and  $\lambda_{S4}$ ,  $\lambda_{P4}$ , showing subtraction when  $\lambda_{P3}$  is  $90^\circ$  out of phase with respect to  $\lambda_{P4}$ .

To verify the principle of operation of this system, a VPI simulation was first performed using the set-up of Figure 6.6 with no modulating signal applied to the modulator. The signal wavelengths were set to  $\lambda_{S1} = 1553.59\text{nm}$  (193.1 THz),  $\lambda_{S2} = 1553.51\text{nm}$  (193.11 THz),  $\lambda_{S3} = 1553.43\text{nm}$  (193.12 THz) and  $\lambda_{S4} = 1553.35\text{nm}$  (193.13 THz) respectively. The output power of each of these signal sources was -10 dBm. The pump wavelengths were generated from the same WDM comb generation module. The pump wavelengths were selected as 1553.19 nm (193.15 THz), 1553.15 nm (193.155 THz), 1553.11 nm (193.16 THz) and 1553.07 nm (193.165 THz) respectively for  $\lambda_{P1}$ ,  $\lambda_{P2}$ ,  $\lambda_{P3}$  and  $\lambda_{P4}$ . Experimentally, multiple pump wavelengths can be produced with a deterministic phase relationship using a mode locked laser [57]. The power level of these pump wavelengths at the input of the HNLF was also set to -10 dBm.

The FWM of the corresponding signal and pump wavelengths in the HNLF generates a common idler wavelength at 1552.79 nm (193.2 THz). Figure 6.7 (a) shows that the mixing of  $\lambda_{S1}$  and  $\lambda_{P1}$  produces an idler at the target wavelength with a power level of -30.3 dBm. Similarly,  $\lambda_{S2}$  and  $\lambda_{P2}$  produce an idler at the same wavelength with a power level of -30.11 dBm, shown in Figure 6.7 (b).

In the simulation the '0' in the template is set by manipulating the phase of the corresponding pump wavelength to be at  $90^\circ$  with respect to the other pumps using the waveshaper. With both  $\lambda_{P1}$  and  $\lambda_{P2}$  set in phase and mixed with  $\lambda_{S1}$  and  $\lambda_{S2}$ , the resultant idler was at the same target frequency with a power level of -24.87 dBm as seen in Figure 6.7 (c). Comparing this power level with the power of the individual mixing it is evident that the optical fields have added in phase which results in a 6 dB increment in the total output power. In order to verify the process of subtraction, the phase of  $\lambda_{P3}$  was set to be  $90^\circ$  out of phase with respect to  $\lambda_{P4}$ . These pump wavelengths were mixed with  $\lambda_{S3}$  and  $\lambda_{S4}$  to produce an idler at the target wavelength with a power level of only -75dBm as depicted in Figure 6.7 (f). This is much less than the power level achieved in the individual mixing process.

The next step was to apply the 1011 modulating signal to the Mach-Zehnder modulator. Intensity modulation was used to modulate the signal wavelengths at 10 Gb/s. After modulation each



of the four wavelengths represent 1011 by the presence or absence of optical power and are delayed based on their bit position as seen at Figure 6.6 (ii). The modulated carriers are then combined with the template wavelengths 1101 where '0' is represented by the same power level as a '1' but with a  $\pi/2$  radians phase shift with respect to the wavelengths representing the '1's. The mixing products follow the concept of Figure 6.7. After filtering of the required idler wavelengths and detection by the photoreceiver, the detected electrical waveforms due to each mixing term are shown in Figure 6.8. Figures 6.8 (a), (b), (c) and (d) show the detected waveforms for individual mixings. Figure 6.8 (e) shows the combined mixing product, which is a summation of Figures 6.8 (a)-(d), and which is a representation of the correlation function. It is to be noted that Figure 6.8 (c) represents the mixing product which involves the template wavelength representing '0'. The mixing product has a  $\pi$  radians phase difference with respect to other mixing products and therefore is subtracted from the other additive signals.

When the input bit pattern matches the template pattern, as is the case here, a correlation peak occurs at the middle of the correlation function. The peak value of the correlation function is three units, corresponding to the number of '1's in the template. This approach provides a correlation function with fewer unwanted 'noise' peaks and an improved noise floor compared to that obtained for the correlation scheme described in Chapter 4. This is because some of the noise bits (unwanted peaks) are cancelled in the subtraction process. For this technique a template wavelength representing a '0' is phase shifted and FWM can result in a '-1' at the output which can cancel an unwanted '1'.

When the input bit stream does not match the template pattern, the peak value of the correlation function is less than the maximum value of three units. Figure 6.9 shows the detected waveforms for a mismatched condition with an input bit stream of 1100 and the template remains 1101. In this case, a peak value of 2 units is reached in the correlation function, which indicates a mismatch, and there is no correlation peak in the middle of the correlation function.

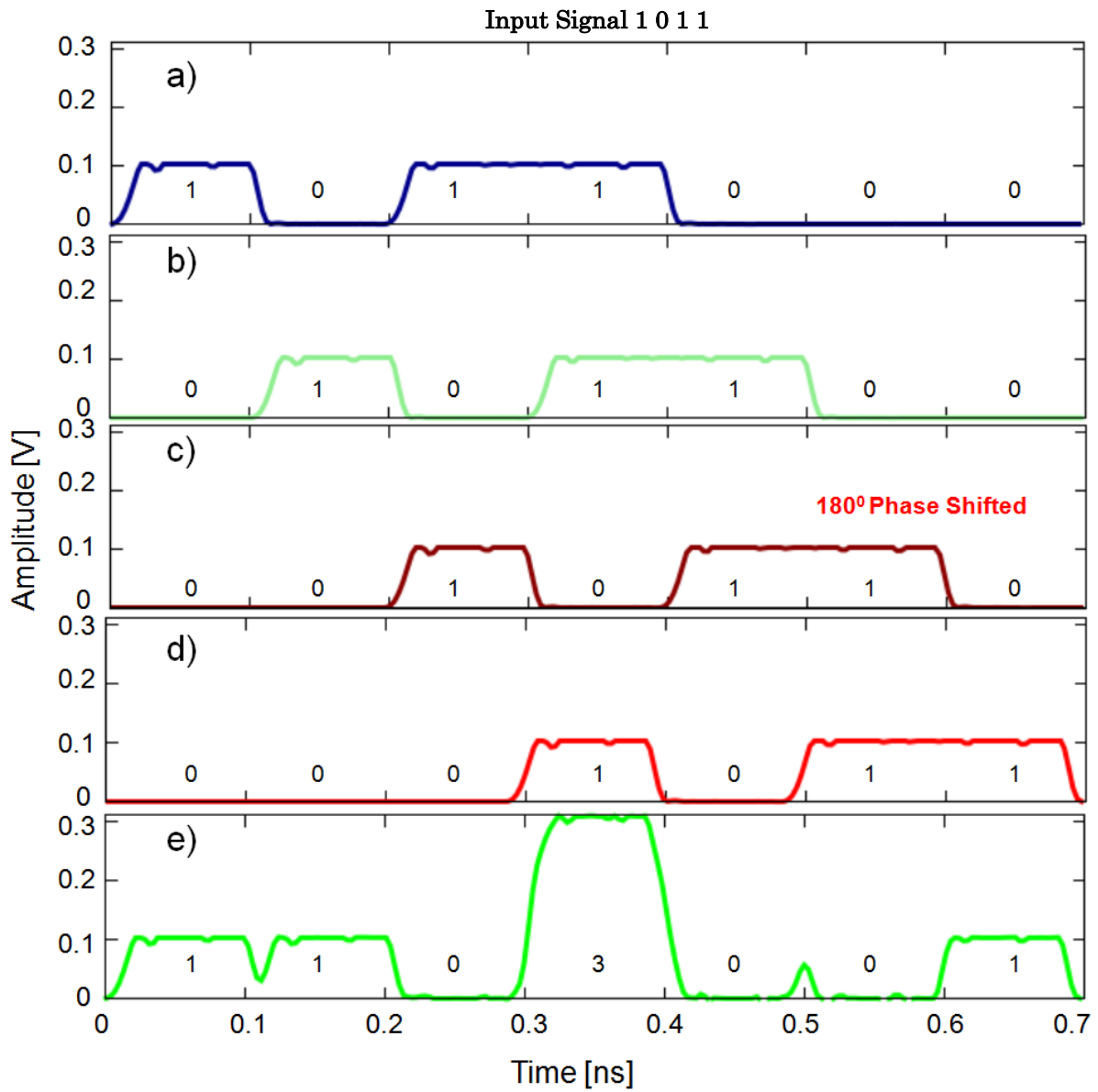


**FIGURE 6.8** Detected electrical waveforms for the matched condition due to the a) mixing of  $\lambda_{S1}$  and  $\lambda_{P1}$ , b) mixing of  $\lambda_{S2}$  and  $\lambda_{P2}$ , c) mixing of  $\lambda_{S3}$  and  $\lambda_{P3}$ , d) mixing of  $\lambda_{S4}$  and  $\lambda_{P4}$  and e) the output correlation function which is a summation of plots a) – d).

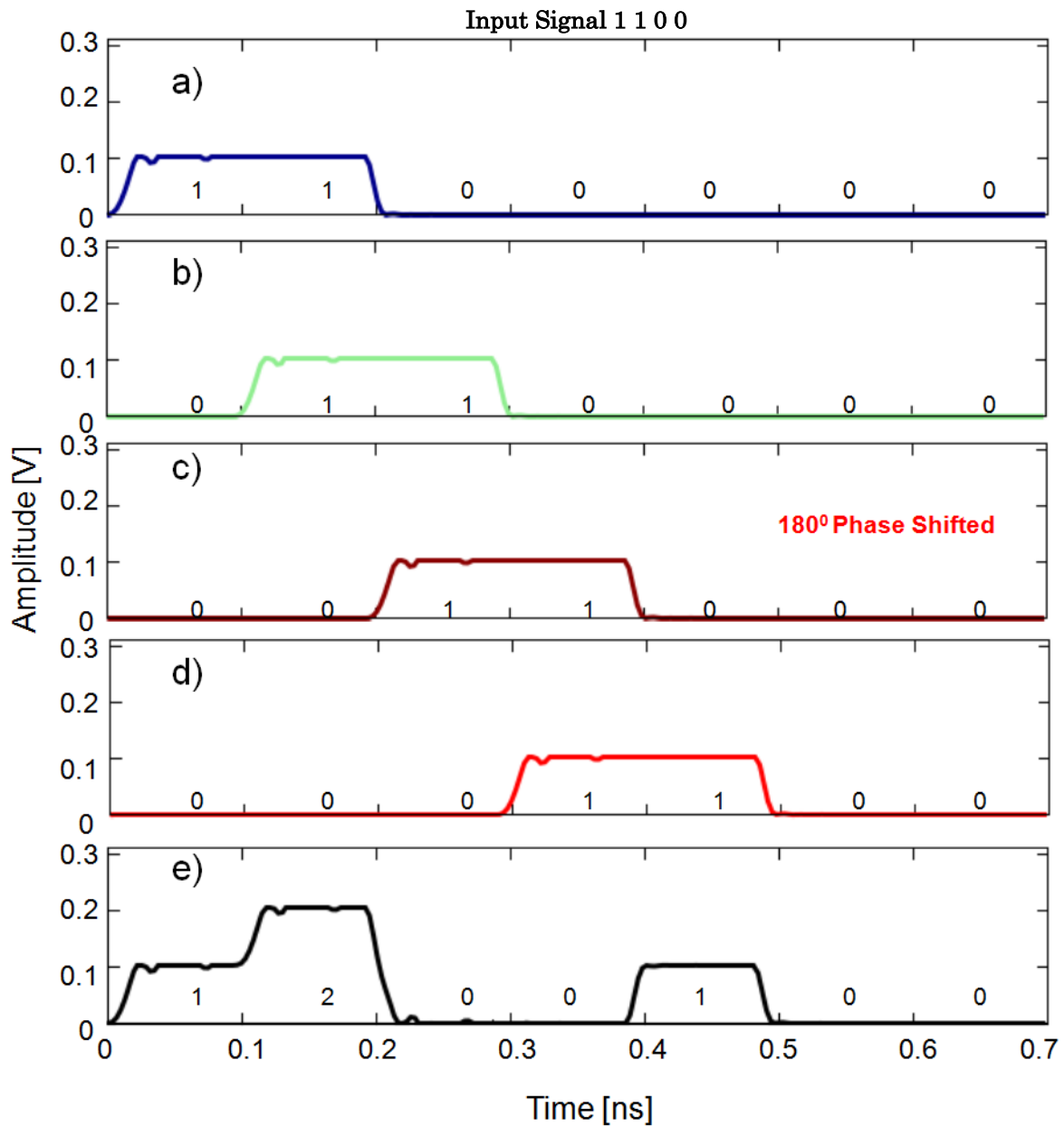


FIGURE 6.9 Detected electrical waveform for a mismatched condition due to the a) mixing of  $\lambda_{S1}$  and  $\lambda_{P1}$ , b) mixing of  $\lambda_{S2}$  and  $\lambda_{P2}$ , c) mixing  $\lambda_{S3}$  and  $\lambda_{P3}$ , d) mixing of  $\lambda_{S4}$  and  $\lambda_{P4}$  and e) the output correlation function which is a summation of plots a) – d).

Figure 6.10 represents the correlation function realised when the modulating signal is a pseudorandom 10 Gb/s bit stream. The bit stream is continually compared with the template. A match between any 4 input bits and the template is indicated when the correlation function reaches a maximum value of 3 units.

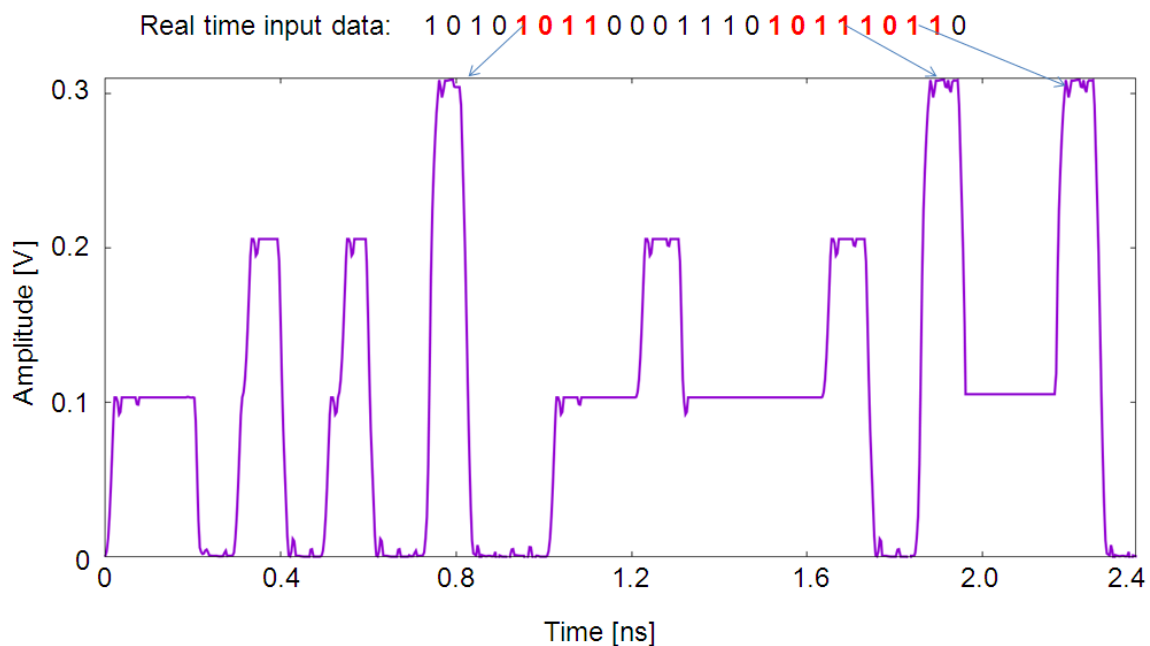


FIGURE 6.10 Output correlation function obtained for a real time 10Gb/s input bit stream.

### 6.3.1.2. Conclusion

Using this correlation approach a significant improvement of the noise floor is achievable by utilizing the cancellation of unwanted bits in the correlation function. However the ultimate contrast is not much better than previously demonstrated correlation schemes. A truth table exercise predicted that a significant improvement in correlation contrast is achievable by using phase modulation (PM) instead of intensity modulation. The next section examines the simulation results obtained using a phase modulator in place of the MZM to modulate the carrier wavelengths.

### 6.3.2. Simulation using Phase Modulation

Using intensity modulation of the signal wavelengths in the approach outlined above, even though a significant improvement of the noise floor is achievable through cancellation of unwanted bits in the correlation function, the ultimate contrast is not much better than previously demonstrated

correlation schemes [9, 24, 27, 29, 38]. This section examines the simulation results obtained using a phase modulator in place of the MZM to modulate the carrier wavelength, keeping the rest of the set-up unchanged. Using phase modulation a ‘1’ is represented by a +ve 1 and a ‘0’ is represented by a –ve 1. The carrier wavelengths are now modulated with input electrical bitstream of 1011 using the PM. The carrier wavelengths are now modulated with input electrical bitstream of 1011 using the PM. The simulation was designed as shown in Figure 6.11.

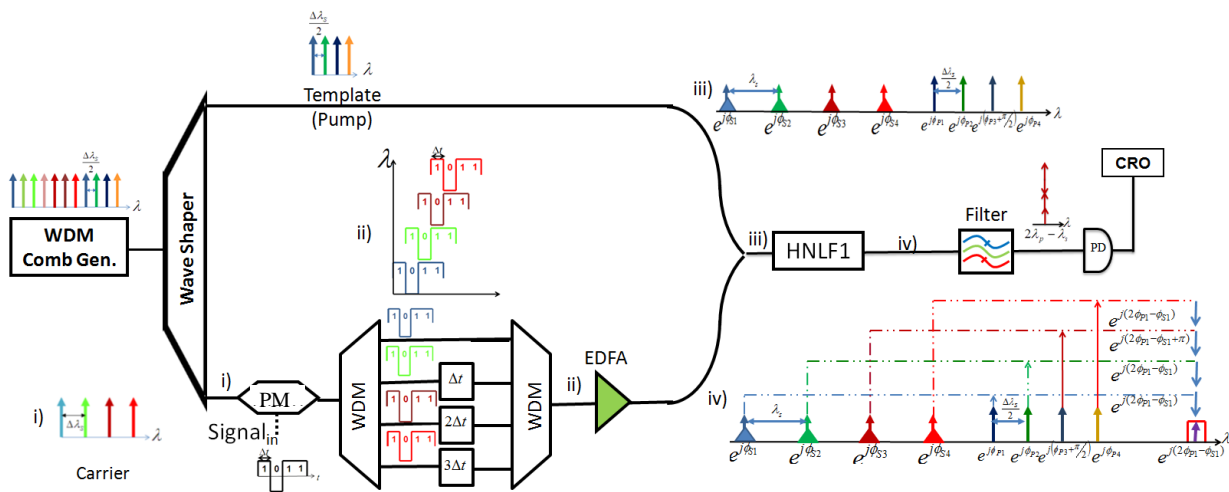


**FIGURE 6.11** Simulation set-up in VPItransmissionMaker 9.0 to verify a negative accumulation based correlation scheme for a 4-bit duration pattern length when a phase modulator (PM) is used.

### 6.3.2.1. Characterization and results

Using the set-up of Fig. 6.11 the four carrier wavelengths are modulated by a phase modulator with an input modulating signal of 1011. After modulation each of the four wavelengths is delayed based on their bit position as shown at Figure 6.11 (ii). The modulated carriers are then combined with the template wavelengths representing 1101 where ‘0’ is represented by the same power level as a ‘1’ but with a  $\pi/2$  radians phase shift with respect to the wavelengths representing the ‘1’s. The mixing products follow the concept of Figure 6.7. The wavelength representing ‘0’ in the template generates a mixing product which has a  $\pi$  radians phase difference with respect to the other mixing products and therefore is subtracted from the other additive signals. This approach produces a

correlation function with reduced noise peaks and an improved noise floor as some of the noise bits (unwanted peaks) were cancelled in the subtraction process.

Figures 6.12 (a), (b), (c) and (d) show the optical signal detected at the target wavelength due to each mixing term when the input signal is matched with the template 1101. Figure 6.12 (e) shows the correlation function which has a peak value of 4 units. This peak is higher than the peak value of 3 units achieved using intensity modulation of the signal wavelengths and achieved by earlier correlation techniques. This can be explained by performing a “truth table” exercise, as seen in Table 6.1 where intensity modulation and phase modulation for the matched case are compared. Using phase modulation of the carrier wavelengths, a ‘0’ is represented by a signal with a  $180^\circ$  phase shift. This mixes with a phase shifted pump wavelength to produce a ‘1’ where previously there was no signal. Also, the correlation peak reached to a value proportional to the number of bits in the pattern which is another improvement with respect to previous correlation methods where the correlation peak reaches a value proportional only to the number of 1’s in the bit pattern. Once again, for this technique, a template wavelength representing a ‘0’ is phase shifted and FWM can result in a ‘-1’ at the output which can cancel an unwanted ‘1’. Table 6.1 below shows the improvement which occurs in terms of noise cancellation (unwanted ‘1’s cancel) by using phase modulation instead of intensity modulation. Appendix 1 shows a “truth table” exercise which presents the expected received optical signal using phase modulation of the carrier wavelengths for all possible input bit patterns when the template bit pattern is 1101.

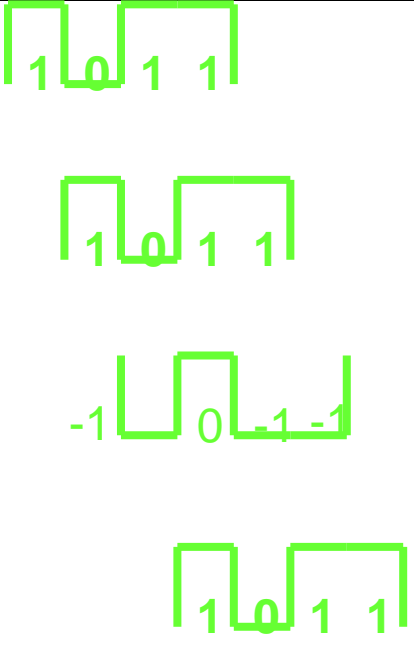
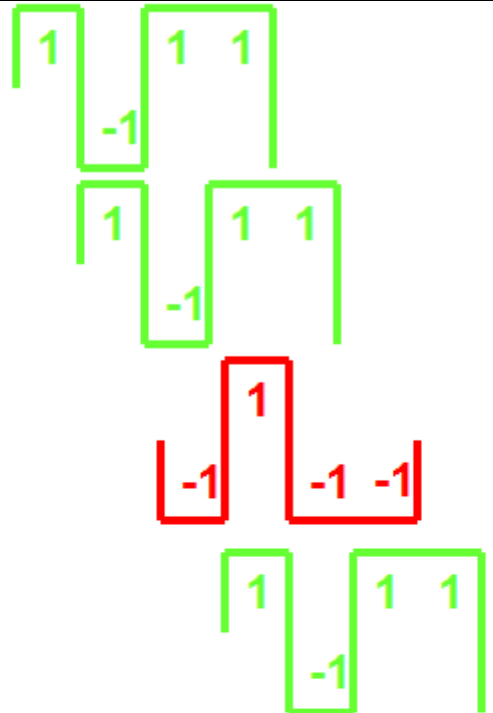
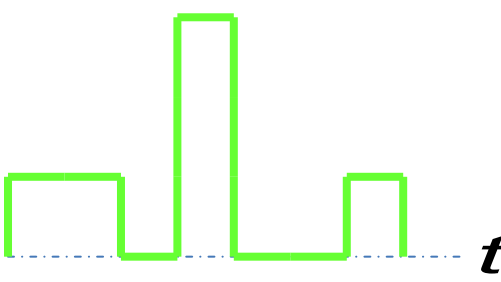
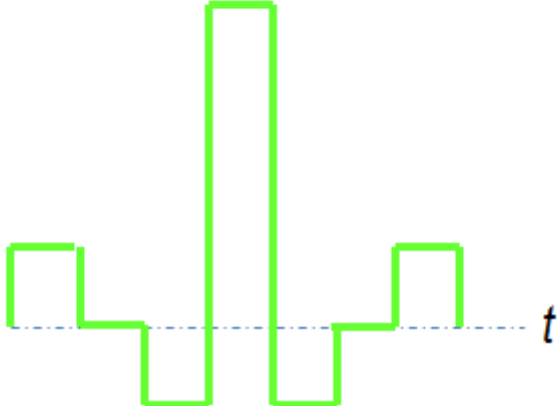
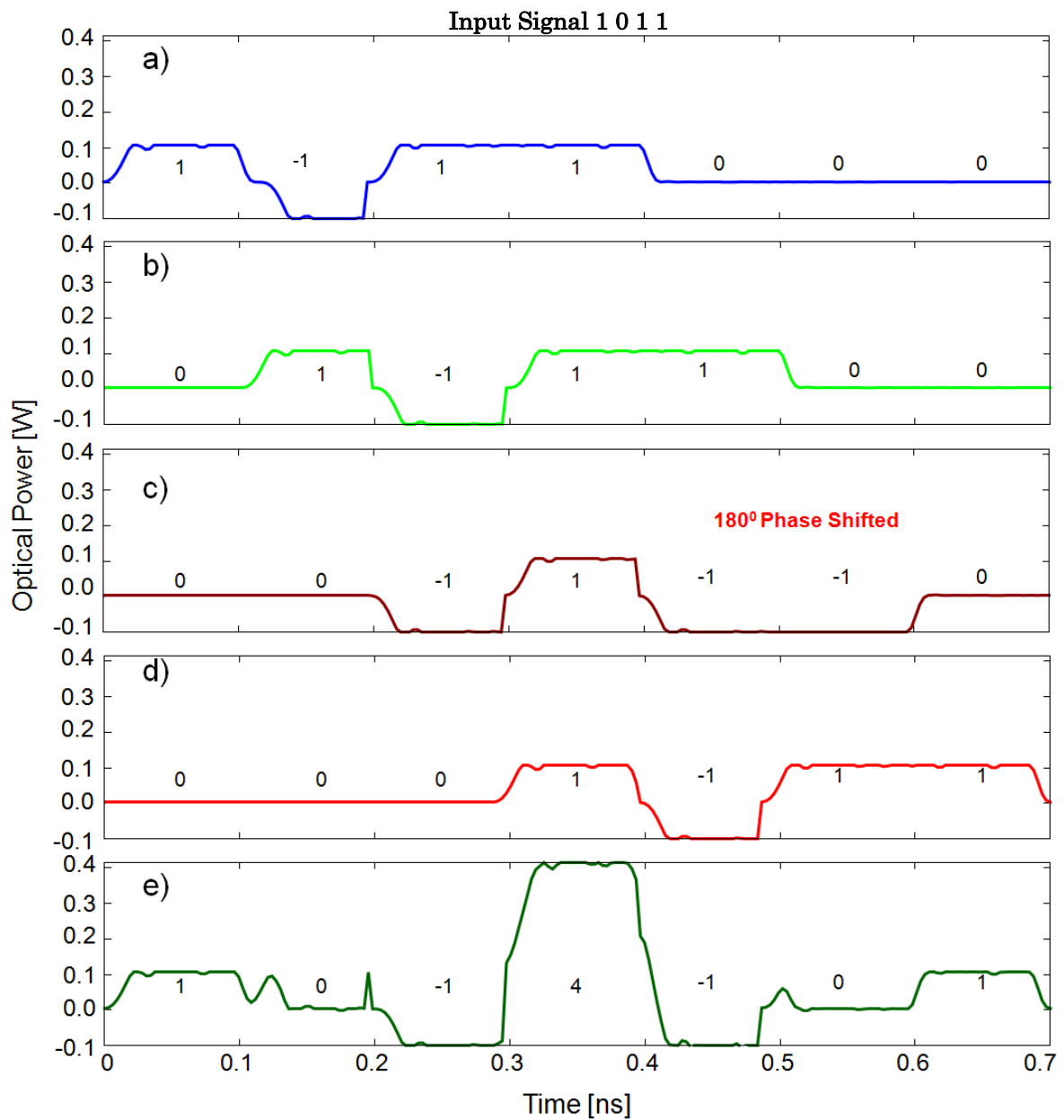
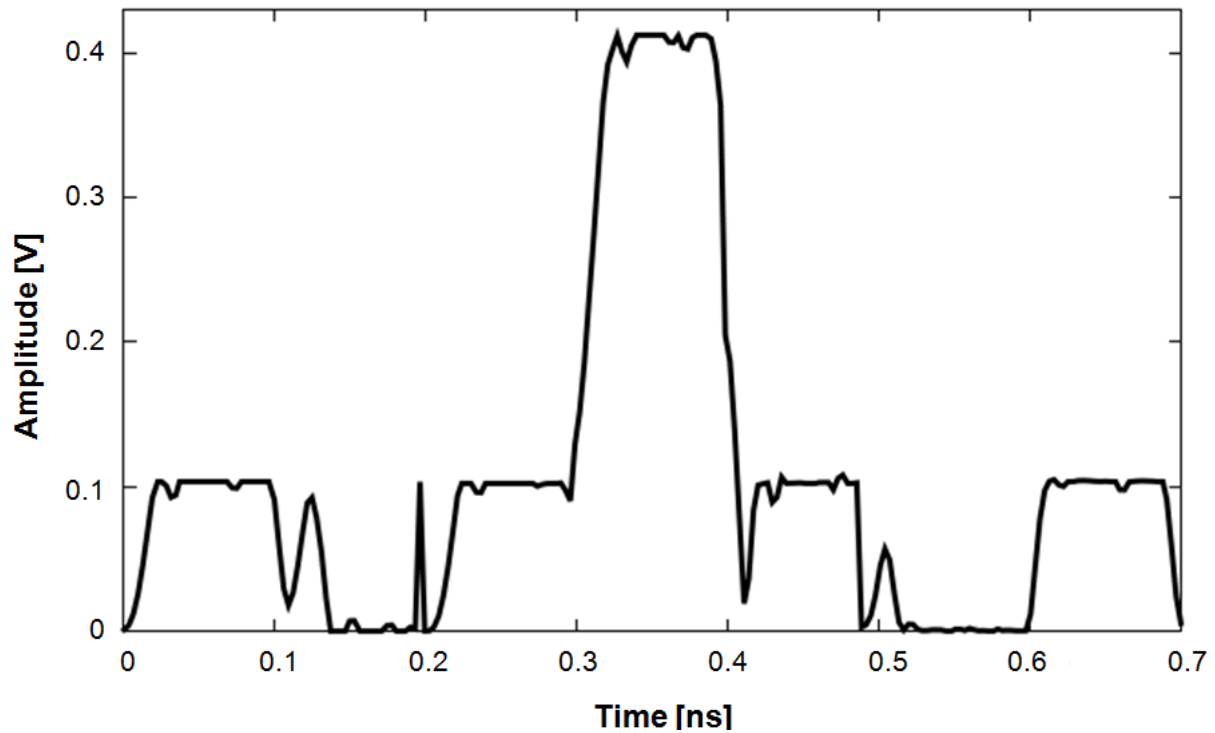
Intensity Modulation for the matched condition 1011	Phase Modulation for the matched condition 1011
	
	

Table 6.1 “Truth table” comparison of intensity modulation and phase modulation showing optical waveforms for each wavelength and the resultant optical waveform for the matched case.



**FIGURE 6.12** Received Optical waveforms for the matched condition at the target wavelength due to the a) mixing of  $\lambda_{S1}$  and  $\lambda_{P1}$ , b) mixing of  $\lambda_{S2}$  and  $\lambda_{P2}$ , c) mixing of  $\lambda_{S3}$  and  $\lambda_{P3}$ , d) mixing of  $\lambda_{S4}$  and  $\lambda_{P4}$  and e) the output correlation function with negative accumulation which is a summation of plots a) – d).





**FIGURE 6.13** Detected electrical waveform at the output of the Photoreceiver.

Figure 6.13 shows detected electrical waveform due to the resultant optical waveform for the matched case. As is visible in the figure the correlation peak reached a value of 4 units which is larger than the maximum achievable 3 units for the intensity modulation case.

Figure 6.14 shows the optical waveforms for the worst case mismatched condition with the input pattern of 1001. Like Figure 6.12, here in Figure 6.14 all the individual mixing products are demonstrated in (a) – (d). Figure 6.14 (e) shows the correlation function with a peak value of 2 units which is the worst possible mismatched condition. It is important to note that although optical power is always positive, the phase of the optical field is changing.

Input Signal 1 0 0 1

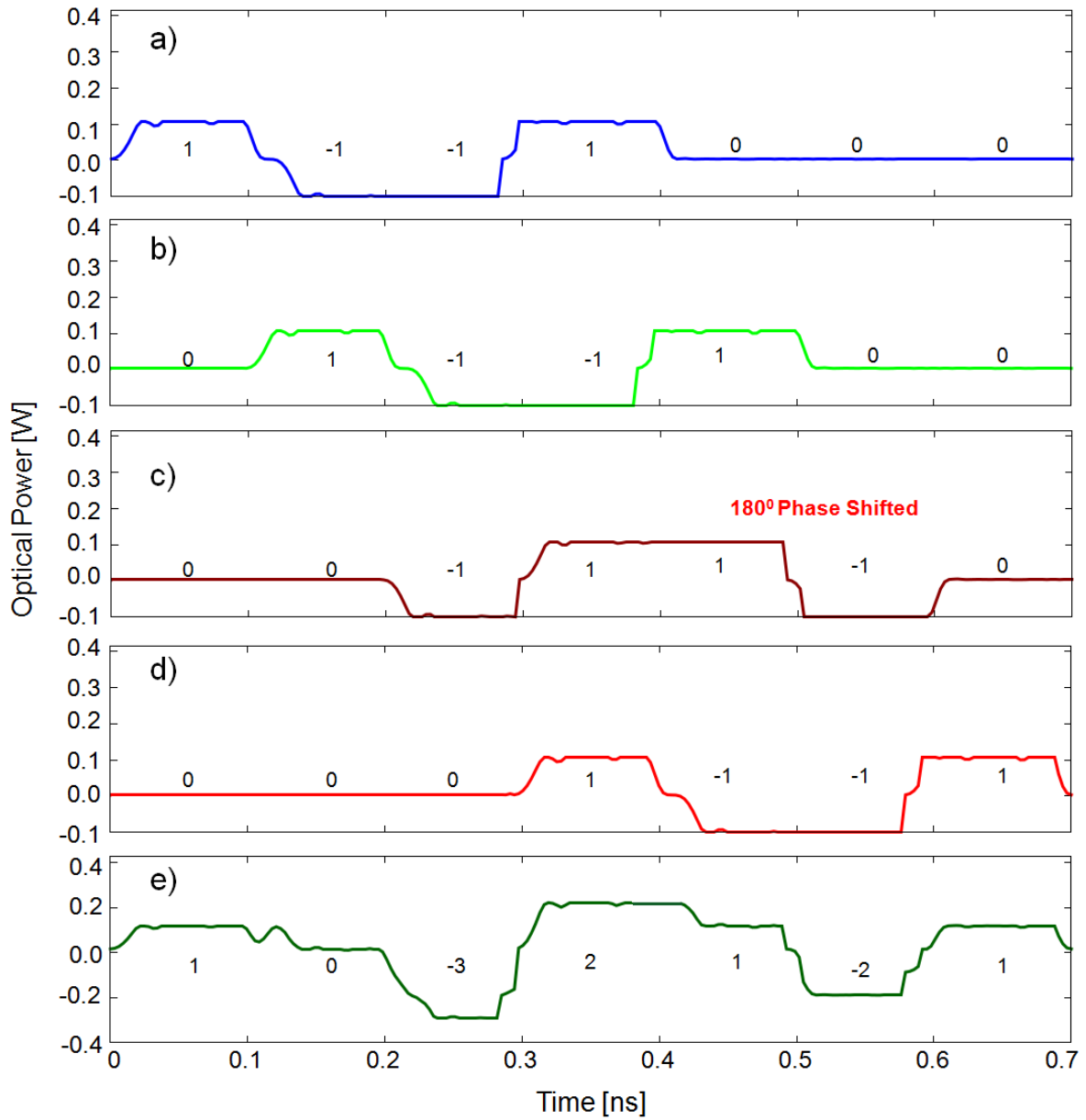


FIGURE 6.14 Received optical waveforms for a mismatched condition due to the. a) mixing of  $\lambda_{S1}$  and  $\lambda_{P1}$ , b) mixing of  $\lambda_{S2}$  and  $\lambda_{P2}$ , c) mixing of  $\lambda_{S3}$  and  $\lambda_{P3}$ , d) mixing of  $\lambda_{S4}$  and  $\lambda_{P4}$  and e) the output correlation function with negative accumulation which is a summation of plots a) – d).

## 6.4 CONCLUSION

In this chapter a novel technique to achieve subtraction of optical fields based on four wave mixing and the use of a common target idler wavelength has been presented. Changing the relative phase of a pump wavelength can change the sign of the field at the idler wavelength causing addition or subtraction of signals. This concept has been used to demonstrate a new photonic correlation scheme where signal wavelengths are modulated by an input electrical bit stream and are then differentially delayed before being mixed with pump wavelengths representing a reference or template bit pattern in a length of highly nonlinear optical fiber. The technique provides negative accumulation in the correlation function.

This technique has been demonstrated using *VPItransmissionMaker 9.0* based simulations. Both intensity modulation and phase modulation of the signal carrier wavelengths by the input bit pattern have been performed. The technique produces a correlation function with enhanced contrast between the correlation peak and other unwanted peaks due to cancellation in the subtraction process. Phase modulation shows an even larger difference between the correlation peak of matched and unmatched signals compared with other photonic correlation techniques previously demonstrated. Unlike the previously demonstrated schemes in Chapter 4 and 5 or other existing schemes, this scheme does not rely on the addition of optical power. So, the noise power of unwanted bits does not increase as the number of bits  $N$  increases. Rather, in most of the cases, a higher number of 1's can lead to a higher number of cancellations and hence improved contrast. Using this scheme, as the number of bits increases there can be a higher number of cancellations which leads to enhanced contrast between the correlation peak and other unwanted peaks. The maximum number of lags ' $N$ ' is however limited depending on the range of wavelengths where the fibre dispersion in the HNLFF is zero, and hence the FWM has maximum efficiency, and the minimum achievable wavelength separation which is determined by the filter resolution of the Waveshaper. In this case, the zero dispersion range of the HNLFF is from 1540nm to 1560nm which is 20nm. The best achievable separation is 20GHz or 0.16nm. This defines that the proposed system with the current available

equipment is limited to a maximum of 125 bits (20nm/0.16nm). For the HNLF the dispersion in the 1540-1560nm was not zero but very small (-0.19 ps/nm-km)

A paper on the subtraction principle was presented at the 2013 IEEE Photonics Conference titled "*Optical Subtraction using Nonlinear Mixing*" (see Appendix IV) . Further to this, the suggested negative accumulation based correlation concept has been published in the IEEE Photonics Journal under the title "*A Photonic Correlation Scheme Using FWM with Phase Management to Achieve Optical Subtraction*" (see Appendix V).

## **7. CONCLUSION AND FUTURE WORK**

The aim of this thesis research was to investigate the use of nonlinear four wave mixing (FWM) in highly nonlinear optical fibre (HNLF) in order to achieve correlation of an input bit stream with a reference template pattern. A secondary goal was to employ FWM to realize negative accumulation optically in a correlator and thus remove the need for the use of electronic processing when subtraction between optical signals is required.

A novel correlation technique using FWM was proposed and experimentally demonstrated. A refinement of the system allowed software control of the reference bit pattern and allowed remoting of the input bit stream. Furthermore, a novel concept for the subtraction of optical powers based on FWM with phase management of pump wavelengths was proposed and analysed. Simulation of a correlator based on this technique using VPItransmissionMaker software showed better contrast compared to previously demonstrated photonic correlation schemes. A summary of each of these achievements is given below.

### **7.1 OUTCOMES OF THE WORK**

In Chapter 4 of this thesis, a novel photonic correlation technique based on matched filtering using four wave mixing in a length of highly nonlinear optical fibre was proposed and demonstrated experimentally for the first time. The technique uses FWM to mix a number of CW laser wavelengths with a pump wavelength which has been modulated by an input bit stream in order to produce copies of the input signal at the output idler wavelengths. Photonic correlation of a 4 bit input signal with a reference bit pattern was demonstrated. Although the technique was demonstrated using only a 4 bit pattern, it is important to note that the technique is scalable to larger bit patterns. The relatively small bit pattern length of 4 bits was a limitation of the number of output ports on the Waveshaper processor

which was used to filter out the idler wavelengths, each representing a bit. A multiport Waveshaper would enable the filtering of more wavelengths, allowing more bits in the bit pattern.

It was also noted that in the experimental demonstration a fibre delay network was used to generate the required wavelength dependent time delays corresponding to multiples of a bit period instead of using a dispersive fibre. This limitation was because the concept was demonstrated with a bit rate of only 100 Mb/s due to the unavailability of a high speed pattern generator. At much higher bit rates the use of a dispersive fibre to achieve the required time delays would be easier and exhibit much less insertion loss than using the fiber delay network which was used here.

The work described in Chapter 4 was presented at the 2012 IEEE Topical Meeting on Microwave Photonics held at Noordwijk, The Netherlands, in September 2012. The paper was titled “*Nonlinear Mixing Based Photonic Correlation*” (see Appendix II).

In Chapter 5, a further improvement to the nonlinear mixing based scheme was described and experimentally demonstrated. This refinement used a software controlled optical processor to select the template bit pattern. This is an advance on state-of-the-art photonic correlators in the literature which select optical wavelengths to represent a template bit pattern by physically turning lasers ON or OFF. This new approach allows the pump wavelength to be modulated with the input bit pattern and transmitted from a remote location for correlation. This work was published in IEEE Photonics Technology Letters in a paper titled “*HNLB Based Photonic Pattern Recognition using Remote Transmitter*” (see Appendix III).

In Chapter 6 a novel scheme to achieve subtraction of two optical signals based on four wave mixing with phase management of pump wavelengths was proposed and demonstrated. The scheme involves changing the phase of a pump wavelength by  $90^\circ$  ( $\pi/2$  radians) which produces an idler wavelength with a  $180^\circ$  ( $\pi$  radians) phase shift with respect to other idlers at the same wavelength. The scheme was successfully demonstrated using VPItransmissionMaker 9.0 simulations. This work was presented at the 2013 IEEE Photonics Conference in September 2013 in a paper titled “*Optical Subtraction using Nonlinear Mixing*” (see Appendix IV).

This subtraction principle was then utilized in a new photonic correlation scheme which achieves subtraction of optical fields and hence allows accumulation of negative signals. This correlation scheme was demonstrated using VPItransmissionMaker 9.0 simulations at a bit rate of 10Gb/s and was shown to give better contrast and noise floor with respect to previously demonstrated photonic correlation schemes. Both intensity modulation and phase modulation of carrier wavelengths was investigated.

This work was published in the IEEE Photonics Journal in December 2013 in a paper titled “*A Photonic Correlation Scheme Using FWM with Phase Management to Achieve Optical Subtraction*” (see Appendix V).

## **7.2 FUTURE WORK**

Successful research always leads to some further development. The initial aim of the current research presented here was to exploit FWM to implement a correlation scheme and then to achieve negative accumulation optically utilizing the mixing process. The outcome of the experiments described here prove that the initial aim has been achieved. However, to meet the challenge presented by only having a low speed electronic pattern generator, the system required a lot of manipulation especially on the dispersion based delay network and it was only tested for a 100 Mbps data rate. The reason for using FWM in the research is that FWM has been shown to work well for very high speed signals in other applications. An obvious area for future work is to demonstrate the correlation scheme at much higher bit rates using a high speed pattern generator and the dispersion in a length of fibre to achieve the required time delays. Operation with longer bit patterns and should also be investigated.

The simulation results of the negative accumulation based correlation scheme provided evidence of achieving all-optical subtraction and showed an improvement in the correlation contrast as well as the noise floor of the correlation function. An experimental verification of the concept is yet to be done and further applications of the concept are yet to be considered. The use of a correlator with

negative accumulation in an application such as serial time-encoded amplified microscopy (STEAM) will be an exciting forthcoming research in ultrafast image processing.

### **7.3 CONCLUSION**

In conclusion, a new nonlinear mixing based correlation technique has been proposed and demonstrated. The technique allows remoting of the transmitter. It has been proposed as a part of future work that a test using a high speed data rate is to be performed and work will continue on improving the correlation contrast. All optical subtraction has been demonstrated using VPI simulations at a data rate of 10 Gbps. A quantitative analysis of the concept is yet to be done experimentally. With a more refined model it may be possible to explore the use of this correlation technique in various applications including STEAM and ultrafast real time image processing.



## **LIST OF ACRONYMS**

### **A**

AWG	Arrayed Wavelength Grating
ASE	Amplified Spontaneous Emission

### **B**

BW	Bandwidth
----	-----------

### **D**

DE	Dispersive element
----	--------------------

### **E**

E/O	Electrical-to-optical conversion
EOM	Electro-optic modulator
EDFA	Erbium-doped fibre amplifier

### **F**

FBG	Fibre Bragg grating
FT	Fourier transforms
FWM	Four wave mixing

### **G**

GVD	Group velocity dispersion
-----	---------------------------

### **H**

HNLF	Highly nonlinear fibre
------	------------------------

## **I**

IM Intensity modulator

## **M**

MLL Mode-locked laser

MZM Mach-Zehnder modulator

## **O**

O/E Optical-to-electrical conversion

## **P**

PC Polarization controller

PD Photodiode

PS-FBG Phase shifted fibre Bragg grating

PM Phase modulator

PM-IM Phase-modulation to intensity-modulation

## **R**

RF Radio frequency

## **S**

SBS Stimulated Brillouin scattering

SPM Self-phase modulation

SOA Semiconductor optical amplifier

STEAM Serial Time Encoded Amplified Microscopy

## **X**

XPM Cross-phase modulation

## REFERENCES:

- [1] J. Capmany, B. Ortega, and D. Pastor, "A tutorial on microwave photonic filters," *Journal of Lightwave Technology*, vol. 24, pp. 201-229, 2006.
- [2] J. P. Yao, "Microwave Photonics," *Journal of Lightwave Technology*, vol. 27, pp. 314-335, Jan-Feb 2009.
- [3] K. Wilner and A. P. V. D. Heuvel, "Fiber-optic delay lines for microwave signal processing," *Proc. IEEE*, vol. 64, p. 3, 1976.
- [4] A. Loayssa, J. Capmany, M. Sagues, and J. Mora, "Demonstration of incoherent microwave photonic filters with all-optical complex coefficients," *IEEE Photonic Technology Letters*, vol. 18, pp. 1744-1746, 2006.
- [5] J. Capmany and D. Novak, "Microwave photonics combines two worlds," *Nature Photonics*, vol. 1, pp. 319-330, Jun 2007.
- [6] A. J. Seeds and K. J. Williams, "Microwave photonics," *Journal of Lightwave Technology*, vol. 24, pp. 4628-4641, Dec 2006.
- [7] J. G. Liu, T. H. Cheng, Y. K. Yeo, Y. X. Wang, L. F. Xue, N. H. Zhu, *et al.*, "All-optical continuously tunable delay with a high linear-chirp-rate fiber Bragg grating based on four-wave mixing in a highly-nonlinear photonic crystal fiber," *Optics Communications*, vol. 282, pp. 4366-4369, Nov 15 2009.
- [8] M. D. P. Lam A. Bui , Trung D. Vo , Niusha Sarkhosh , Hossein Emami , Benjamin J. Eggleton , and Arnan Mitchell "Instantaneous frequency measurement system using optical mixing in highly nonlinear fiber," *Optics Express*, vol. 17, pp. 22983-22991 2009.
- [9] Y. Dai and J. Yao, "Microwave Correlator Based on a Nonuniformly Spaced Photonic Microwave Delay-Line Filter," *IEEE Photonic Technology Letters*, vol. 21, pp. 969-971, 2009.
- [10] S. Xiao and A. M. Weiner, "Coherent photonic processing of microwave signals using spatial light modulator: programmable amplitude filters," *Journal of Lightwave Technology*, vol. 24, pp. 2523-2529, 2006.
- [11] J. Mora, S. Sales, M. D. Manzanedo, R. Garcia-Olcina, J. Capmany, B. Ortega, *et al.*, "Continuous tuning of photonic transversal filter based on the modification of tapped weights," *IEEE Photonic Technology Letters*, vol. 18, pp. 1594-1596, 2006.
- [12] M. Sagues, R. G. Olcina, A. Loayssa, S. Sales, and J. Capmany, "Multi-tap complexcoefficient incoherent microwave photonic filters based on optical single-sideband modulation and narrow band optical filtering," *Optics Express*, vol. 16, pp. 295-303, 2008.

- [13] A. Ortigosa-Blanch, J. Mora, J. Capmany, B. Ortega, and D. Pastor, "Tunable radiofrequency photonic filter based on an actively mode-locked fiber laser," *Optics Letters*, vol. 31, pp. 709-711, 2006.
- [14] J. H. Lee, Y. M. Chang, Y. G. Han, S. B. Lee, and H. Y. Chung, "Fully reconfigurable photonic microwave transversal filter based on digital micromirror device and continuous-wave, incoherent supercontinuum source," *Applied Optics*, vol. 46, pp. 5158-5167, 2007.
- [15] J. Mora, L. R. Chen, and J. Capmany, "Single-bandpass microwave photonic filter with tuning and reconfiguration capabilities," *Journal of Lightwave Technology*, vol. 26, pp. 2663-2670, 2008.
- [16] E. Hamidi, "Photonic Processing of Ultra-broadband Radio Frequency Waveforms," Doctor of Philosophy, School of Electrical and Computer Engineering, Purdue University, USA, 2010.
- [17] J. G. Proakis, *Digital Communications*, 4 ed. New York: McGraw-Hill, 2001.
- [18] W. M. Lovelace and J. K. Townsend, "The effects of timing jitter and tracking on the performance of impulse radio," *IEEE Journal of Selected Areas Communication*, vol. 20, pp. 1646-1651, 2002.
- [19] R. A. Scholtz, D. M. Pozar, and W. Namgoong, "Ultra-wideband radio," *Journal of Applied Signal processing*, vol. 3, pp. 252-272, 2005.
- [20] I. S. Lin and A. M. Weiner, "Selective correlation detection of photonicalllygenerated ultra-wideband RF signals," *Journal of Lightwave Technology*, vol. 26, pp. 2692-2699, 2008.
- [21] C. Pulikkaseril, L. A. Stewart, M. A. F. Roelens, G. W. Baxter, S. Poole, and S. Frisken, "Spectral modeling of channel band shapes in wavelength selective switches," *Optics Express*, vol. 19, 2011.
- [22] F. Abou-Galala and B. L. Anderson, "Real-time all-optical performance monitoring using optical bit-shape correlation," *Applied Optics*, vol. 48, 2009.
- [23] Y. Han, "All-optical Microwave signal processing," Master of Applied Science, Electrical Engineering and Computer Science, University of Ottawa, Ottawa, 2011.
- [24] Y. Park and J. Azana, "Optical signal processors based on a time-spectrum convolution," *Optics Letters*, vol. 35, pp. 796-798, Mar 15 2010.
- [25] A. Malacarne, R. Ashrafi, Y. Park, and J. Azana, "Reconfigurable Optical DPSK Pattern Recognition based on Incoherent Optical Processing," *2011 IEEE Photonics Conference (Pho)*, pp. 373-374, 2011.
- [26] V. Torres-Company and L. R. Chen, "All-fiber joint-transform correlator for time-multiplexed signals," *Optics Letters*, vol. 34, pp. 3385-3387, 2009.
- [27] S. H. Kim, K. Goda, A. Fard, and B. Jalali, "Optical time-domain analog pattern correlator for high-speed real-time image recognition," *Optics Letters*, vol. 36, pp. 220-222, 2011.

- [28] A. Kaur, K. Singh, and B. Utreja, "Performance analysis of semiconductor optical amplifier using four wave mixing based wavelength Converter for all Optical networks.," *International Journal of Engineering Research and Applications*, vol. 3, p. 5, 2013.
- [29] R. Kibria, L. Bui, and M. Austin, "Nonlinear Mixing Based Photonic Correlation," in *2012 IEEE International Topical Meeting on Microwave Photonics*, Noordwijk, The Netherlands, 2012.
- [30] R. Kibria, L. A. Bui, A. Mitchell, and M. W. Austin, "HNLF Based Photonic Pattern Recognition using Remote Transmitter," *IEEE Photonic Technology Letters*, vol 26, pp. 457-460, 2014.
- [31] R. Kibria and M. W. Austin, "Optical Subtraction using Nonlinear Mixing " in *2013 IEEE Photonics Conference* Seattle, USA, 2013.
- [32] R. Kibria, L. A. Bui, A. Mitchell, and M. W. Austin, "A Photonic Correlation Scheme Using FWM with Phase Management to Achieve Optical Subtraction," *IEEE Photonic Journal*, vol 5, issue 6, 2013.
- [33] M. Leonov and V. Kitaev, "Multi-Channel Correlation of Wideband RF Signals In Hybrid CPU+FPGA System," presented at the 14th Electronics New Zealand Conference (ENZCon), Newzeland, 2007.
- [34] B.K.Mishra, L. Jolly, and K. Mhatre, "Performance analysis of third order nonlinearities in optical communication system " *International Journal of Scientific & Engineering Research*, vol. 4, p. 4, 2013.
- [35] D. Ferris, "The CABB Correlator," presented at the Next Generation Correlators for Radio Astronomy and Geodesy, 2006.
- [36] (2013).<http://www2.nict.go.jp/aeri/sts/stmg/K5/VSSP/index-e.html>. Available at: <http://www2.nict.go.jp/aeri/sts/stmg/K5/VSSP/index-e.html>
- [37] Y. Park, A. Malacarne, and J. Azana, "Real-Time Group-Delay Monitoring of Ultra-Broadband Dispersive Devices by Incoherent Light Interferometry," *2011 Conference on Lasers and Electro-Optics (Cleo)*, 2011.
- [38] A. Malacarne, R. Ashrafi, Y. Park, and J. Azana, "Reconfigurable optical differential phase-shift-keying pattern recognition based on incoherent photonic processing," *Optics Letters*, vol. 36, pp. 4290-4292, Nov 1 2011.
- [39] A. VanderLugt, "Signal detection by complex spatial filtering," *IEEE Transactions on Information Theory*, vol. 10, pp. 139-145, 1964.
- [40] V. H. Diaz-Ramirez, V. Kober, and J. Alvarez-Borrego, "Pattern recognition with an adaptive joint transform correlator," *Applied Optics*, vol. 45, 2006.
- [41] D. A. Jackson and J. D. C. Jones, "Proposed Topologies for a Fiber-Optic-Based 1-GHz Clipped Digital Correlator," *Optics Letters*, vol. 11, pp. 824-826, 1986.

- [42] A. G. Podoleanu and D. A. Jackson, "Combined electronic clipped correlator and fibre-optic correlator," *Electronics Letters*, vol. 31, pp. 1492-1494, 1995.
- [43] P. Tortoli, F. Guidi, and C. Alzeni, "Digital versus SAW matched filter implementation for RADAR pulse compression," in *IEEE Ultrasonic Symp. ULISYS*, 1994, pp. 199-202.
- [44] C. Bhattacharya and G. Patel, "A Fast Implementation of Correlation of Long Data Sequences for Coherent Receivers," *IEEE Transactions on Circuits and Systems-II: Analog and Digital Signal Processing*, vol. 49, pp. 430-433, 2002.
- [45] R. A. Minasian, "Photonic signal processing of microwave signals," *IEEE Transactions on Microwave Theory and Techniques*, vol. 54, pp. 832-846, Feb 2006.
- [46] C. W. Thiel. (6th January, 2013). *Four-wave mixing and its applications*. accessed at <http://www.physics.montana.edu/students/thiel/docs/FWMixing.pdf>
- [47] S. P. Singh and N. Singh, "Progress in Electromagnetics Research," *Nonlinear Effects in Optical Fibers: Origins, Management and Applications*, vol. 73, pp. 249-275, 2007.
- [48] N. A. Mohammed, M. M. Ragab, and M. H. Aly, "Four Wave Mixing based wavelength conversion using different types of fibres," *International Journal of Engineering Science and Technology*, vol. 4, pp. 324-330, 2012.
- [49] S. Asimakis, P. Petropoulos, F. Poletti, J. Y. Y. Leong, R. C. Moore, K. E. Frampton, *et al.*, "Towards efficient and broadband four-wave-mixing using short-length dispersion tailored lead silicate hollow fibers," *Optics Express*, vol. 15, pp. 596-601, 2007.
- [50] A. Camerlingo, F. Parmigiani, X. Feng, F. Poletti, P. Horak, W. H. Loh, *et al.*, "Wavelength Conversion in a Short Length of a Solid Lead-Silicate Fiber," *IEEE Photonic Technology Letters*, vol. 22, pp. 628-630, 2010.
- [51] P. A. Andersen, T. Tokle, Y. Geng, C. Peucheret, and P. Jeppesen, "Wavelength Conversion of a 40-Gb/s RZDPSK Signal Using Four-Wave Mixing in a Dispersion-Flattened Highly Nonlinear Photonic Crystal Fiber," *IEEE Photonic Technology Letters*, vol. 17, pp. 1908-1910, 2005.
- [52] J. H. Lee, W. Belardi, K. Furusawa, P. Petropoulos, Z. Yusoff, T. M. Monro, *et al.*, "Four-Wave Mixing Based 10-Gb/s Tunable Wavelength Conversion Using a Hollow Fiber With a High SBS Threshold," *IEEE Photonic Technology Letters*, vol. 15, pp. 440-442, 2003.
- [53] (15th January). [http://www.fiber-optics.info/articles/fiber\\_nonlinearities](http://www.fiber-optics.info/articles/fiber_nonlinearities).
- [54] S. H. Lee, H. W. Jung, S. H. Kim, D. w. Kim, and K. H. Kim, "Measurement of nonlinear coefficient of a highly nonlinear fiber based on peak four-wave mixing signal generation conditions," *Optics Communications*, vol. 284, p. 4, 2011.
- [55] L. A. Bui, M. D. Pelusi, T. D. Vo, N. Sarkhosh, H. Emami, B. J. Eggleton, *et al.*, "Instantaneous frequency measurement system using optical mixing in highly nonlinear fiber," *Optics Express*, vol. 17, pp. 22983-22991, Dec 7 2009.

- [56] E.J.M. Verdurmen, G.D. Khoe, A.M.J. Koonen, and H. d. Waardt, "All-Optical data format conversion from WDM to OTDM based on FWM," *Microwave and Optical Technology Letters*, vol. 48, p. 3, 2006.
- [57] D. Peter and S. Hong, "Multiwavelength modelocked lasers," USA Patent, 2003.

# APPENDIX I

Shown below is a “truth table” exercise which presents the expected received optical signal using phase modulation of the carrier wavelengths for all possible input bit patterns when the template bit pattern is 1101, as discussed in Section 6.3.2.1.

Truth table:

The template is fixed 1101. It will have different output for different input combinations.

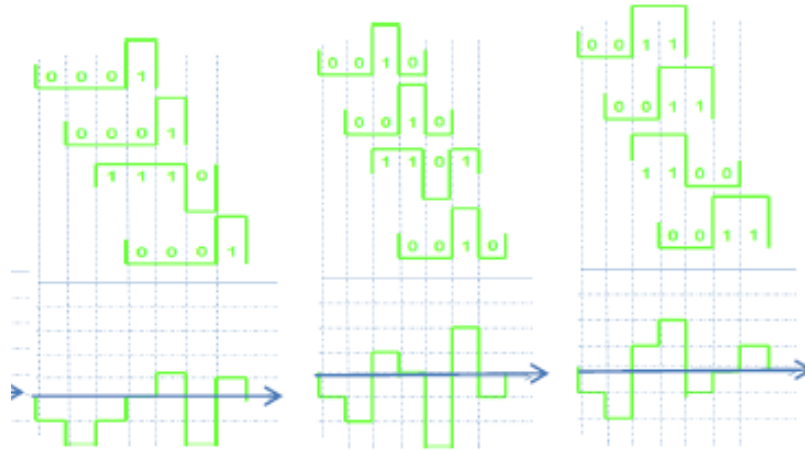
For input 0000:

For input 0001

For input 0010

For input 0011

Not a possible test case.

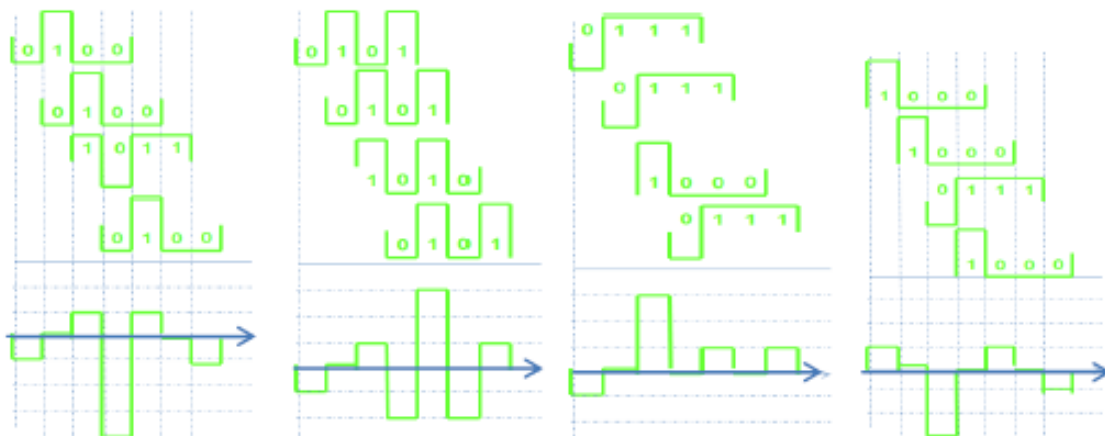


For input 0100:

For input 0101:

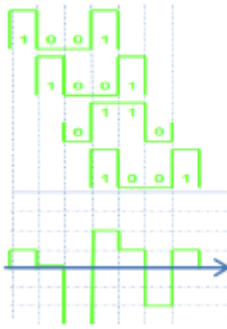
For input 0111:

For input 1000:

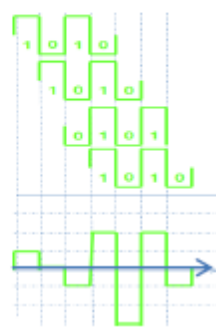




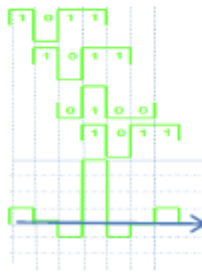
For input 1001



For input 1010



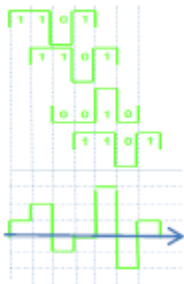
For input 1011:



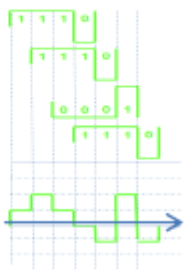
For input 1100



For input 1101:



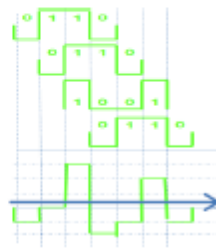
For input 1110



For 1111

Not a possible test case

For 0110



## **APPENDIX II**

This Appendix contains the paper published in the proceedings of the IEEE International Topical Meeting on Microwave Photonics, 2012.

# Nonlinear Mixing Based Photonic Correlator

Refat Kibria, Lam Anh Bui and Michael W. Austin

School of Electrical & Computer Engineering, RMIT University, Melbourne, Australia  
 refat.kibria@student.rmit.edu.au

**Abstract**—We propose a novel correlation technique based on matched filtering using four wave mixing (FWM) in a length of highly nonlinear fiber (HNLf). A pump wavelength which is modulated by an input bit stream is mixed with wavelength channels to generate idler wavelengths which also carry the bit stream. The idler wavelengths are differentially delayed and summed at a photodetector to produce the required correlation function. This scheme has been experimentally demonstrated and the measured results verify the proposed concept. The technique allows remoting of the transmitter.

**Keywords**— Correlation, Four Wave Mixing (FWM), highly nonlinear fiber (HNLf), Microwave photonics (MWP), Pattern recognition

## I. INTRODUCTION

Microwave photonic systems have attracted much research interest due to their broad bandwidth, low dispersion, low RF dependent attenuation and their ability to provide parallel processing [1]. A major application of microwave photonics is the processing of RF signals in the optical domain. RF processing can be done electronically but a major limitation is the speed of the electronics. The solution to this problem is to process RF signals in the optical domain. Optical approaches have been utilized to realize a range of RF processing tasks. These include filtering [1, 2], phase shifting [2], and frequency up and down conversion [1-3]. In this paper, we propose, for the first time, a pattern recognition or correlation technique based on the use of a matched filter using four wave mixing in a length of highly nonlinear fiber.

A pattern recognition technique based on a matched filter was presented in [4], in which the reference bit pattern is encoded as discrete optical wavelengths which are modulated by a binary input signal. The wavelengths are then differentially delayed in a dispersive medium before they are detected with a high frequency photodetector in which many versions of the binary signals carried by the different wavelengths are summed. Correlation of the binary input signal and the encoded reference bit pattern is thus obtained at the photodetector output.

In this paper, a modification of the matched filter concept in [4] is presented which allows remoting of the transmitter by copying the bit pattern from one optical channel to many channels in order to realise the matched filter concept. In the area of signal processing, optical four wave mixing (FWM) has been used to perform frequency conversion [5, 6], spatial information processing [4, 5] and frequency measurement [7].

Here, we propose the correlation concept using a remote transmitter by exploiting the use of FWM in a length of HNLf to mix wavelength channels with a pump wavelength which has been modulated by an input bit stream in order to produce copies of the input signal at the output idler wavelengths.

The paper is organized as follows. Section II explains the principle of operation. Section III describes the practical demonstration, Section IV presents the system characterization and Section V presents the experimental results and discussion. A conclusion is then given in Section VI.

## II. PRINCIPLE OF OPERATION

Figure 1(a) presents the correlation system in [4] in which a reference bit pattern is encoded on to discrete optical wavelengths. In particular, the reference bit pattern is inverted in time and ‘1’s and ‘0’s are represented by the presence and absence of optical wavelengths respectively.

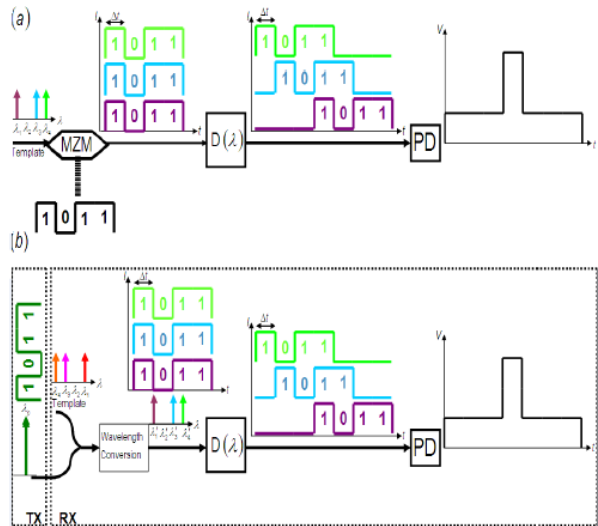


Figure 1. Illustration of the working principle of (a) the scheme demonstrated in [4] and (b) the proposed HNLf based scheme with possible remote transmitter.

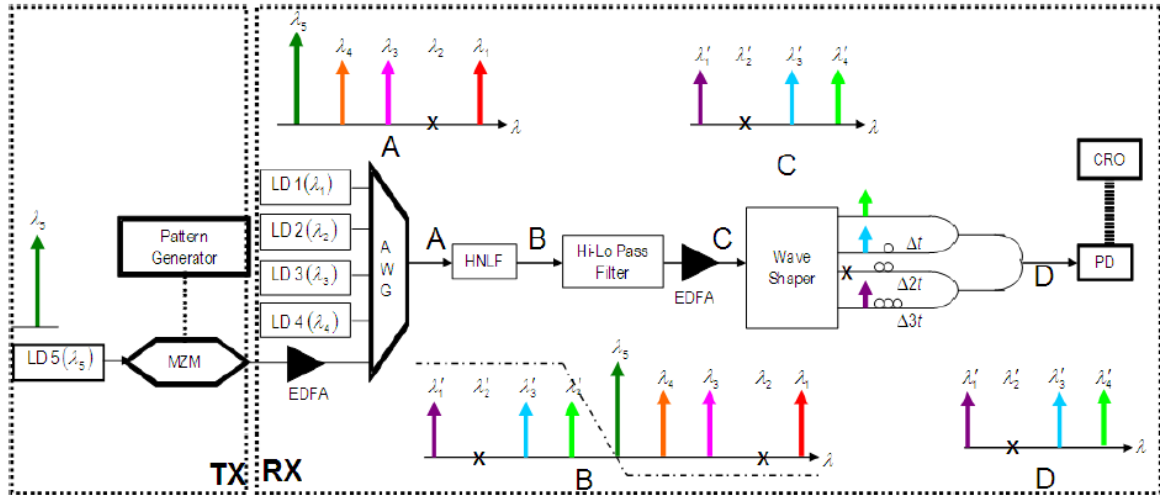


Figure 2. Experimental set-up for the proposed HNLf based remote transmitter correlation scheme

In [4] the wavelengths are combined and modulated by the input bit pattern using a Mach Zehnder Modulator (MZM). The wavelengths are then differentially delayed using dispersion. The wavelengths and the dispersion are selected such that after the dispersive delay, the wavelength channels separate in time according to the bit position they represent. The wavelengths are then combined and the summed optical power at a photodetector is measured, which is the desired correlation function.

In the proposed system of Figure 1(b), the bit pattern on one wavelength is copied to several other wavelengths using wavelength conversion; in particular FWM wavelength conversion is used. The pump wavelength is first modulated by the input bit stream and then is mixed with a number of wavelength channels in a length of HNLf which creates numerous idler wavelengths. The pump wavelength can be modulated with the signal and transmitted from a remote location and hence this approach allows the signal to be transmitted from a remote location for correlation. The reference bit pattern or template is determined by the choice of the wavelength channels. The idler wavelengths are filtered and differentially delayed using lengths of fiber with delays corresponding to multiples of a bit period and then summed at a photodetector to provide the correlation function.

### III. PRACTICAL DEMONSTRATION

The experimental set-up for the proposed system is shown in Figure 2. CW lasers are turned on to represent the template. In this experiment the template was chosen to be a 4 bit long binary word of 1011. So, lasers are turned on to represent 1101 (inverted representation of the template). At the transmitter, the input bit pattern was chosen to be 1011 with a bit duration of  $T = 10$  ns (bit rate = 100 Mb/s). The pump wavelength  $\lambda_5$  at the transmitter is set at 1546.95 nm and is modulated with the input bit stream using a MZM. The input bit stream originates from a Programmable Pattern Generator. At the receiver, the modulated pump wavelength is combined with the wavelengths representing the template. An EDFA is used to

increase the pump power to ensure that it has higher power than that of the other wavelengths for efficient wavelength conversion. The wavelengths of the four channels are selected to be 1549.41 nm ( $\lambda_1$ ), 1550.2 nm ( $\lambda_2$ ), 1551.84 nm ( $\lambda_3$ ) and 1553.63 nm ( $\lambda_4$ ). To select 1101,  $\lambda_5$  is turned off. The optical power of each of these wavelength channels at the input of the 1 km of HNLf is maintained at 1 dBm and the power of the modulated pump is 8 dBm. FWM in the HNLf generates numerous idler wavelengths of which 1544.5 nm ( $\lambda'_1$ ), 1543.7 nm ( $\lambda'_2$ ) and 1540.7 nm ( $\lambda'_3$ ) are the idlers of interest for the reference template of 1101. These idlers all contain a copy of the input signal (Figure 2 [B & C]).

After mixing in the HNLf all the mixing products are passed through an optical filter to remove the high power pump and the original wavelength channels. The filter is a low pass filter with a cut-off wavelength at 1545.4 nm (Figure 2 [B]). The pump and the original wavelength channels are attenuated significantly and the idlers pass through. The output of the filter consists of the required idler wavelengths with a few other low power unwanted idlers.

All these idler wavelengths are input to an optical processor (Waveshaper) which removes the unwanted idlers and forwards the wanted wavelengths to a delay network formed by lengths of fiber patch cord. The differential delay between each output port of the Waveshaper was adjusted to a 1 bit duration ( $\bullet t = 10$ ns, equivalent to the time delay in a 2m patch cord).  $\lambda'_1$  is forwarded to port 1 with zero relative delay.  $\lambda'_2$  is forwarded to port 2 with a 1 bit delay.  $\lambda'_3$  is forwarded to port 4 with a 3 bit delay. The outputs of the different ports are combined using 3 dB couplers and the combined optical signal is detected using a photodetector.

### IV. CHARACTERIZATION

In order to verify that the optical signals at various stages of the system are as expected, the optical signal at different stages was measured using an OSA and the differential delay between wavelengths was measured using an oscilloscope.

Figure 3(a) shows the pump and the wavelength channels at the input of the HNLF. The pump power is 7 dB higher than that of the other wavelengths. Figure 3(b) shows the mixing products at the output of the HNLF. All the input channels, pump and several mixing products are present in the spectrum. The pump and the other input channels have much higher power than the required idlers. A low pass filter is employed to eliminate the high power signal wavelengths. Figure 3(c) shows the output of this filter. The pump and other channels are attenuated significantly and only the required idlers with several other low power unwanted idlers remain in the spectrum. Figure 3(d) shows the idler wavelengths  $\lambda_1'$ ,  $\lambda_3'$  and  $\lambda_4'$  measured at the output of the Waveshaper. The power of these wavelengths was set to be -11 dBm to get equal power in each idler wavelength.

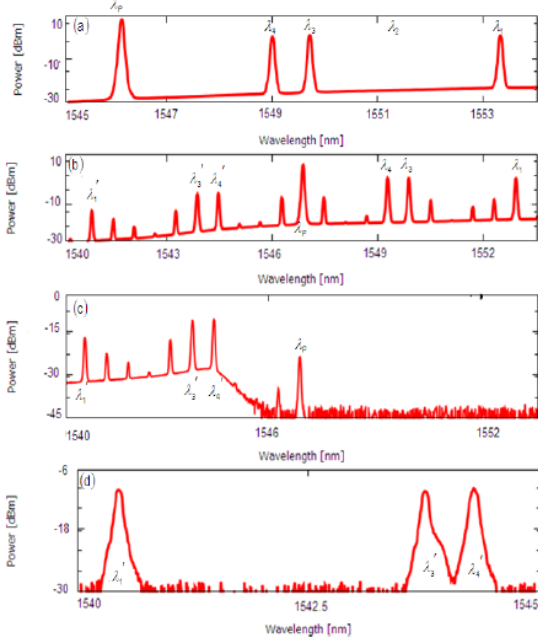


Figure 3. (a) Pump and channel wavelengths at the HNLF input. (b) Mixing products at the output of the HNLF. (c) Output of the low pass filter (filtering the high power pump and the input channels). (d) Idler wavelengths at the output of the Wave shaper.

After the Waveshaper, the idler wavelengths of Figure 3(d) are differentially delayed using fiber patch cords connected to different ports of the Waveshaper. As mentioned previously,  $\lambda_4'$  is forwarded to port 1 with zero relative delay,  $\lambda_3'$  is forwarded to port 2 with a 1 bit delay and  $\lambda_1'$  is forwarded to port 4 with a 3 bit delay. Figures 4(a)–4(c) show the measured photodetector output when each of the wavelengths  $\lambda_1'$ ,  $\lambda_3'$  and  $\lambda_4'$  is individually delayed and incident on the photodetector. The measured results show the expected delays.

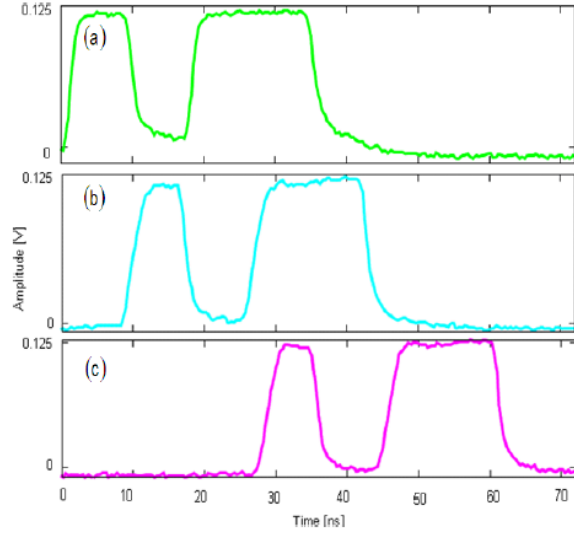


Figure 4. (a) Measured photodetector output when only  $\lambda_4'$  is present. (b) Measured photodetector output when only  $\lambda_3'$  is present. It is differentially delayed by a 1 bit delay. (c) Measured photodetector output when only  $\lambda_1'$  is present. It is differentially delayed by a 3 bit delay.

## V. RESULTS AND DISCUSSION

Having characterized the system and showed that it performs as expected, we now demonstrate the correlation. In Figure 5, the solid blue line shows the measured correlation function at the photodetector output when all three idler wavelengths are present and the input bit pattern (1011) matches the reference bit pattern. When there is a match between the input bit pattern and the reference bit pattern, a correlation peak occurs at the middle of the correlation function, which is at the end of the original bit pattern. The height of the correlation peak is equal to the height of a '1' multiplied by the number of '1's in the template, which in this case is 3 ( $3 \times 0.125 \text{ V} = 0.375 \text{ V}$ ).

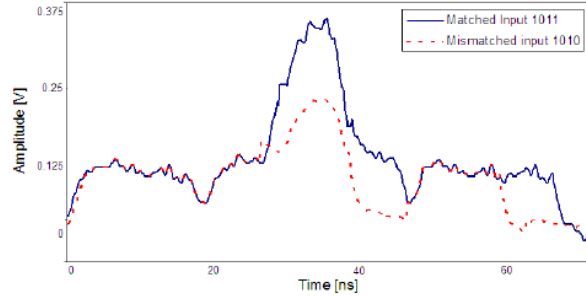


Figure 5. Measured correlation output when all three wavelengths are present and the input bit pattern (1011) matches the reference bit pattern and the output with a mismatched input signal (1010).

The red dotted line in Figure 5 shows the correlation function when the input bit pattern (1010) does not match the reference bit pattern. Since this bit stream is not the same as the template, the height of the correlation peak is smaller than

that for the matched case. The results achieved here are similar to those obtained using the linear scheme in [4].

In setting up the experiment, filtering out the high power pump and the wavelength channels was a challenge and therefore the wavelengths were carefully selected to match the filter cut-off wavelength. Also, unavailability of a high speed pattern generator lead us to operate the system with a bit rate as low as 100 Mbps. It is obvious that with a high speed pattern generator the proposed scheme can replicate the dispersive delay scheme of [4] and generating a several bit delay would be easier and with much less insertion loss than using the fiber delay network which was used here.

## VI. CONCLUSION

A novel photonic correlation technique which uses four wave mixing in a length of nonlinear optical fiber has been proposed and demonstrated. Contrary to the system in [4], the proposed scheme will allow the use of a remote transmitter. Future work will include implementation of the template using a software controlled optical processor only.

## ACKNOWLEDGEMENT

Comments on this work from Professor Arnan Mitchell have been invaluable and the authors acknowledge his input.

## REFERENCES

- [1] J. P. Yao, "Microwave Photonics," *Journal of Lightwave Technology*, vol. 27, pp. 314-335, Jan-Feb 2009.
- [2] A. J. Seeds and K. J. Williams, "Microwave photonics," *Journal of Lightwave Technology*, vol. 24, pp. 4628-4641, Dec 2006.
- [3] J. Capmany and D. Novak, "Microwave photonics combines two worlds," *Nature Photonics*, vol. 1, pp. 319-330, June 2007.
- [4] Y. Park and J. Azaña, "Optical signal processors based on a time-spectrum convolution," *Optics Letters*, vol. 35, pp. 796-798, 2010.
- [5] Y. Dai and J. Yao, "Microwave Correlator Based on a Nonuniformly Spaced Photonic Microwave Delay-Line Filter," *IEEE Photonics Technology Letters*, vol. 21, pp. 969-971, 2009..
- [6] R. A. Minasian, "Photonic signal processing of microwave signals," *IEEE Transactions on Microwave Theory and Techniques*, vol. 54, pp. 832-846, Feb 2006.
- [7] L. A. Bui, M. D. Pelusi, T. D. Vo, N. Sarkhosh, H. Emami, B. J. Eggleton, and A. Mitchell, "Instantaneous frequency measurement system using optical mixing in highly nonlinear fiber," *Optics Express*, vol. 17, pp. 22983-22991, 2009.

## **APPENDIX III**

This appendix contains the paper published in the IEEE Photonic Technology Letters in January 2014.



# HNLF-Based Photonic Pattern Recognition Using Remote Transmitter

Refat Kibria, Lam Bui, Arnan Mitchell, and Michael W. Austin, *Member, IEEE*

**Abstract**—In this letter, a novel correlation technique based on matched filtering using four wave mixing with possible remote transmission is proposed. A pump wavelength, which is modulated by an input bit pattern is mixed with wavelength channels in a highly nonlinear fiber to generate idler wavelengths, which also carry the bit stream. Specific idler wavelengths are selected using software control of an optical processor to generate the reference template. These idlers are then differentially delayed and summed at a photodetector to produce the required correlation function. This scheme has been experimentally demonstrated and the measured results verify the proposed concept.

**Index Terms**—Correlation, four wave mixing (FWM), highly nonlinear fiber (HNLF), microwave photonics (MWP), pattern recognition.

## I. INTRODUCTION

MICROWAVE photonics has been used to successfully realize a range of RF processing tasks including filtering [1]–[3], phase shifting [4], and frequency up and down conversion [1]–[4]. In this letter we propose, for the first time, a matched filter based pattern recognition or correlation technique where the template library signal can be software controlled for the ease of operation and the signal processing can be done in a remote location from the transmitter.

Correlation, or more generally speaking, finding the similarity between two signals, is a core signal processing technique used in many applications such as radar, radio astronomy and high-energy physics [5]. The process of correlation involves delaying one signal with respect to the other, multiplication of the two signals and integration. The correlation of two continuous complex signals  $S_1(t)$  and  $S_2(t)$  is given by

$$r(\tau) = S_1(t) * S_2(t) = \lim_{T \rightarrow \infty} \frac{1}{2T} \int_{-T}^T S_1(t) S_2^*(t - \tau) dt \quad (1)$$

In Equation (1),  $\tau$  is the lag or delay between the signals. The number of lags is an important feature defining the resolution capabilities of a correlator. However, the incurred execution time or time complexity for wideband correlation is a challenge using electronic processing because of bandwidth

limitations. A solution to this problem is to use photonic processing of the electronic signals.

In [6], a pattern recognition technique based on a matched filter was presented in which the reference or template bit pattern is encoded as discrete optical wavelengths. These wavelengths are each modulated by the input bit pattern and then differentially delayed in a dispersive medium before they are summed and detected with a high frequency photodetector.

Correlation of the binary input signal and the encoded reference bit pattern is obtained at the photodetector output. A key problem with this technique is that all the photonic processing is done near the source of the input bit pattern whereas in a practical system it may be desirable to isolate the signal processing from the source of the input signal. Also, for this technique a new reference bit pattern requires a new template which is selected by physically turning lasers on and off, which has obvious disadvantages.

A different correlation technique based on nonlinear mixing was proposed in [7]; however the template was also selected by physically turning laser diodes on or off. In this letter, we propose a nonlinear mixing based correlation scheme where the template is selected using software control of an optical processor. Because of this, changing and controlling the template can be done from a remote location. The proposed correlation scheme uses four wave mixing (FWM) in a length of highly nonlinear fiber (HNLF) to mix template wavelengths with a pump wavelength which has been modulated by an input bit stream in order to produce copies of the input signal at the output idler wavelengths. The technique allows the possibility of a remote transmitter. The performance criterion of such system is also discussed in this letter.

The letter is organized as follows. Section II explains the principle of operation. Section III describes the experimental set-up and Section IV presents the system characterization. Section V presents and discusses the experimental results. A conclusion is given in Section VI.

## II. PRINCIPLE OF OPERATION

Fig. 1 shows a schematic of the correlation system presented in [6] in which a reference bit pattern is encoded using discrete optical wavelengths. The reference bit pattern is inverted in time and ‘1’s and ‘0’s are represented by the presence and absence of optical wavelengths respectively.

These wavelengths are each modulated by a binary input signal bit pattern using a Mach-Zehnder Modulator (MZM). The wavelengths are then differentially delayed using dispersion in a length of single-mode fiber. The wavelengths and

Manuscript received October 10, 2013; revised November 24, 2013; accepted December 18, 2013. Date of publication January 2, 2014; date of current version February 5, 2014.

The authors are with the School of Electrical and Computer Engineering, RMIT University, Melbourne 3000, Australia (e-mail: refat.kibria@student.rmit.edu.au; lam.bui@rmit.edu.au; arnan.mitchell@rmit.edu.au; michael.austin@rmit.edu.au).

Color versions of one or more of the figures in this letter are available online at <http://ieeexplore.ieee.org>.

Digital Object Identifier 10.1109/LPT.2013.2296506

1041-1135 © 2014 IEEE. Translations and content mining are permitted for academic research only. Personal use is also permitted, but republication/redistribution requires IEEE permission. See [http://www.ieee.org/publications\\_standards/publications/rights/index.html](http://www.ieee.org/publications_standards/publications/rights/index.html) for more information.



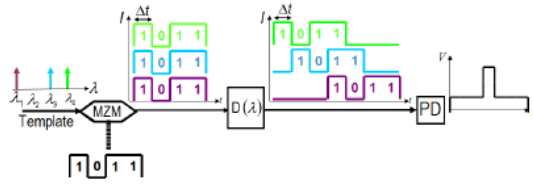


Fig. 1. Illustration of the working principle of the correlation scheme demonstrated in [6].

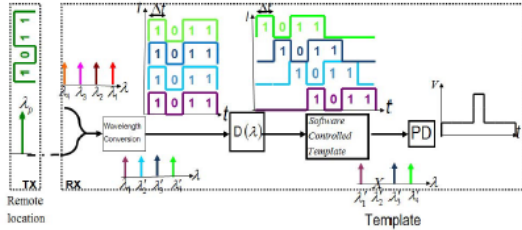


Fig. 2. Illustration of the working principle of the proposed HNLF based correlation scheme with possible remote transmitter and software controlled template.

the dispersion are selected such that after the dispersive delay, the wavelength channels separate in time according to the bit position they represent. The wavelengths are then summed on a high frequency photodetector (PD) which produces the desired correlation function.

In the system proposed here, seen in Fig. 2, a pump wavelength is first modulated by the input bit stream, possibly at a remote location, and then mixed with a number of wavelengths in a length of HNLF. The number of wavelengths used equals the number of bits in the input bit pattern. FWM in the HNLF creates numerous idler wavelengths, each with a copy of the input bit pattern.

The reference bit pattern or template is determined by selecting particular idler wavelengths generated by the FWM process using a software controlled optical processor. These idler wavelengths are differentially delayed with delays corresponding to multiples of a bit period and then summed at a photodetector to provide the correlation function. The advantage of this technique allows the pump wavelength to be modulated with the signal and transmitted from a remote location for correlation. Instead of selecting the reference template by turning lasers on or off, all the lasers at the receiver are kept on.

III. EXPERIMENTAL SETUP

The experimental set-up for the proposed system is shown in Fig. 3. At the transmitter, the pump wavelength  $\lambda_5$  (1546.95nm) is modulated by the input bit pattern using a MZM. In this experiment the bit pattern is 4 bits long and was chosen to be 1011 with a bit duration of 10ns (bit rate = 100Mb/s). The input bit stream originates from a Programmable Pattern Generator. The modulated pump wavelength is then transmitted to the receiver end using polarization maintenance (PM) fibre. All the equipment used in transmitter

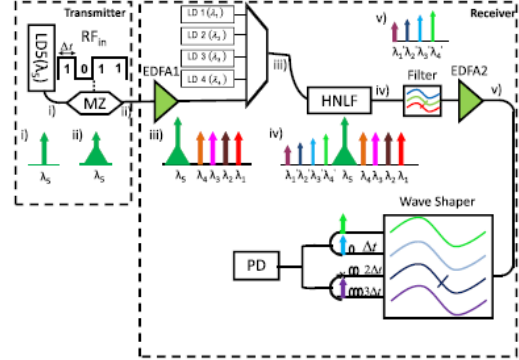


Fig. 3. Experimental Set-up.

and receiver end are PM equipment, which includes fibres, couplers, AWG, MZM, Waveshaper etc. This is to ensure that polarization is maintained and should not have much impact on the final output.

At the receiver, four CW lasers with wavelengths  $\lambda_1 - \lambda_4$  are used to represent the number of bits in the pattern. The modulated pump wavelength is amplified using an EDFA and then combined with the CW wavelengths using an AWG. The five wavelengths then pass to a 1km length of highly nonlinear fibre. The pump wavelength is amplified to ensure that it has a higher power than that of the other wavelengths for efficient FWM wavelength conversion.

The wavelengths of the four CW lasers are selected to be 1549.41 nm ( $\lambda_4$ ), 1550.2 nm ( $\lambda_3$ ), 1551.84 nm ( $\lambda_2$ ) and 1553.63 nm ( $\lambda_1$ ). The template was chosen to be a 4 bit long binary word of 1101 (inverted representation of the desired signal). The optical power of each of these wavelengths at the input of the HNLF is 8 dBm and the power of the modulated pump is 16 dBm.

The HNLF used here is a 1km length of standard PM-HNLF from OFS [8]. FWM in the HNLF generates numerous idler wavelengths of which 1540.7nm ( $\lambda_1'$ ), 1542.9nm ( $\lambda_2'$ ), 1543.7nm ( $\lambda_3'$ ) and 1544.5nm ( $\lambda_4'$ ) are the idlers of interest. These idler wavelengths each contain a copy of the input bit pattern (Fig. 3 [iv]). After mixing in the HNLF, all the mixing products pass through an optical filter to remove the high power pump and the original laser wavelengths. The filter is a low pass filter with a cut-off wavelength at 1545.4nm. The pump and the original wavelength channels are attenuated significantly and the idlers pass through. The output of the filter consists of the required idler wavelengths with a few other low power unwanted idlers.

All these idler wavelengths are amplified and are then input to an optical processor (Finisar Waveshaper 4000s) which is programmed to only pass the idler wavelengths which represent the reference bit pattern, in this case  $\lambda_1', \lambda_3'$  and  $\lambda_4'$ .

These wavelengths are then input to a delay network formed by lengths of fibre patch cord. A fibre delay network was used instead of using the dispersion in a length of single-mode fibre because for the low bit rate used, a delay of one-bit period

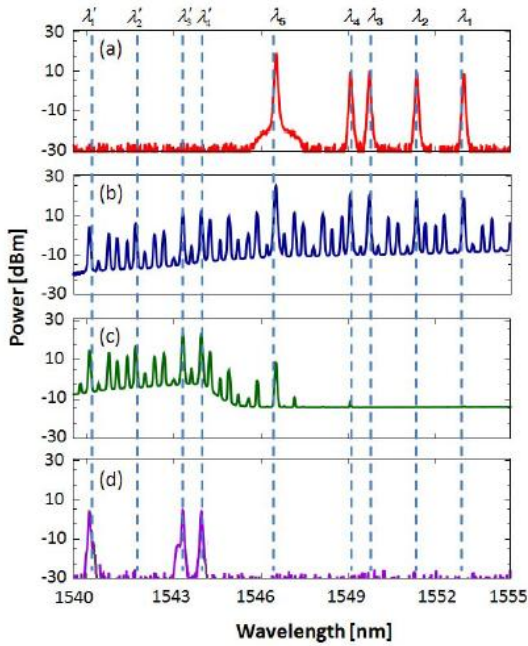


Fig. 4. (a) Pump and CW laser wavelengths at the input of the HNLF, (b) mixing products at the output of the HNLF, (c) output of the low pass filter (filtering the high power pump and the input channels), (d) idler wavelengths measured at the photodetector.

would require a length of  $\sim 600\text{km}$ . The differential delay between each output port of the Waveshaper was adjusted to a 1 bit duration ( $\Delta t = 10\text{ns}$ , equivalent to the time delay in a 2m long fibre patch cord).  $\lambda_4'$  is forwarded to port 1 with zero relative delay,  $\lambda_3'$  is forwarded to port 2 with a 1 bit delay and  $\lambda_1'$  is forwarded to port 4 with a 3 bit delay. The outputs of the different ports are then combined using 3 dB couplers and the combined optical signal is detected using a photodetector.

IV. CHARACTERIZATION

The system was characterized by measuring the optical signal at different stages using an OSA. The differential delay between wavelengths was measured by observing the photodetector output with an oscilloscope.

Fig. 4(a) shows the pump and the CW wavelengths at the input of the HNLF. The pump power is 8 dB higher than that of the other wavelengths. Fig. 4(b) shows the mixing products at the output of the HNLF. All the input wavelengths, the pump and many mixing products are present in the spectrum. The pump and the input wavelengths have much higher power than the required idler wavelengths. A low pass filter is employed to eliminate these high power wavelengths. Fig. 4(c) shows the output of this filter. The pump and the original wavelengths are attenuated significantly and only the required idlers with several other low power unwanted idlers remain in the spectrum. Fig. 4(d) shows the desired idler wavelengths  $\lambda_1'$ ,  $\lambda_3'$  and  $\lambda_4'$  measured at the input to the photodetector.

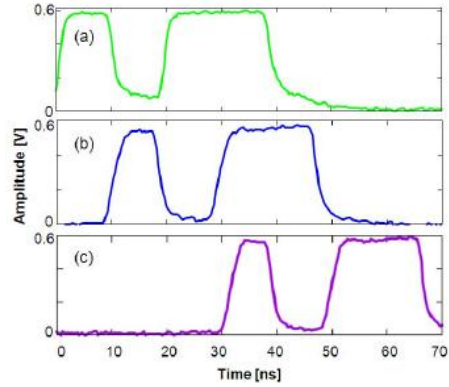


Fig. 5. (a) Measured photodetector output when only  $\lambda_4'$  is present. (b) Measured photodetector output when only  $\lambda_3'$  is present. It is differentially delayed by a 1 bit delay compared to  $\lambda_4'$ . (c) Measured photodetector output when only  $\lambda_1'$  is present. It is differentially delayed by a 3 bit delay compared to  $\lambda_4'$ .

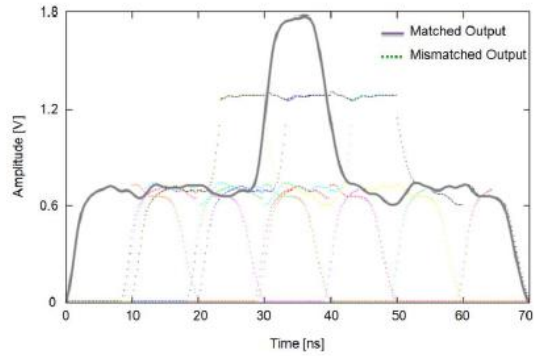


Fig. 6. Measured correlation output for all possible combinations of input bit patterns. The solid line indicates the output for a matched bit pattern.

The power of each of these wavelengths was adjusted by the Waveshaper to be equal.

After the Waveshaper, the idler wavelengths shown in Fig. 4(d) are differentially delayed using fiber patch cords connected to different output ports of the Waveshaper. Fig. 5(a)–(c) show the measured photodetector output when each of the wavelengths is individually delayed and incident on the photodetector. The measured results show the expected relative time delays.

V. RESULTS AND DISCUSSION

Having characterized the system and showed that it performs as expected, we now demonstrate the correlation. In Fig. 6, the thick solid line shows the measured correlation function at the photodetector output when all three idler wavelengths are present and the input bit pattern (1011) matches the reference bit pattern. When there is a match between the input bit pattern and the reference bit pattern, a correlation peak occurs at the middle of the correlation function, which is at the end of the original bit pattern. The height of the measured



correlation peak is equal to the height of a '1' detected for each wavelength (0.6 V) multiplied by the number of '1's in the template, which in this case is 3 ( $3 \times 0.6 \text{ V} = 1.8 \text{ V}$ ).

The dotted plots in Fig. 6 show the measured correlation functions for all possible mismatched conditions. The height of the correlation peak is smaller than that for the matched case. The maximum output for a mismatched signal is  $2 \times 0.6 = 1.2 \text{ V}$ . The results achieved here are similar to those obtained using the scheme in [6].

Although the proposed concept has been demonstrated here using only a 4 bit pattern, it is important to note that the technique is scalable to larger bit patterns. Scalability depends on a number of factors. Firstly, it depends on the number of idler wavelengths which can be efficiently generated and filtered using four wave mixing. Efficient four wave mixing requires HNLFF with low dispersion. The HNLFF used here exhibits low dispersion ( $-0.19 \text{ ps/km.nm}$ ) over the wavelength range 1540–1560nm. This determines the range of possible signal wavelengths. The wavelength spacing in this range depends on the resolution of the filter used to filter out the idler wavelengths. Assuming a filter resolution of 20GHz, an upper limit on the number of possible wavelengths in this 20nm range, and therefore the number of signal bits, is 125.

In the letter reported here, the 4 bits was a limitation of the number of output ports on the Waveshaper which was used to filter out the idler wavelengths, each representing a bit. A multiport Waveshaper would enable the filtering of more wavelengths, allowing more bits in the bit pattern.

A second issue to note is that although a fiber delay network was used here, this is not necessary. A simple dispersive medium could be used to achieve the required wavelength dependent time delays. Unfortunately, the concept was demonstrated with a bit rate of only 100 Mb/s due to the unavailability of a high speed pattern generator. In this case it was easier to use a fibre delay network instead of a dispersive fibre to achieve the large time delays corresponding to multiples of a bit period. At higher bit rates than that used here, single-mode fiber could be used as a dispersive medium to achieve the required time delays for the idler wavelengths, as in [6]. Generating a several bit delay would be easier and with much less insertion loss than using the fiber delay network which was used here.

The required time delay increases as the number of bits increases. For  $N$  bits, a maximum time delay of  $(N - 1) \times$  the bit duration is required. At 40Gb/s, the bit duration is 25ps. For a 16 bit pattern, a maximum delay of 375 ps is required. Assuming wavelength spacings of 0.8nm, a length of 1.8km of SMF could be used to achieve the delays.

Another factor which can limit the scalability of this scheme, as well as that demonstrated in [6], is the visibility of the correlation peak for the matched case, i.e. how different is the correlation peak for the matched signal from the maximum

output for a mismatched signal. Since the output of the photodetector is due to the summation of several optical signals at different wavelengths, and each wavelength produces a signal current plus a noise current, successful detection of the matched case depends on the signal current produced by each '1' as well as the noise current produced by each wavelength.

For the matched case, the maximum value of the output signal will be due to the number of '1's in the signal ( $N$ ), whereas the maximum output for a mismatched case will be proportional to  $(N - 1)$  times the output for each '1', as seen in Fig. 6. The maximum output current when  $N$  wavelengths are incident on the photodetector will include  $N$  noise currents, whereas the maximum output for a mismatched case will include  $(N - 1)$  noise currents. Using the concept of the quality factor or  $Q$  factor which is a figure of merit commonly used in digital optical fiber systems, where the  $Q$  factor is defined as the difference between the average levels of '1's and '0's divided by the sum of their standard deviations due to the noise, it can be shown that the  $Q$  factor for the detected signal in the matched case will be proportional to  $(2N - 1)^{-1}$ . Therefore, for this correlation technique, the visibility of the matched case decreases as the number of '1's in the reference bit pattern increases.

## VI. CONCLUSION

A novel photonic correlation technique based on matched filtering using FWM has been proposed and demonstrated. Contrary to the systems in [6] and [7], the scheme proposed here will allow the use of a remote transmitter and selection of the reference template using software control. Future letter will include modification of the system to enable correlation of analogue signals which involves the accumulation of negative signals.

## REFERENCES

- [1] J. Capmany, B. Ortega, D. Pastor, and S. Sales, "Discrete-time optical processing of microwave signals," *J. Lightw. Technol.*, vol. 23, no. 2, pp. 702–723, Feb. 2005.
- [2] J. Capmany and D. Novak, "Microwave photonics combines two worlds," *Nature Photon.*, vol. 1, pp. 319–330, Jun. 2007.
- [3] J. P. Yao, "Microwave photonics," *J. Lightw. Technol.*, vol. 27, no. 3, pp. 314–335, Feb. 1, 2009.
- [4] A. J. Seeds and K. J. Williams, "Microwave photonics," *J. Lightw. Technol.*, vol. 24, no. 12, pp. 4628–4641, Dec. 2006.
- [5] M. Leonov, "Method and implementation of multi-channel correlation in the hybrid CPU+FPGA system," M.S. thesis, School Eng., Auckland Univ. Technol., Auckland, New Zealand, 2009.
- [6] Y. Park and J. Azaña, "Optical signal processors based on a time-spectrum convolution," *Opt. Lett.*, vol. 35, no. 6, pp. 796–798, 2010.
- [7] R. Kibria, L. A. Bui, and M. W. Austin, "Nonlinear mixing based photonic correlator," in *Proc. IEEE Int. Topical Meeting Microw. Photon.*, Noordwijk, The Netherlands, Sep. 2012, pp. 30–33.
- [8] OFS Specialty Photonics Division, Broendby, Denmark. (2013). *HNLFF Standard* [Online]. Available: <http://ofscatalog.specialtyphotonics.com>

## **APPENDIX IV**

This appendix contains the paper published in the proceedings of IEEE Photonics Conference, 2013.

# Optical Subtraction using Nonlinear Mixing

Refat Kibria and Michael W. Austin

School of Electrical & Computer Engineering, RMIT University, Melbourne, Australia

## Abstract

A novel technique to achieve subtraction of two optical signals based on Four Wave Mixing is presented. It utilizes the subtraction of idler wavelengths by applying a  $\pi/2$  radians relative phase shift between pump wavelengths.

## I. INTRODUCTION

Microwave photonics has been used to successfully realize a range of RF processing tasks including filtering [1-3], phase shifting [4], and frequency up and down conversion [1-4]. In this paper we propose, for the first time, a photonic technique to realize subtraction of two optical signals.

Subtraction is a widely used signal processing task. Typically, subtraction of two optical signals is achieved electronically using balanced photodetectors [5], however processing of optical signals in the electronic domain exhibits the usual problems of limited bandwidth and processing speed. Processing in the optical domain is a more attractive approach.

In this paper, a four wave mixing (FWM) based scheme is illustrated to achieve subtraction optically. The optical wavelengths for the mixing process were selected carefully following the principle of [6], so that the mixing products occur at the same idler wavelength. The relative phase of the pump wavelengths produces optical subtraction.

The paper is organized as follows. Section II explains the principle of operation. Section III describes the simulation set-up and Section IV presents and discusses the simulation results. Section V concludes the paper.

## II. PRINCIPLE OF OPERATION

The principle of operation of the proposed scheme is to utilize the inherent property of four wave mixing to achieve the subtraction of two optical signals optically. FWM of signal and pump wavelengths creates idlers at sum and difference wavelengths which carry information from the original wavelengths. As in [6], if a number of signal and pump wavelengths are selected such that the signal wavelengths have a separation of twice that of the pump wavelengths, then FWM of each signal and pump will create idlers at a common target wavelength, as shown in Figure 1 [see Appendix]. The optical power at this target idler wavelength depends on the relative phase

of each mixing product at that wavelength. Subtraction of an idler can be achieved if the pump of that mixing product has a  $\pi/2$  radian phase shift with respect to the other pumps. The resultant idler for that particular mixing term will have a  $\pi$  phase difference with respect to the other and their sum will be a subtraction between two signals.

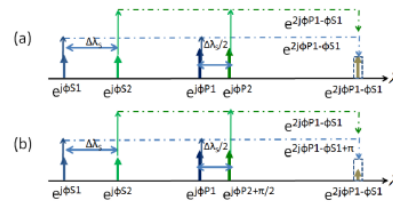


Fig. 1. Principle of operation. a) Selection of wavelengths based on the scheme in [6] for addition b) Illustration of the subtraction process by applying a  $\pi/2$  relative phase shift to one pump wavelength.

## III. Simulation Set-up

A simulation of the proposed scheme has been performed using VPiTransmission Maker 9.0 (Figure 2). A WDM comb generator is used as an optical source to obtain wavelengths with a deterministic phase relationship. An optical processor is designed to pass signal wavelengths in one arm and pump wavelengths in the other arm. The Wavelength shaper can also change the phase of a pump wavelength as required. The pump and signal wavelengths are then combined and fed into a highly nonlinear fiber (HNLF). The output of the HNLF contains the nonlinear FWM products.

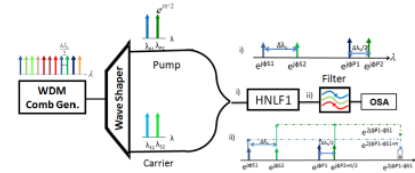


Fig. 2. Simulation schematic to achieve optical subtraction.

This work is supported by a RMIT University International Post Graduate Research Scholarship.

A bandpass filter is used to pass only the required idler and eliminate all other wavelength components. The power level at the target idler is monitored using an OSA to observe the addition and subtraction process

#### IV. RESULTS

Figure 3 shows the simulation results when the signal and pump wavelengths are all in phase. Signal  $\lambda_{S1}$  and pump  $\lambda_{P1}$  mix and generate an idler at  $2\lambda_{P1}-\lambda_{S1}$  with a power level of -30 dBm. Likewise,  $\lambda_{S2}$  and  $\lambda_{P2}$  generate an idler at the same wavelength with the same power level of -30dBm. When  $\lambda_{S1}$ ,  $\lambda_{S2}$ ,  $\lambda_{P1}$  and  $\lambda_{P2}$  are all present, the optical fields of the two idlers add in phase, resulting in a power level of -24 dBm.

Figure 4 shows the simulation results when the phase of pump  $\lambda_{P2}$  is phase shifted by  $90^\circ$  with respect to  $\lambda_{P1}$ . As before, the mixing of  $\lambda_{S1}$  and  $\lambda_{P1}$  produces an idler at  $2\lambda_{P1}-\lambda_{S1}$  with a power level of -30 dBm, as does the mixing of  $\lambda_{S2}$  and  $\lambda_{P2}$ . However, the two idlers are now  $180^\circ$  out of phase. When  $\lambda_{S1}$ ,  $\lambda_{S2}$ ,  $\lambda_{P1}$  and  $\lambda_{P2}$  are all present, the optical fields of the idlers subtract and produce a power level of -80 dBm.

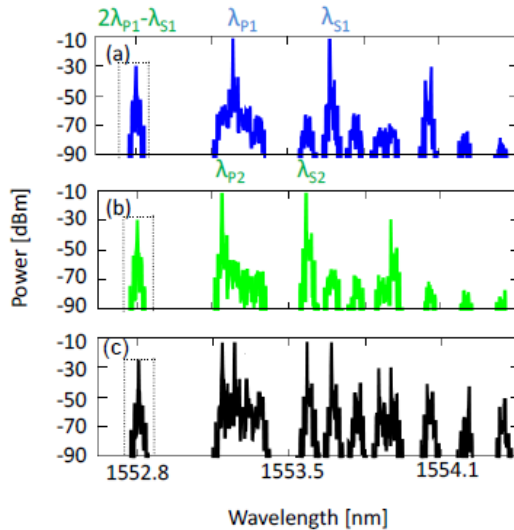


Fig. 3. Simulation results illustrating the addition process. a) Signal wavelength  $\lambda_{S1}$  and pump wavelength  $\lambda_{P1}$  generate an idler at  $2\lambda_{P1}-\lambda_{S1}$ . b)  $\lambda_{S2}$  and  $\lambda_{P2}$  mix and generate an idler at the same wavelength as in a). c)  $\lambda_{S1}$ ,  $\lambda_{S2}$ ,  $\lambda_{P1}$  and  $\lambda_{P2}$  generate two idlers at the same wavelength which add in phase, producing a 6dB increase in optical power.

#### V. CONCLUSION

In this paper subtraction of optical signals has been demonstrated using FWM for the first time. The application of the concept in different real-time signal processing schemes is to be tested in future.

#### APPENDIX

The signal wavelengths are  $\lambda_{S1}$  and  $\lambda_{S2} = \lambda_{S1} + \Delta\lambda_S$   
The pump wavelengths are  $\lambda_{P1}$  and  $\lambda_{P2} = \lambda_{P1} + \Delta\lambda_S/2$   
Applying FWM, the mixing products are:

$\lambda_{S1}$  and  $\lambda_{P1} \Rightarrow 2\lambda_{P1} - \lambda_{S1}$  and  $\lambda_{S2}$  and  $\lambda_{P2} \Rightarrow 2\lambda_{P1} + \Delta\lambda_S - \lambda_{S1} - \Delta\lambda_S = 2\lambda_{P1} - \lambda_{S1}$ . If  $\lambda_{P2}$  has a phase shift of  $90^\circ$ , the mixing product is at  $2\lambda_{P1} - \lambda_{S1}$  with a phase shift of  $180^\circ$ .

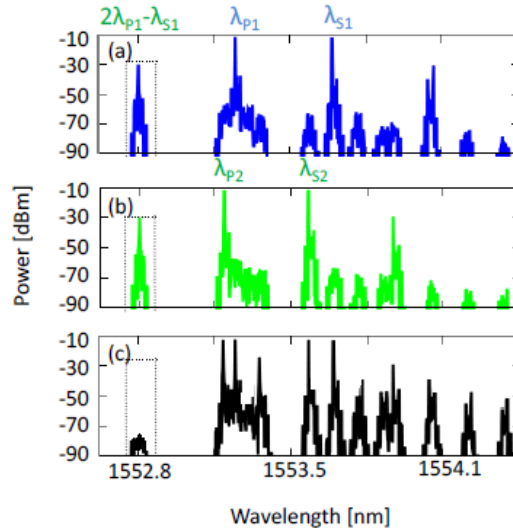


Fig. 4. Simulation results illustrating the optical subtraction process. a) Signal wavelength  $\lambda_{S1}$  and pump wavelength  $\lambda_{P1}$  generate an idler at  $2\lambda_{P1}-\lambda_{S1}$ . b)  $\lambda_{S2}$  and  $\lambda_{P2}$ , which is  $90^\circ$  phase shifted with respect to  $\lambda_{P1}$ , generate an idler at the same wavelength as in a) but with a  $180^\circ$  phase shift. c)  $\lambda_{S1}$ ,  $\lambda_{S2}$ ,  $\lambda_{P1}$  and  $\lambda_{P2}$  mix and generate two idlers at the same wavelength which are  $180^\circ$  out of phase, producing a subtraction.

#### ACKNOWLEDGMENT

The authors gratefully acknowledge the contributions of Prof. Aman Mitchell and Dr. Lam Bui for their insight and comments regarding the work.

#### REFERENCES

- [1] J. Capmany, *et al.*, "Discrete-time optical processing of microwave signals," *Journal of Lightwave Technology*, vol. 23, pp. 702-723, Feb 2005.
- [2] J. Capmany and D. Novak, "Microwave photonics combines two worlds," *Nature Photonics*, vol. 1, pp. 319-330, Jun 2007.
- [3] J. P. Yao, "Microwave Photonics," *Journal of Lightwave Technology*, vol. 27, pp. 314-335, Jan-Feb 2009.
- [4] A. J. Seeds and K. J. Williams, "Microwave photonics," *Journal of Lightwave Technology*, vol. 24, pp. 4628-4641, Dec 2006.
- [5] S. H. Kim, *et al.*, "Optical time-domain analog pattern correlator for high-speed real-time image recognition," *Optics Letters*, vol. 36, p. 956-958, 2011.
- [6] E.J.M. Verdurmen, *et al.*, "All-Optical data format conversion from WDM to OTDM based on FWM," *Microwave and Optical Technology Letters*, vol. 48, p. 1177-1179, 2006.

## APPENDIX V

This appendix contains the paper published in the IEEE Photonics Journal in December 2013.

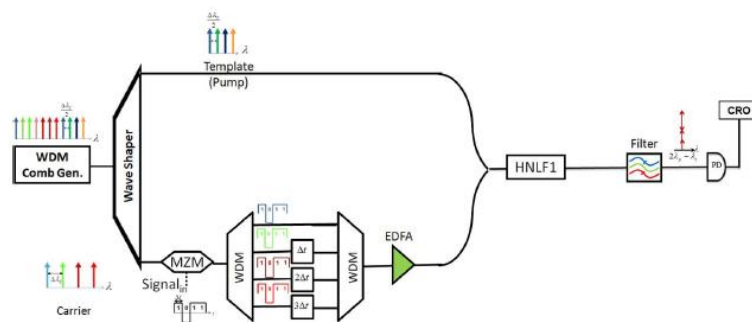


Open Access

# (IPC) A Photonic Correlation Scheme Using FWM With Phase Management to Achieve Optical Subtraction

Volume 5, Number 6, December 2013

Refat Kibria  
Lam A. Bui  
Arnan Mitchell  
Michael W. Austin, Member, IEEE



DOI: 10.1109/JPHOT.2013.2287555  
1943-0655 © 2013 IEEE





# (IPC) A Photonic Correlation Scheme Using FWM With Phase Management to Achieve Optical Subtraction

Refat Kibria, Lam A. Bui, Arnan Mitchell, and  
Michael W. Austin, *Member, IEEE*

School of Electrical and Computer Engineering, RMIT University, Melbourne Vic. 3000, Australia

DOI: 10.1109/JPHOT.2013.2287555  
1943-0655 © 2013 IEEE

Manuscript received September 15, 2013; revised October 11, 2013; accepted October 11, 2013. Date of publication October 28, 2013; date of current version November 26, 2013. This work was supported under an RMIT University International Postgraduate Research Scholarship. This paper describes work presented at the 2013 IEEE Photonics Conference. Corresponding author: R. Kibria (e-mail: refat.kibria@student.rmit.edu.au; refat-cse@sust.edu).

**Abstract:** In this paper, a photonic correlation scheme that allows accumulation of negative signals is presented. The scheme uses four-wave mixing of pairs of signal and pump wavelengths, which are chosen such that they create idler wavelengths at a common wavelength. The total optical power at this target idler wavelength depends on the relative phase of each pump and signal wavelength. This concept has been applied to form a correlator where signal wavelengths are modulated by an input bit stream and mixed with pump wavelengths representing a reference bit pattern. This approach provides a correlation function with smaller unwanted noise peaks due to cancellation in the subtraction process. Simulation of the proposed correlation technique has been used to verify the concept using both intensity and phase modulation of the signal wavelengths.

**Index Terms:** Four wave mixing, microwave photonics, pattern recognition, photonic correlation.

## 1. Introduction

Correlation of electrical signals with negative values is difficult using photonics since optical signals are always positive [1]–[3]. In this paper, a novel correlation scheme based on four wave mixing (FWM) is presented which can achieve accumulation of negative correlation signals. The key concept of this work is to utilize an inherent property of FWM to achieve the subtraction of two optical signals optically [4]. FWM of signal and pump wavelengths creates idler wavelengths at sum and difference wavelengths which carry information from the original wavelengths. If a number of signal and pump wavelength pairs are selected such that the signal wavelengths have a separation equal to twice that of the pump wavelengths, then FWM of each signal and pump wavelength pair will create an idler wavelength at a common target wavelength. The optical power at this target idler wavelength depends on the relative phase of each mixing product at that wavelength. Subtraction of an idler can be achieved if the pump wavelength of that mixing product has a  $\pi/2$  radian or  $90^\circ$  phase shift with respect to the other pump wavelengths [4]. The resultant idler for that particular mixing term will have a  $\pi$  radian or  $180^\circ$  phase difference with respect to the other idlers at the same wavelength which will result in a subtraction of optical fields. This subtraction principle is utilized to achieve a negative accumulation based correlator. Fig. 1 illustrates this principle.



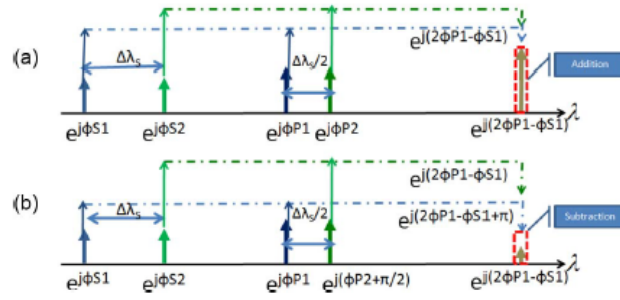


Fig. 1. Principle of operation. (a) Selection of wavelengths based on the scheme in [5] for addition. (b) Illustration of the subtraction process by applying a  $\pi/2$  radian relative phase shift to one pump wavelength.

In Fig. 1, the signal wavelengths are  $\lambda_{S1}$  and  $\lambda_{S2}$  ( $= \lambda_{S1} + \Delta\lambda_S$ ) and the pump wavelengths are  $\lambda_{P1}$  and  $\lambda_{P2}$  ( $= \lambda_{P1} + \Delta\lambda_S/2$ ). In terms of frequency, the signal frequencies are  $\omega_{S1}$  and  $\omega_{S2}$ , where  $\omega_{S2} = \omega_{S1} + \Delta\omega_S$ , and the pump frequencies are  $\omega_{P1}$  and  $\omega_P$ , where  $\omega_{P2} = \omega_{P1} + \Delta\omega_S/2$ . Four wave mixing of  $\omega_{P1}$  and  $\omega_{S1}$  produces an idler frequency at  $2\omega_{P1} - \omega_{S1}$  ( $\approx 2\lambda_{P1} - \lambda_{S1}$ ). Likewise, FWM of  $\omega_{P2}$  and  $\omega_{S2}$  produces an idler at  $2(\omega_{P1} + \Delta\omega_S/2) - (\omega_{S1} + \Delta\omega_S) = 2\omega_{P1} + \Delta\omega_S - \omega_{S1} - \Delta\omega_S = 2\omega_{P1} - \omega_{S1}$  ( $\approx 2\lambda_{P1} - \lambda_{S1}$ ). If the pump wavelengths are in phase [Fig. 1(a)], the resultant idlers add at the common wavelength. If  $\lambda_{P2}$  has a phase shift of  $\pi/2$  radians compared to  $\lambda_{P1}$  [Fig. 1(b)], the mixing product due to  $\lambda_{P2}$  has a phase shift of  $P$  radians compared to the mixing product due to  $\lambda_{P1}$  resulting in subtraction of the optical fields.

Simulation results of this principle are presented in [4]. In this paper, we use this technique to demonstrate a correlation scheme which can achieve accumulation of negative signals. The correlation process is demonstrated for both intensity and phase modulation of the signal wavelengths and it is concluded that phase modulation is the preferred modulation technique since it achieves a greater contrast between correlated and uncorrelated signals.

## 2. Optical Signal Subtraction

Before presenting the correlation technique, we present simulation results demonstrating the optical subtraction scheme described above. A simulation of the subtraction scheme was performed using “*VPItransmissionMaker 9.0*” software. A WDM comb generator was used as an optical source to obtain signal and pump wavelengths with a deterministic phase relationship and an optical processor was used to change the phase of a pump wavelength as required.

Pump and signal wavelengths were combined and fed into a length of highly nonlinear fiber (HNLFF) which had a nonlinear coefficient  $\gamma = 20 \text{ W}^{-1}\text{km}^{-1}$  and zero dispersion in the 1540 to 1560 nm range. The output of the HNLFF contains the FWM products. The power level at the target idler wavelength was measured to observe the addition and subtraction process.

Fig. 2(i) shows the simulation results when the signal and pump wavelengths are all in phase. Signal  $\lambda_{S1}$  and pump  $\lambda_{P1}$  mix and generate an idler at  $2\lambda_{P1} - \lambda_{S1}$  with a power level of  $-30$  dBm. Likewise,  $\lambda_{S2}$  and  $\lambda_{P2}$  generate an idler at the same wavelength with the same power level of  $-30$  dBm. When  $\lambda_{S1}$ ,  $\lambda_{S2}$ ,  $\lambda_{P1}$ , and  $\lambda_{P2}$  are all present, the optical fields of the two idlers add in phase, resulting in a power level of  $-24$  dBm (a 6 dB increase).

Fig. 2(ii) shows the simulation results when the phase of pump  $\lambda_{P2}$  is phase shifted by  $90^\circ$  with respect to  $\lambda_{P1}$ . As before, the mixing of  $\lambda_{S1}$  and  $\lambda_{P1}$  produces an idler at  $2\lambda_{P1} - \lambda_{S1}$  with a power level of  $-30$  dBm, as does the mixing of  $\lambda_{S2}$  and  $\lambda_{P2}$ . However, the two idlers are now  $180^\circ$  out of phase. When  $\lambda_{S1}$ ,  $\lambda_{S2}$ ,  $\lambda_{P1}$ , and  $\lambda_{P2}$  are all present, the optical fields of the idlers subtract and produce a power level of  $-80$  dBm.

## 3. Correlation Technique

In the proposed correlation technique, a number of carrier or signal wavelengths are each modulated by an input electrical bit stream which is to be correlated with a reference or template bit

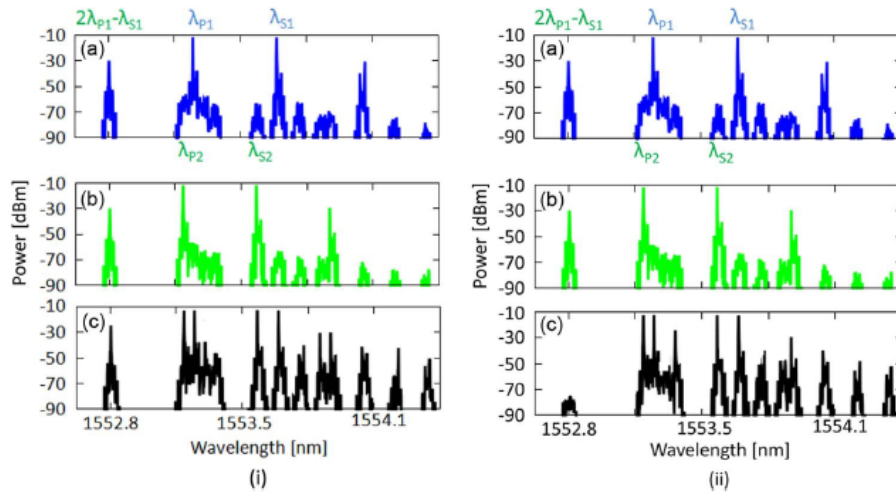


Fig. 2. Simulation results illustrating the addition process in (i) and subtraction process in (ii).

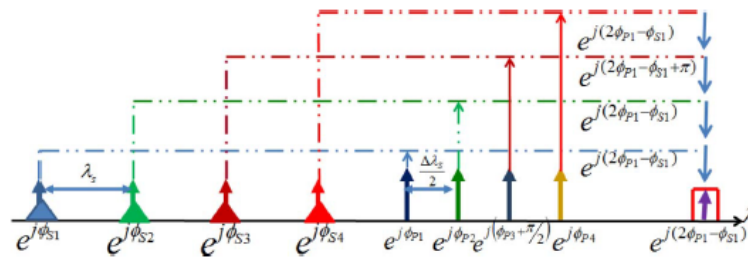


Fig. 3. Principle of operation of the proposed negative accumulation technique with pump wavelengths representing the template 1101.

pattern. The modulated signal wavelengths are then dispersed or delayed so there is a relative delay of a one bit time duration between adjacent wavelengths, as in [2], and combined with an equal number of pump wavelengths, which represent the template bit pattern. The pump wavelengths have an equal power level and those representing a “0” exhibit a  $\pi/2$  radians phase shift with respect to those representing a “1”. The spacing between the pump wavelengths is selected to be the half the spacing between the signal wavelengths, as explained above, such that the individual mixing processes generate the same unique idler wavelength [4], [6]. The signal and pump wavelengths are mixed in a length of highly nonlinear optical fiber to produce the required idler wavelengths.

As an example of this process, consider the correlation of a four bit pattern (let it be 1011 for this example). To represent the four bits, four wavelengths are selected to act as carrier wavelengths which are modulated with the input electrical bit stream. As the method is a convolution method, the pump wavelengths are selected as a time inverted version of the reference bit pattern, in this case 1101, to get the correlation coefficient [2]. The third wavelength representing a “0” has a  $\pi/2$  radians phase shift with respect to the wavelengths representing a “1”. FWM of the carrier and pump wavelengths produces idlers at  $2\lambda_{p1} - \lambda_{s1}$ , as shown in Fig. 3, with three additive idlers and one  $180^\circ$  out of phase idler which will subtract from the others. The output at  $2\lambda_{p1} - \lambda_{s1}$  thus provides a correlation coefficient with negative accumulation.

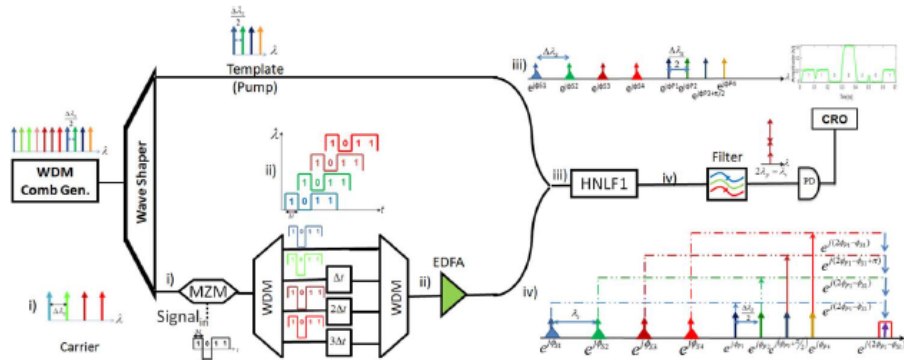


Fig. 4. Simulation set-up in *VPItransmissionMaker 9.0* used to verify the negative accumulation based correlation scheme for a 4-bit duration pattern length when intensity modulation is used.

Simulations have been performed using “*VPItransmissionMaker 9.0*” software to validate this proposed correlation scheme. Both intensity and phase modulation have been used to modulate the signal wavelengths.

### 3.1. Simulation Using Intensity Modulation

The simulation set-up for the correlation scheme using intensity modulation to modulate the signal wavelengths is shown in Fig. 4.

Similar to the simulation for subtraction in [5], a WDM comb generator is used to ensure a deterministic phase relationship among the wavelengths in operation and a wave shaper is used to process the wavelength comb to set the template up. The wave shaper module consists of filters and a phase converter which can manipulate the phase of any input wavelength and can also process any frequency in the spatial domain. In the laboratory, a wave shaper enables software control to shape any pulse or frequency comb. The WDM comb generator module was used to generate a wavelength comb with a  $\Delta\lambda_S/2$  spacing between them. The wave shaper processes the incoming wavelength comb in such a way that one output port provides 4 optical wavelengths with a  $\Delta\lambda_S$  spacing with no manipulation of their phase. These wavelengths represent the carrier wavelengths. The other output port has 4 optical wavelengths with  $\Delta\lambda_S/2$  spacing between them. The phase of these wavelengths can be manipulated to represent the template. In this case, to represent 1101 the phase of the third wavelength was altered to have a  $\pi/2$  radians phase difference with respect to other wavelengths at this port. Therefore, at this output port the pump wavelengths representing 1101 had the same power level with one wavelength phase shifted by  $\pi/2$  radians.

The output port which provides the signal or carrier wavelengths is connected to a quadrature biased Mach–Zehnder modulator (MZM) which is driven by an input 1011 bit pattern at 10 Gb/s. As a result all the carrier wavelengths are modulated by the input bit stream. Since intensity modulation is utilized in this simulation the “1” is represented by the presence of optical power whereas an absence indicates a “0”. The wavelengths then face a differential delay depending on the bit position they represent and are then amplified and combined with the wavelengths representing the template before being fed into a 1 km length of HNL F. The HNL F has a nonlinear coefficient  $\gamma = 20 \text{ W}^{-1} \text{ km}^{-1}$  and zero dispersion in the 1540 to 1560 nm range.

The FWM of pump and carrier wavelengths produces numerous idlers, but one unique idler at  $2\lambda_{P1} - \lambda_{S1}$  is produced for all individual mixings and this particular wavelength is filtered to obtain the correlation function.

To verify the principle of operation, a VPI simulation was first performed using the set-up of Fig. 4 with no modulating signal applied to the modulator. The signal wavelengths were set to  $\lambda_{S1} = 1553.59 \text{ nm}$  (193.1 THz),  $\lambda_{S2} = 1553.51 \text{ nm}$  (193.11 THz),  $\lambda_{S3} = 1553.43 \text{ nm}$  (193.12 THz) and  $\lambda_{S4} = 1553.35 \text{ nm}$  (193.13 THz), respectively. The output power of these signal sources was set to  $-10 \text{ dBm}$ . The pump wavelengths were generated from the same WDM module. The pump



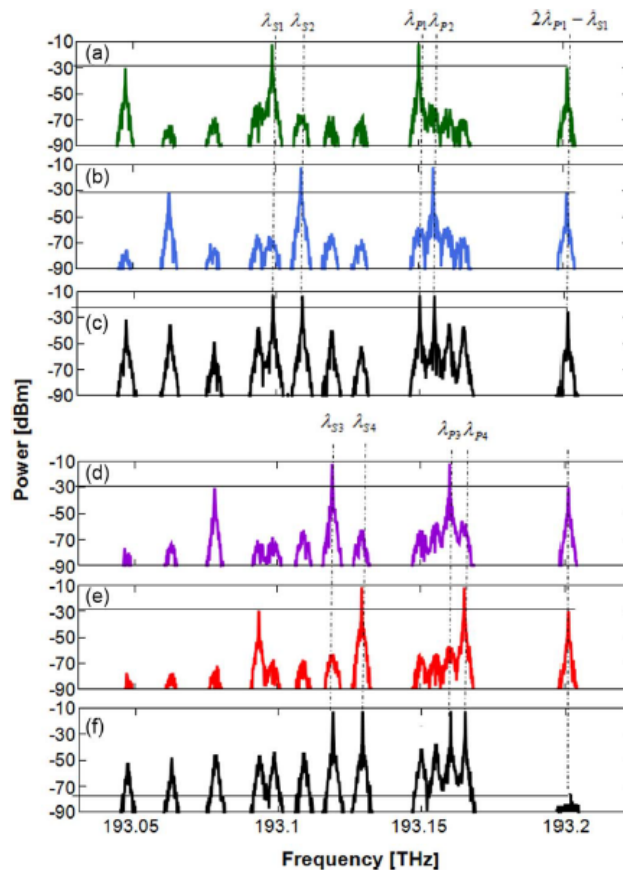


Fig. 5. Proof of concept. (a) Individual mixing result of  $\lambda_{S1}$  and  $\lambda_{P1}$ , (b) individual mixing product of  $\lambda_{S2}$  and  $\lambda_{P2}$ , (c) mixing product  $\lambda_{S1}$  and  $\lambda_{P1}$ , and  $\lambda_{S2}$  and  $\lambda_{P2}$ , showing an addition when  $\lambda_{P1}$  and  $\lambda_{P2}$  are in phase, (d) individual mixing result of  $\lambda_{S3}$  and  $\lambda_{P3}$ , (e) individual mixing result of  $\lambda_{S4}$  and  $\lambda_{P4}$  and (f) mixing product of  $\lambda_{S3}$ ,  $\lambda_{P3}$ , and  $\lambda_{S4}$  and  $\lambda_{P4}$ , showing subtraction when  $\lambda_{P3}$  is  $90^\circ$  out of phase with respect to  $\lambda_{P4}$ .

wavelengths were selected as 1553.19 nm (193.15 THz), 1553.15 nm (193.155 THz), 1553.11 nm (193.16 THz) and 1553.07 nm (193.165 THz), respectively for  $\lambda_{P1}$ ,  $\lambda_{P2}$ ,  $\lambda_{P3}$ , and  $\lambda_{P4}$ . The power level of these pump wavelengths at the input of the HNLFF was also set  $-10$  dBm.

Four wave mixing of the corresponding signal and pump wavelengths in the HNLFF generates a common idler wavelength at 1552.79 nm (193.2 THz). Fig. 5(a) shows that the mixing of  $\lambda_{S1}$  and  $\lambda_{P1}$  produces an idler at the target wavelength with a power level of  $-30.3$  dBm. Similarly,  $\lambda_{S2}$  and  $\lambda_{P2}$  produce an idler at the same wavelength with a power level of  $-30.11$  dBm, shown in Fig. 5(b).

With both  $\lambda_{P1}$  and  $\lambda_{P2}$  set to be in phase and mixed with  $\lambda_{S1}$  and  $\lambda_{S1}$ , the resultant idler was at the same target wavelength with a power level of  $-24.87$  dBm, as seen in Fig. 5(c). Comparing this power level with the power of individual mixing it is evident that the optical fields have added in phase which results in a 6 dB increment in the total output power. In order to verify the process of subtraction, the phase of  $\lambda_{P3}$  was set to be  $90^\circ$  out of phase with respect to  $\lambda_{P4}$ . These pump wavelengths were mixed with  $\lambda_{S3}$  and  $\lambda_{S4}$  to produce an idler at the target wavelength with a power level of only  $-75$  dBm as depicted in Fig. 5(f). Subtraction of power levels has been achieved in this case.

The next step was to apply the 1011 modulating signal to the modulator. After modulation, each of the four wavelengths which represent 1011 are delayed based on their bit position as seen at Fig. 4(ii). The modulated carriers are then combined with the template wavelengths and mixed in the HNLFF. The mixing products followed the concept of Fig. 5. After filtering of the required idler

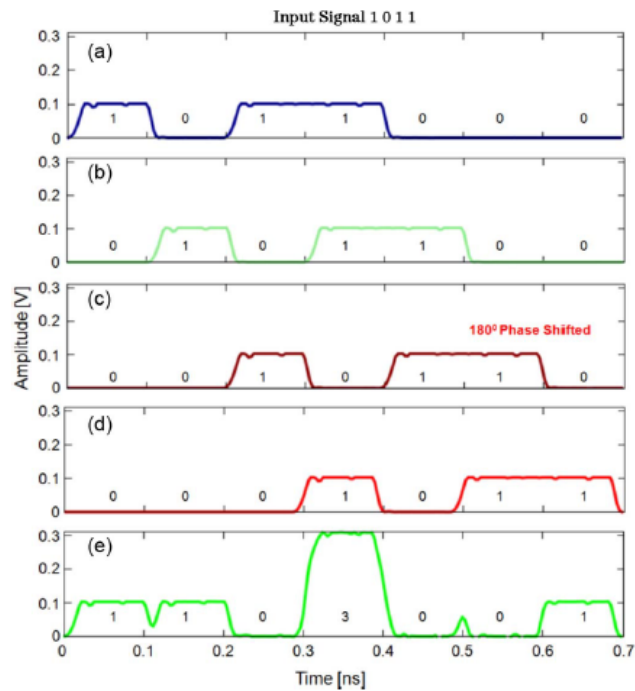


Fig. 6. Detected electrical waveforms of each mixing term at the idler wavelength for the matched condition showing (a) mixing of  $\lambda_{S1}$  and  $\lambda_{P1}$ , (b) mixing of  $\lambda_{S2}$  and  $\lambda_{P2}$ , (c) mixing of  $\lambda_{S3}$  and  $\lambda_{P3}$ , (d) mixing of  $\lambda_{S4}$  and  $\lambda_{P4}$  and (e) the output correlation function which is a summation of plots (a)–(d).

wavelengths and detection by a photodetector, the detected electrical waveforms due to each mixing term are shown in Fig. 6. Fig. 6(a)–(d) show the detected waveforms for individual mixing terms at the target idler wavelength. Fig. 5(e) shows the combined mixing product, which is a summation of Fig. 6(a)–(d) which represents the correlation function. It is to be noted that Fig. 6(c) represents the mixing product which involves the template wavelength representing “0”. The mixing product has a  $\pi$  radians phase difference with respect to the other mixing products and therefore is subtracted from the other additive signals.

When the input bit pattern matches the template pattern, as is the case here, a correlation peak occurs at the middle of the correlation function. The height of this correlation peak is equal to the height of a “1” detected for each wavelength multiplied by the number of “1”s in the template, in this case three. The correlation technique described here results in smaller unwanted ‘noise’ peaks because some of the noise bits are canceled in the subtraction process. When the input bit stream does not match the template pattern, the peak value of the correlation function is less than the maximum value of three units. Fig. 7 shows the detected waveforms for a mismatched condition when the input bit stream is changed to 1100 and the template remains 1101. A peak value of 2 units is reached in the correlation function which indicates a mismatch.

If the modulating signal is a continuous pseudorandom bit stream rather than a fixed 4 bit pattern, the incoming bit stream is continuously compared with the template and a match between any 4 input bits and the 1101 template is indicated when the correlation function reaches a maximum value of 3 units. This is shown in Fig. 8.

### 3.2. Simulation Using Phase Modulation

Using intensity modulation of the signal wavelengths in the approach outlined above, even though a significant improvement of the noise floor is achievable through cancellation of unwanted bits in the correlation function, the ultimate contrast is not much better than previously demonstrated

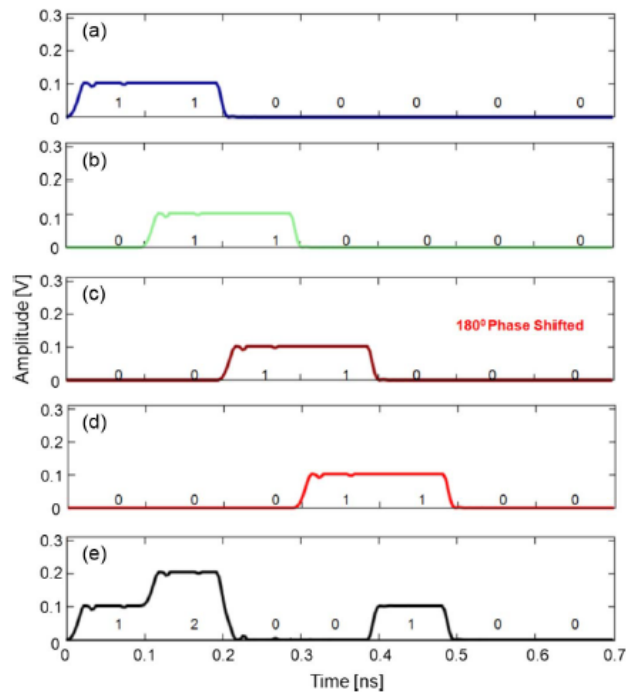


Fig. 7. Detected electrical waveforms of each mixing term at the idler wavelength for a mismatched condition showing (a) mixing of  $\lambda_{S1}$  and  $\lambda_{P1}$ , (b) mixing of  $\lambda_{S2}$  and  $\lambda_{P2}$ , (c) mixing of  $\lambda_{S3}$  and  $\lambda_{P3}$ , (d) mixing of  $\lambda_{S4}$  and  $\lambda_{P4}$ , and (e) the output correlation function which is a summation of plots (a)–(d).

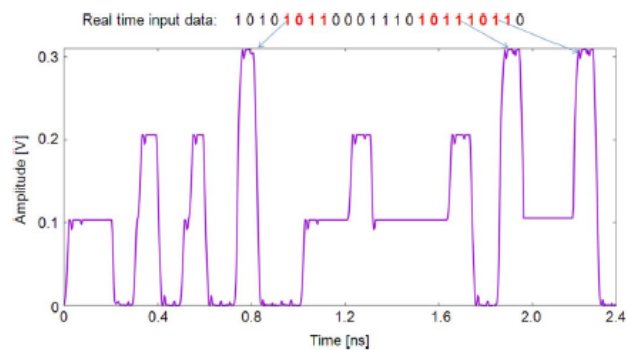


Fig. 8. Output correlation function obtained for a continuous 10Gb/s input bit stream.

correlation schemes [2], [3], [6]–[8]. By performing a truth table exercise it was realized that a significant improvement in correlation contrast is achievable by using phase modulation (PM) instead of intensity modulation. This section examines the simulation results obtained using a phase modulator in place of the MZM to modulate the carrier wavelength.

By replacing the MZM intensity modulator with a phase modulator and keeping the rest of the setup of Fig. 4 unchanged, the carrier wavelengths can be phase modulated by the input bit stream. Using phase modulation, a “1” is represented by a +ve 1 and a “0” is represented by a –ve 1.

FWM of the carrier and pump wavelengths produces idler wavelengths at a common target wavelength, as before. Because positive and negative optical fields can cancel, the resulting correlation signal exhibits an enhanced contrast between the correlation peak and other peaks.

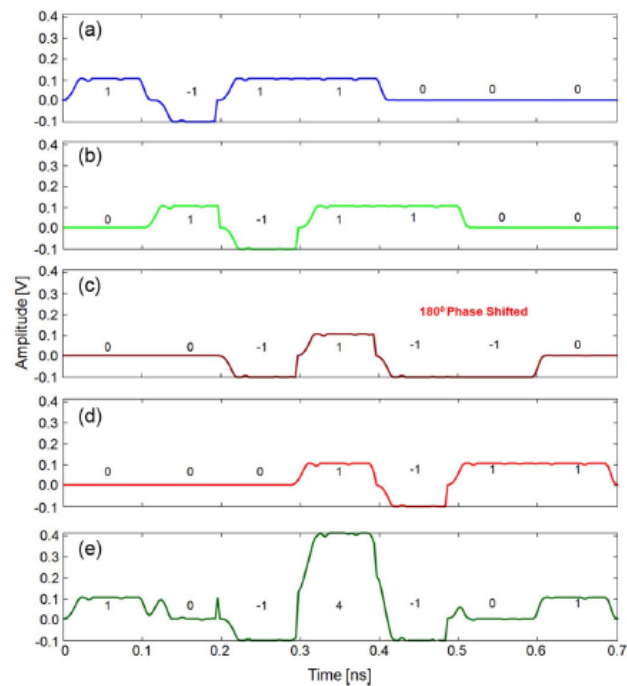


Fig. 9. Detected electrical waveforms of each mixing term at the idler wavelength for the matched condition showing (a) mixing of  $\lambda_{S1}$  and  $\lambda_{P1}$ , (b) mixing of  $\lambda_{S2}$  and  $\lambda_{P2}$ , (c) mixing of  $\lambda_{S3}$  and  $\lambda_{P3}$ , (d) mixing of  $\lambda_{S4}$  and  $\lambda_{P4}$ , and (e) the output correlation function with negative accumulation which is a summation of plots (a)–(d).

Fig. 9(a)–(d) show the electrical waveforms at the output of the photodetector due to each mixing term at the target idler wavelength when the input signal is matched with the template 1101. Fig. 9(e) shows the correlation function which has a peak value of 4 units. This peak is higher than the peak value of 3 units achieved using intensity modulation of the signal wavelengths and achieved by other earlier correlation techniques. In addition, the contrast between the correlation peak and other peaks is at least two units which is a notable improvement with respect to previous correlation methods where the contrast is only 1 unit.

All possible input bit patterns were simulated and Fig. 10 shows the worst case mismatched condition when the input pattern is 1001. In this case the peak value of the correlation is two units, as seen in Fig. 10(e). Therefore, there is at least a 2 unit difference in contrast between the correlation peaks for the matched and mismatched bit patterns.

#### 4. Conclusion

A novel technique to achieve subtraction of optical fields based on four wave mixing and the use of a common target idler wavelength has been presented. Changing the relative phase of a pump wavelength can change the sign of the field at the idler wavelength causing addition or subtraction of signals. This concept has been used to demonstrate a new photonic correlation scheme where signal wavelengths are modulated by an input electrical bit stream and are then differentially delayed before being mixed with pump wavelengths representing a reference or template bit pattern in a length of highly nonlinear optical fiber. This technique has been demonstrated using *VPItransmissionMaker 9.0* based simulations. Both intensity and phase modulation of signal carrier wavelengths by the input bit pattern have been performed. The technique shows a correlation function with better contrast between the correlation peak and other unwanted peaks due to



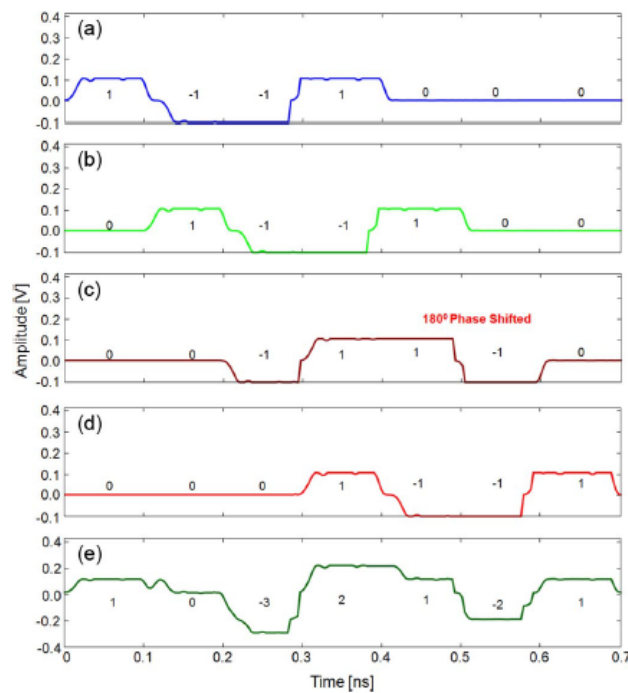


Fig. 10. Detected electrical waveforms of each mixing term at the idler wavelength for a mismatched condition showing (a) mixing of  $\lambda_{S1}$  and  $\lambda_{P1}$ , (b) mixing of  $\lambda_{S2}$  and  $\lambda_{P2}$ , (c) mixing of  $\lambda_{S3}$  and  $\lambda_{P3}$ , (d) mixing of  $\lambda_{S4}$  and  $\lambda_{P4}$ , and (e) the output correlation function with negative accumulation which is a summation of plots (a)–(d).

cancelation in the subtraction process. Phase modulation shows a larger difference between the correlation peak of matched and unmatched signals compared with other photonic correlation techniques previously demonstrated.

## References

- [1] R. Kibria, L. A. Bui, A. Mitchell, and M. W. Austin, "HNLf based photonic pattern recognition using remote transmitter," *IEEE Photon. Technol. Lett.*, under review.
- [2] Y. Park and J. Azana, "Optical signal processors based on a time-spectrum convolution," *Opt. Lett.*, vol. 35, no. 6, pp. 796–798, Mar. 15, 2010.
- [3] R. Kibria, L. Bui, and M. Austin, "Nonlinear mixing based photonic correlator," in *Proc. IEEE Int. Top. Meet. Microw. Photon.*, Noordwijk, The Netherlands, 2012, pp. 30–33.
- [4] R. Kibria and M. W. Austin, "Optical subtraction using nonlinear mixing," presented at the IEEE Photonics Conference, Bellevue, WA, USA, 2013, Paper WC1.3.
- [5] E. J. M. Verdumen, G. D. Khoe, A. M. J. Koonen, and H. D. Waardt, "All-optical data format conversion from WDM to OTDM based on FWM," *Microw. Opt. Technol. Lett.*, vol. 48, no. 5, pp. 992–994, May 2006.
- [6] A. Malacarne, R. Ashrafi, Y. Park, and J. Azana, "Reconfigurable optical differential phase-shift-keying pattern recognition based on incoherent photonic processing," *Opt. Lett.*, vol. 36, no. 21, pp. 4290–4292, Nov. 1, 2011.
- [7] S. H. Kim, K. Goda, A. Fard, and B. Jalali, "Optical time-domain analog pattern correlator for high-speed real-time image recognition," *Opt. Lett.*, vol. 36, no. 2, pp. 220–222, Jan. 2011.
- [8] Y. Dai and J. Yao, "Microwave correlator based on a nonuniformly spaced photonic microwave delay-line filter," *IEEE Photon. Technol. Lett.*, vol. 21, no. 14, pp. 969–971, Jul. 2009.